CHARACTERIZATION OF *CAENORHABDITIS ELEGANS* AS A *MYCOBACTERIUM MARINUM* VIRULENCE MODEL

A Dissertation

by

DON THUSHARA NUWAN GALBADAGE

Submitted to the Office of Graduate and Professional Studies of
Texas A&M University
in partial fulfillment of the requirements for the degree of

DOCTOR OF PHILOSOPHY

Chair of Committee,	Jeffrey D. Cirillo
Committee Members,	Robert C. Alaniz
	Helene L. Andrews-Polymenis
	Xiaorong Lin
	Jon T. Skare
Head of Program,	Warren Zimmer

May 2017

Major Subject: Medical Sciences

ABSTRACT

Mycobacterium marinum is a medically important aquatic pathogen that causes cutaneous granulomatous lesions in humans and a chronic tuberculosis-like granulomatous disease in ectotherms. *M. marinum* is commonly used as a model to facilitate understanding of *M. tuberculosis (Mtb)* virulence and pathogenesis. However, there are limitations for use of *M. marinum* as a model for *Mtb* because *M. marinum* have optimal growth temperature <33°C and they are not respiratory pathogens. *Caenorhabditis elegans* have been used as a host to study various pathogens because of the many molecular tools available and their genetic tractability. We infected *C. elegans* with *M. marinum* and characterized nematode morbidity and mortality. *C. elegans* infected with *M. marinum* for 24 hours display a mortality rate of >80% within two days post-infection. In contrast, nematodes infected with the non-pathogenic mycobacterial species *M. smegmatis* have a mortality rate of <15%. *C. elegans* infected with *M. marinum* also displayed extensive pathology and colonization when compared to nematodes infected with *M. smegmatis*. Our observations demonstrate that *M. marinum* are pathogenic to *C. elegans* and suggest that these nematodes can be used for analysis of *M. marinum* virulence factors. We characterized a mycobacterial *luxR1* gene locus in *M. marinum* that plays a role in *Mtb* virulence and macrophage infection. *M. marinum luxR1* is transcribed in a common transcript with the *pcd* gene that has been suggested to play a role in biofilm formation. *M. marinum* mutants of *luxR1* and *pcd* genes were characterized for their roles in growth, colony morphology, sliding motility, biofilm

formation, macrophage infection and *C. elegans* infections. We show that the *Mm-luxR1* gene plays a role in several *M. marinum* virulence related phenotypic characteristics. Mitogen activated protein kinase (MAPK) cell signaling pathways are critical mediators of host innate immune response to pathogens and it is known that mycobacterial species activate all major MAPK pathways upon host cell contact. Probing the role of *C. elegans* p38 MAPK pathway in response to mycobacterial infections revealed differences in host innate immune responses to pathogenic and non-pathogenic mycobacteria. A p38 MAPK *pmk-1* mutant of *C. elegans* is hypersensitive to both *M. marinum* and *M. smegmatis* infection, while nematodes with an intact MAPK pathway are resistant to *M. smegmatis* but not *M. marinum*. This study establishes *C. elegans* as a new model for analysis of mycobacterial virulence and mechanisms of immune protection.

DEDICATION

This dissertation is dedicated to my kindhearted and loving parents who always encouraged, supported and believed in me throughout my educational and research experience at Texas A&M University, College of Medicine.

ACKNOWLEDGEMENTS

I thank my committee chair, Dr. Jeffrey Cirillo for providing me with the opportunity, resources and guidance to carry-out my graduate research project and mentoring me to help me be a become a better scientist. I also thank my committee members, Drs. Robert C. Alaniz, Helene L. Anderws-Polymenis, Xiaorong Lin, and Jon T. Skare, for their guidance and constructive comments throughout the course of this research.

I thank Dr. Julian Leibowitz, our MD/PhD program coordinator for his guidance and support throughout my time in medical school and graduate school. Thanks also go to my friends and colleagues in the Cirillo lab, Suat, post-doctoral fellows, graduate students and undergraduate students for their assistance and support during my time with the Cirillo group. I thank fellow graduate student Tonya Shepherd for her assistance and collaboration in my laboratory work. I acknowledge the support and assistance I received in lab from undergraduate students Dixi Patel, Anna Woojung (Anna) Kim and Pascal Lagendijk. I also thank the department faculty and staff for making my time at Texas A&M University College of Medicine, Microbial Pathogenesis and Immunology Department a great and positive experience.

Finally, I thank my mother and father for their unwavering support, encouragement and faith in me during all of my educational training. Thanks also go to my brother, sister, cousins and close relatives for their encouragement and support throughout my training.

NOMENCLATURE

ADC	Albumin dextrose complex
AHL	N-acyl homoserine lactone
AI	Autoinducer
CFU	Colony forming unit
CR	Complement receptor
DNA	Deoxyribonucleic acid
EE	Early endosomes
LAM	Lipoarabinomannan
LE	Late endosomes
LPS	Lipopolysaccharide
MADC	Middlebrook albumin dextrose complex
MAPK	Mitogen-activated protein kinase
MBL	Mannose-binding lectin
MIM	Macrophage infection mutant
MKP	Mitogen-activated protein kinase phosphatase
Mm	*Mycobacterium marinum*
MOI	Multiplicity of infection
Ms	*Mycobacterium smegmatis*
Mtb	*Mycobacterium tuberculosis*
OD	Optical density

PAMP	Pathogen-associated molecular pattern
PCD	Piperideine-6-carboxylate dehydrogenase
PCR	Polymerase chain reaction
PRR	Pattern recognition receptors
qPCR	Quantitative PCR (real-time PCR)
RACE	Rapid amplification of cDNA ends
RNA	Ribonucleic acid
RNAi	RNA interference
RT-PCR	Reverse transcriptase PCR
SEM	Standard error of the mean
TEM	Transmission electron microscope
TLC	Thin layer chromatography
TLR	Toll-like receptor

TABLE OF CONTENTS

Page

LIST OF FIGURES

Page

LIST OF TABLES

Page

CHAPTER I

INTRODUCTION AND LITERATURE REVIEW

I.1 Mycobacterial Infections and Pathogenesis

Mycobacterial species are important human pathogens causing diseases including tuberculosis, leprosy, severe skin lesions and infections in immune compromised patients that can be lethal if left untreated (Corti and Palmero, 2008; Cruz-Knight and Blake-Gumbs, 2013; Rodrigues and Lockwood, 2011; Tebruegge and Curtis, 2011). Mycobacteria are non-motile, rod-shaped, acid-fast, slow growing and obligate aerobic bacteria that are often successful pathogens (Vilcheze et al., 2011). They are facultative intracellular parasites and different mycobacteria have chosen niches where they colonize and establish infection. *M. tuberculosis* use macrophages as their primary site of infection while *M. leprae* has an affinity for Schwann cells (Cruz-Knight and Blake-Gumbs, 2013; Rodrigues and Lockwood, 2011). Pathogenic mycobacteria *M. tuberculosis* and *M. avium*, are able to establish systemic disease where as others, including *M. leprae*, *M. marinum* and *M. ulcerans*, cause pathology in cutaneous or subcutaneous tissues, due to their growth temperature of slightly lower than mammalian physiological temperature, to survive and cause disease (Sizaire et al., 2006; Tebruegge and Curtis, 2011). Therefore, mycobacterial pathogens cause a wide array of diseases including; lung infections, systemic infections via dissemination, motor-sensory nerve damage and dermatological manifestations. Severity and extent of pathology of these

infections are determined by the pathogenic strain of mycobacteria involved and the magnitude of the host immune response (Bobosha et al., 2014; Rovina et al., 2013).

Mycobacterium tuberculosis (*Mtb*) infects nearly one-third of the world's population, causing chronic granulomatous lung infection and latent tuberculosis (Bloom and Murray, 1992; Dye, 2006; Dye et al., 1999). Even though current TB treatments are effective against *Mtb,* the prevalence of multidrug resistant (MDR) and extreme drug resistant (XDR) forms of *Mtb* is increasing (Zumla et al., 2012). MDR and XDR have a higher prevalence in immune compromised patients, making the treatment of TB an even larger problem (Hesseling et al., 2012; Munsiff et al., 1997). The incidence of TB in HIV positive patients has increased to the point that tuberculosis is now considered an AIDS defining disease (Aaron et al., 2004). Even though *Mtb* has been studied for several decades, the molecular mechanisms of pathogenesis are not fully understood. A better understanding of pathogenic processes used by *Mtb* will help in the development of novel treatments and more effective vaccines. Mycobacterial pathogens are successful intracellular pathogens adapted to counter the host immune response at various stages of disease. Identifying these processes is an important step toward controlling mycobacterial diseases and eliminating an age-old pathogen.

Mtb is usually first encountered by the host immune system by resident macrophages in lung alveoli within humans exposed to aerosolized droplets containing the bacteria. Type II pneumocytes and dendritic cells are also important as they readily internalize mycobacteria and are effective antigen presenters that lead to the activation of T cells as well as the humoral immune response (Bermudez and Goodman, 1996;

Bodnar et al., 2001; Gonzalez-Juarrero and Orme, 2001; Tascon et al., 2000). *Mtb* is thought to use complement receptors, toll-like receptor II and mannose receptors on the surface of macrophages for the attachment and phagocytosis in the macrophages. Mycobacteria upregulate mannose receptors to their advantage ensuring its internalization into macrophages by direct attachment to mycobacterial cell surface mannose residues such as mannose-capped lipoarabinomannan (LAM) (Gaynor et al., 1995; Kang et al., 2005; Noss et al., 2001; Schlesinger, 1993). Once phagocytosed, *Mtb* remain within a phagosome that is formed by an actin-dependent process (Mooren et al., 2012). These *Mtb* laden phagosomes undergo complex maturation to form early endosomes (EE) containing Rab5 vesicular receptors (Brumell and Grinstein, 2004; Vieira et al., 2002). While EEs usually mature to form late endosomes (LE) containing Rab7 receptors, which are then able to fuse with lysosomes to form phagolysosomes, *Mtb* laden EEs do not undergo this maturation process (He et al., 2012; Liu and Modlin, 2008; Vergne et al., 2004b). *Mtb* is an effective intracellular pathogen that alters phagolysosome biogenesis to its advantage and survives within macrophage phagosomes. These *Mtb* defense mechanisms prevent activation of the host immune system, preventing the cell from undergoing apoptosis and inhibiting activation of a proinflammatory cytokine response (Rosenberger and Finlay, 2003).

After establishing infection within macrophages in the lung, *Mtb* grow and survive for extended periods of time. Macrophages secrete chemokines that initiate migration of neutrophils, monocytes, and lymphocytes to the site of infection, but these immune cells are not effective in reducing the bacterial load or eliminating the pathogen

(Fenton and Vermeulen, 1996; van Crevel et al., 2002). These immune cells together with macrophages form an organized cell complex, known as a granuloma, walling off pathogenic mycobacteria in a caseating center to contain the infection (Davis and Ramakrishnan, 2009). While granulomas are thought to be an effective host immune defense against *Mtb*, the pathogen is able to survive and have a prolonged latent phase and may use granulomas to their advantage during reactivation and dissemination (Keane et al., 1997). *Mtb* has evolved multiple mechanisms to evade and modulate the host immune system and establish chronic infections in humans, leading to over 2 billion people latently infected worldwide and causing close to 3 million deaths annually (Dye et al., 1999).

I.2 *Mycobacterium marinum* as a Model Pathogen

The study of *Mtb* can be facilitated through use of other mycobacterial species, such as *Mycobacterium marinum*, as model organisms (Deng et al., 2011; Stinear et al., 2008; Tobin and Ramakrishnan, 2008). *M. marinum* is a pathogenic *Mycobacterium* found in fresh and sea water ecosystems worldwide (Petrini, 2006). It causes a tuberculosis-like granulomatous infection in fish and amphibians (Gauthier and Rhodes, 2009; Kaattari et al., 2006; Ramakrishnan et al., 1997; Swaim et al., 2006a). *M. marinum* is also a natural human pathogen causing cutaneous granulomatous lesions and can sometimes present in a similar manner to rheumatoid arthritis (Adhikesavan and Harrington, 2008; Ang et al., 2000; Jernigan and Farr, 2000; Osorio et al., 2010; Sauder and Hanke, 1978; Slany et al., 2012). *M. marinum* does not cause systemic disease in

humans because its optimal growth temperature is <33^{o}C, and is normally unable to grow well at 37^{o}C (Clark and Shepard, 1963a). The advantages of using *M. marinum* for study of *Mtb* pathogenic processes is that it can be studied under BSL-2 conditions and has a generation time of 4 hours, compared to a generation time of more than 20 hours for *Mtb*. *M. marinum* is also experimentally useful because of the conservation of genetic traits between *Mtb* and *M. marinum*, and between their respective natural hosts, and this translates into shared virulence determinants (Tobin and Ramakrishnan, 2008). *M. marinum* can be manipulated using molecular tools, and genes of interest can be more easily studied with relative ease. Therefore the orthologs of genes of interest in *M. tuberculosis* can be more easily studied in *M. marinum*. It is ultimately important to directly compare the functions of *M. tuberculosis* and *M. marinum* orthologs to identify their similarities and differences. But use of *M. marinum* should allow more parid progress during detailed analysis of their mechanisms of action.

To better understand mycobacterial pathogenesis including that of *Mtb*, host-pathogen interactions need to be dissected (Koul et al., 2004). Macrophage cell-lines are commonly used for in vitro assays to examine the processes of adherence, attachment, entry and intracellular growth (Cosma et al., 2003). Animal models, including mice and guinea pigs, are well established and commonly used for the study of *Mtb* (Balasubramanian et al., 1994; McMurray, 2001; Shi et al., 2011). The mouse model for study of mycobacterial infections can be somewhat limited, since mice do not display normal granuloma formation and are thought to be relatively resistant when compared to humans (Flynn, 2006). However, neither mice nor guinea pigs can be easily used to

study systemic *M. marinum* infections because *M. marinum* does not normally survive well at mammalian physiologic temperatures (37°C). While mouse models have been used infrequently for the study of *M. marinum* they do not normally allow analysis of systemic infections and are mostly limited to localized infections, such as mouse foot-pad models (Clark and Shepard, 1963b; Mor and Levy, 1985; Mor et al., 1980; Robinson et al., 2007; Subbian et al., 2007a). Systemic *M. marinum* infections and granulomatous disease caused by *M. marinum* infections can be examined in fish and frog models, developed in several laboratories (Cosma et al., 2006). A zebrafish model has been characterized for the study of caseating granuloma development and pathogenesis in *M. marinum* infections (Broussard and Ennis, 2007; Swaim et al., 2006b; Talaat et al., 1998; van der Sar et al., 2004a). However, like the mouse model, the zebrafish model does not display the same disease as is observed in the guinea pig model or during human tuberculosis infections.

I.3 *LuxR* Virulence Gene Locus

Many Gram positive and Gram negative bacterial use small signaling molecules for communication, also known as quorum sensing (QS) (Schauder et al., 2001; Teasdale et al., 2011; Whitehead et al., 2001). Quorum sensing is due to each bacterium constitutively expressing one or more autoinducer molecules. When the population of a particular bacterial species reaches a critical level, the autoinducer signals can suppress or activate target proteins that regulate a cascade of events within the target bacteria (Asad and Opal, 2008). Gram negative species, like *V. fischeri*, commonly use a

luxR/luxI type 1 autoinducer (AI-1) system, which is controlled by highly soluble and diffusible signal molecules that are modifed N-acyl homoserine lactones (AHL) (Beutler et al., 2006). Gram positive and negative bacteria, also often use a second QS system, first described in *V. harveyi,* where a type 2 autoinducer (AI-2) is produced that is removed by the *luxS* gene (Bassler, 2002; Miller and Bassler, 2001; Schauder et al., 2001). A third system, with autoinducer type 3 (AI-3), has recently been described, that uses human epinephrine or norepinephrine as activators (Fuqua and Greenberg, 2002; Kendall et al., 2007). Bacterial communication is not limited to specific species of bacteria. Interspecies communication occurs in complex bacterial communities during infection and biofilm formation (Dunny et al., 1995). QS systems are used by many bacteria, including *Vibrio* species to regulate virulence mechanisms, such as motility, antibiotic production, toxin production, capsule formation, and biofilm formation (Beck von Bodman and Farrand, 1995; Brouillette et al., 2005; Eberl et al., 1996; Gambello et al., 1993; Howard et al., 2006; Karaolis et al., 2005). An analogous set of *lux* system regulators that are induced in *Streptomyces* in response to changes in environment has been identified, studied, and characterized (Takano, 2006). *Streptomyces* are phylogenetically closely related to *Mycobacterium*, and protein orthologs to *Streptomyces* in mycobacteria are often studied.

It is possible that mycobacteria have a *lux* system that contributes to its virulence mechanisms. Mycobacterial species do not have homologs to *luxI* or *luxS* proteins, key components of the AI-1 and AI-2 systems. However, several genes with similarity to *luxR* are present in all mycobacterial species. In the case of *Streptomyces* species, they

carry an ArpA regulatory protein as part of their QS system (Ando et al., 1997; Ohnishi et al., 1999; Yamazaki et al., 2000). A few mycobacterial *luxR* genes are similar to the *arpA* gene in *Streptomyces* species. QS in *Streptomyces* species regulates sporulation and antibiotic synthesis and the signaling molecule is a gamma-butyrolactone (GBL) (Horinouchi and Beppu, 1992, 1994). We hypothesized that similar to ArpA in *Streptomyces*, mycobacterial species have LuxR regulators that are controlled by GBLs and they play a role in virulence.

I.4 Host Innate Immune Response

The innate immune response is the first line of defense against pathogenic bacteria. Innate immunity offer broad protection against invading pathogens from the moment of contact until the adaptive immune response is activated. Even after the activation of the adaptive immune response, the innate immune response works in synergy with adaptive immunity to control and eliminate disease (Marcenaro et al., 2011). In the absence of a successful innate immune response there can be delays or a lack of activation of the pathogen-specific adaptive immune response. The innate immune response is a vital component of host cell signaling pathways and plays a critical role in controlling the overall host immune response (Sirisinha, 2014). Host innate immune system is composed of several non-specific defenses against infectious agents including; a physical epithelial barrier, dendritic cells, natural killer cells, and phagocytic leukocytes.

Eukaryotic hosts recognize pathogen-associated molecular patterns (PAMPs) using a variety of pattern recognition receptors (PRRs) to trigger appropriate immune responses (Kawai and Akira, 2010; Newton and Dixit, 2012). The innate immune response subsequently activates the adaptive immune response through production of cytokines and chemokines, working in synergy with the adaptive immune response to attempt killing of invading pathogens (Iwasaki and Medzhitov, 2010). PRRs recognize conserved structures not present in eukaryotic cells such as lipopolysaccharide (LPS), and trigger many of the aspects of the immune response even after the adaptive immune response takes over (Janeway, 1989, 1992). Activation of the adaptive immune response takes about 5 to 7 days and in the absence of a functional innate immune response this process is delayed or not appropriately activated (Medzhitov and Janeway, 1997). Among other functions, PRRs are also important for activation of the inflammatory response and initiation of apoptosis (Medzhitov and Janeway, 1997).

While the $CD4^+$ T cell immune response plays a critical role in conferring protective immunity against *Mycobacterium tuberculosis* infections, the innate immune response also helps activate and amplify the adaptive immune system (Basu et al., 2012). The innate immune response against *Mtb* occurs in distinct steps. First, host immune cells, such as macrophages and dendritic cells, use cellular receptors including toll-like receptors (TLRs) to bind and phagocytose *Mtb.* These cells then produce an array of cytokines, both anti- and pro-inflammatory mediators that coordinate the host inflammatory response. Finally these effector molecules induce or modulate the host adaptive immune response (van Crevel et al., 2002).

Mycobacteria are thought to be phagocytosed by macrophages and antigen presenting cells by several different ways. Many bacteria, including mycobacteria, can be opsonized with C3 complement factor and attach to the complement receptor (CR) 1, 3 and 4 (Hirsch et al., 1994; Schlesinger, 1993). Non-opsonized mycobacteria can also bind to CR3 and CR4 directly, possibly through their lectin-binding sites (Cywes et al., 1997; Zaffran and Ellner, 1997). Collectin proteins such as plasma factor mannose binding lectins (MBLs) recognize patterns of carbohydrates on the surface of mycobacteria and can assist in phagocytosis (Neth et al., 2000). TLRs are conserved receptors that are involved in the innate immune response and TLR4 plays a role in the recognition, binding of mycobacteria and phagocytosis (Means et al., 1999a; Means et al., 1999b). Once intracellular, *Mtb* is capable of modulating proinflammatory cytokines such as TNF-α, IL-1β, IL-6, IL-12, IFN-γ and anti-inflammatory cytokines, such as IL-4, IL-10 and TGF-β (Dahl et al., 1996; Flynn et al., 1993; Henderson et al., 1997; Hernandez-Pando and Rook, 1994; Ladel et al., 1997; Shaw et al., 2000; Toossi et al., 1995; VanHeyningen et al., 1997). The regulated expression of these host cytokines together with antigen presentation is crucial to initiation of the T-cell mediated adaptive immune response (Hirsch et al., 1999; Mazzaccaro et al., 1996; Sousa et al., 2000). Even after activation of the T cell response the innate immune system and cytokines, such as TNF-α, are important in formation of granulomas and maintenance of *Mtb* in the latent state (Kindler et al., 1989; Mohan et al., 2001; Senaldi et al., 1996).

I.5 *Caenorhabditis elegans* as a Model Host

The nematode *C. elegans* is widely used as a model to study bacterial infections, the innate immune response and host-pathogen interactions (Couillault and Ewbank, 2002; Evans et al., 2008; Garsin et al., 2003; Hodgkin et al., 2000; Singh and Aballay, 2009). *C. elegans* has been used to study Gram-negative (Aballay et al., 2003; Mahajan-Miklos et al., 1999; Sem and Rhen, 2012) and -positive pathogens (Garsin et al., 2001; JebaMercy and Balamurugan, 2012; JebaMercy et al., 2011; Maadani et al., 2007). In the past 15 years *C. elegans* has been utilized to study numerous plant, animal and human microbial pathogens.

Some of the Gram-negative bacteria studied using *C. elegans* as a host include: *Acinetobacter baumannii, Aeromonas hydrophila, Burkholderia cepacia, B. mallei, B. pseudomallei, Burkholderia thailandensis, Escherichia coli, Pseudomonas aeruginosa, Salmonella enterica* serovar Dublin, *S.* enterica serovar Enteritidis, *S. enterica* serovar Typhimurium, *Serratia marcescens, Yersinia pestis,* and *Y. pseudotuberculosis* (Aballay et al., 2000; Couillault and Ewbank, 2002; Darby et al., 1999; Gan et al., 2002; Garigan et al., 2002; Joshua et al., 2003; Kothe et al., 2003; Kurz et al., 2003; Labrousse et al., 2000; O'Quinn et al., 2001; Pujol et al., 2001; Smith et al., 2004; Styer et al., 2005; Tan et al., 1999). Some of the Gram-positive bacteria studied using *C. elegans* as a host include: *Bacillus thuringiensis*, *Enterococcus faecalis, E. faecium., Staphylococcus aureus, Streptococcus dysgalactiae, S. mitis, S. oralis, S. pneumoniae, S. pyogenes, Streptococcus, Group G, Microbacterium nematophilum, Streptomyces albireticuli,* and *S. avermitilis* (Bolm et al., 2004; Garsin et al., 2001; Griffitts et al., 2001; Haber et al.,

1991; Hodgkin et al., 2000; Jansen et al., 2002; Moy et al., 2004; Park et al., 2002; Sifri et al., 2003; Sifri et al., 2002).

Pseudomonas aeruginosa is one of the first human pathogens used to produce an increase in mortality of *C. elegans* upon exposure to it (Mahajan-Miklos et al., 1999). Even to date, mortality remains one of *C. elegans'* most effective and simple read-outs when infected with pathogenic bacteria. There are several other pathological processes in *C. elegans* that are useful in the study of host pathogen interactions. Pathogens such as *E. faecalis, S. marcescens* and *S. enterica* attach to and persist on the gut epithelium of *C. elegans* (Kurz et al., 2003; Maadani et al., 2007; Sem and Rhen, 2012). Natural pathogens of *C. elegans* such as the actinomycete *Streptomyces albireticuli* and the fungus *Drechmeria coniospora* invade the gut epithelium into inner tissues of the nematode (Jansson et al., 1984; Park et al., 2002). Pathogens such as *S. pyogenes, E. faecium* and *P. aeruginosa* cause death of the nematode via toxin-mediated killing (Jansen et al., 2002; Moy et al., 2004; Tan et al., 1999). A pathogenic *Microbacterium nematophilum* forms an adhesive biofilm like structure on the *C. elegans* nematode cuticle, which is involved in its pathogenic process (Hodgkin et al., 2000). Bacterial virulence factors including virulence regulators like quorum-sensing systems, two-component regulators; cell wall components like cell membrane, capsule; and secreted products such as exotoxins, exoenzymes, and type III secretory system have been shown to be important in *C. elegans* infections (Aballay et al., 2000; Bae et al., 2004; Coulthurst et al., 2004; Kothe et al., 2003; Kurz et al., 2003; Tan et al., 1999; Tenor et al., 2004). The importance of bacterial virulence factors along with the ability of

pathogens to induce mortality of *C. elegans*, make it a useful host to study the pathogenic processes involved in the bacterial infections.

There are extensive *C. elegans* mutant libraries that can be used to study the function of nearly any gene of interest. This resource is complemented by the existence of comprehensive RNAi libraries that can knock-down any gene of interest with relative ease. The nematode cellular signaling pathways are well characterized and most of the functions of the genes involved have been determined. *C. elegans* have many conserved genes that are functionally similar to that in higher-eukaryotes and mammalian systems, including humans. *C. elegans* is a valuable model system to study the innate immune responses because of its well characterized genetic environment and the availability of extensive molecular tools, making it possible to perform an array of genetic analyses (Ashrafi et al., 2003; Juang et al., 2013; Kim et al., 2005; Tabach et al., 2013; Taylor and Dillin, 2013; Wilkins et al., 2005).

CHAPTER II

INTRODUCING *CAENORHABDITIS ELEGANS* AS A *MYCOBACTERIUM MARINUM* VIRULENCE MODEL

II.1 Summary

Mycobacterium marinum are pathogenic mycobacteria that cause cutaneous granulomatous lesions in humans and a chronic tuberculosis-like granulomatous disease in ectotherms, including fish and amphibians. *M. marinum* are commonly used to understand *M. tuberculosis (Mtb)* virulence and pathogenesis. They are genetically closely related to *Mtb*, share many virulence genes, cause granulomas and are much easier to handle in the laboratory as compared to *Mtb*. *Caenorhabditis elegans* are used as a host to study various pathogens including *Pseudomonas*, *Staphylococcus*, *Legionella*, *Enterococcus*, *Shigella* and *Proteus* species because of their ease of use and genetic tractability. *C. elegans* have a well characterized innate immune system. Extensive mutant and RNAi libraries exist for analysis of their immune responses, making *C. elegans* a very attractive model. We fed *C. elegans* with *M. marinum* and characterized nematode morbidity and mortality. *C. elegans* fed on *M. marinum* for 24 hours display a mortality rate of >80% within two days post-infection. In contrast, nematodes fed on the non-pathogenic mycobacterial species *M. smegmatis* have a mortality rate of <10%. Using fluorescent tagged *C. elegans*, *M. marinum* and *M. smegmatis* we observed that there is also a difference in localization of pathogenic and non-pathogenic mycobacterial strains, suggesting that *C. elegans* are readily colonized

by pathogenic mycobacteria. Virulent *M. marinum* persist in the pharyngeal, gut and tail regions of the nematode, while avirulent *M. smegmatis* are easily broken down or cleared from the gut. Furthermore, *C. elegans* display different temporal and morphological characteristics based on the virulence of the mycobacterial strain they are infected with. Our observations demonstrate that *M. marinum* are pathogenic to *C. elegans* and suggest that these nematodes can be used for analysis of *M. marinum* virulence. We evaluated the versatility of *C. elegans* as a virulence model for *M. marinum* by infecting them with an array of *M. marinum* mutants with macrophage infection defects. Several mutants were significantly less virulent in *C. elegans* causing reduced mortality rates of 40-65%, suggesting related mechanisms of infection in macrophages and *C. elegans*. This study establishes *C. elegans* as a new model for analysis of mycobacterial virulence and mechanisms of the immune response.

II.2 Introduction

The genus *Mycobacterium* contains some of the most important bacterial pathogens worldwide, including the causative agents of leprosy and tuberculosis (Gutierrez et al., 2009; Stone et al., 2009). Tuberculosis (TB) is one of the most important bacterial infections in humans, representing a global health threat. It causes approximately 2 million deaths annually, leaving more than a third of the world's population latently infected and multi drug resistant TB (MDR-TB) prevalent in all continents. (Chiang et al., 2013; Glaziou et al., 2013; Lynch, 2013; Pan et al., 2005).

Genetically tractable virulence models are extremely valuable for pathogenesis studies, since they allow rapid analysis of complex interactions that are often difficult to study in other mammalian models. Several virulence models are used to study mycobacterial virulence mechanisms, including tissue culture cells, mice, guinea pigs and rabbits (Calderon et al., 2013; Cirillo et al., 2009; Danelishvili et al., 2007a; Danelishvili et al., 2007b; Khounlotham et al., 2009; Kong et al., 2010; Miltner et al., 2005). *C. elegans* is a valuable model system to study host immune responses because of its well characterized genome and the availability of extensive molecular tools, making it possible to perform an array of genetic analyses (Ashrafi et al., 2003; Juang et al., 2013; Kim et al., 2005; Tabach et al., 2013; Taylor and Dillin, 2013; Wilkins et al., 2005). *C. elegans* can be used as a model to study bacterial infections, innate immune response and host-pathogen interactions (Couillault and Ewbank, 2002; Evans et al., 2008; Garsin et al., 2003; Hodgkin et al., 2000; Singh and Aballay, 2009) for both Gram-negative (Aballay et al., 2003; Mahajan-Miklos et al., 1999; Sem and Rhen, 2012) and -positive pathogens (Garsin et al., 2001; JebaMercy and Balamurugan, 2012; JebaMercy et al., 2011; Maadani et al., 2007).

Mycobacterium marinum is commonly used as a virulence model for *M. tuberculosis* due to its rapid growth and ease of use in a laboratory setting (Carvalho et al., 2011; Deng et al., 2011; Prouty et al., 2003; Shiloh and Champion, 2010). By combining easy to use model organisms for the pathogen and host, *M. marinum* and *C. elegans,* respectively, we set out to analyze the host innate immune response against pathogenic mycobacteria. We found that infection of *C. elegans* with the pathogenic

mycobacteria, *M. marinum,* causes significantly higher morbidity and mortality as compared to infection with the non-pathogenic mycobacterial species, *M. smegmatis*. *C. elegans* ingest and are colonized by *M. marinum*, but non-pathogenic mycobacteria are unable to colonize the nematodes and are cleared. *M. marinum* infected *C. elegans* undergo irreversible physiological and morphological changes leading to the death of the nematode. Mortality of *C. elegans* correlates well with virulence of *M. marinum*, suggesting that the nematodes serve as a useful virulence model for mycobacteria.

Genetically tractable and inexpensive lower eukaryotic models for the study of host-pathogen interactions, including yeast, amoebae and *Caenorhabditis elegans*, are extremely valuable, since they allow rapid analysis of complex interactions that are sometimes impossible to fully evaluate in detail in humans or other mammalian models. However, since *M. marinum* does not replicate well over 32°C, mammalian models are mostly limited to skin infections. *M. marinum* pathogenesis has mainly been studied in human, mouse or fish cell-lines including macrophages and epithelial cells (Alibaud et al., 2011; El-Etr et al., 2004; El-Etr et al., 2001; Mehta et al., 2006; Park et al., 2008; Subbian et al., 2007a). Zebrafish and mouse footpads have been used to study pathogenesis of *M. marinum* since they can model temperatures at or below 32^{o}C (Adams et al., 2011; Ehlers, 2010; Fortune and Rubin, 2007; Ramakrishnan, 2013; Subbian et al., 2007b; Takaki et al., 2013; Tobin et al., 2012; Weerdenburg et al., 2012), but no previous studies have demonstrated the ability to use *C. elegans* as a virulence model for *M. marinum*.

The nematode *C. elegans* is widely used as a model to study bacterial infections, innate immune response and host-pathogen interactions (Couillault and Ewbank, 2002; Evans et al., 2008; Garsin et al., 2003; Hodgkin et al., 2000; Singh and Aballay, 2009). *C. elegans* has been established for study of Gram-negative (Aballay et al., 2003; Mahajan-Miklos et al., 1999; Sem and Rhen, 2012) and Gram-positive pathogens (Garsin et al., 2001; JebaMercy and Balamurugan, 2012; JebaMercy et al., 2011; Maadani et al., 2007). *C. elegans* is a valuable model system to study immune responses because of its well characterized genetics and the availability of extensive molecular tools, making it possible to perform an array of genetic analyses (Ashrafi et al., 2003; Juang et al., 2013; Kim et al., 2005; Tabach et al., 2013; Taylor and Dillin, 2013; Wilkins et al., 2005).

Our experimental results indicate that infection of *C. elegans* with the pathogenic mycobacteria, *M. marinum* causes significant morbidity and mortality in nematodes as compared to infection with a non-pathogenic mycobacterial species, *M. smegmatis*. Infected *C. elegans* undergo morphological changes and most gravid nematodes undergo bagging (bag of worms) and are unable to recover. We show that *C. elegans* ingest *M. marinum* and act as a simple but effective model to study *M. marinum* pathogenesis and the innate immune response. The versatility of our model was displayed using *M. marinum* mutants that display a reduction in nematode mortality. Therefore, this model system can be used to analyze host-pathogen interactions from the side of both the host and pathogen in great detail.

II.3 Experimental Procedures

II.3 (A) Bacteria Growth Conditions

Strain M, a wild-type clinical isolate of *M. marinum* (Ramakrishnan, 1997), *M. smegmatis* strain mc^2155 and *E. coli* strain OP50 were used for *C. elegans* infection to characterize host pathogen interactions. Two constitutively expressing tdTomato fluorescent mycobacterial strains (ψmm91 and ψmm23) were derived by transforming *M. marinum* and *M. smegmatis* with a multi-copy plasmid, pJDC60 (pFJS8ΔGFP::tdTomato, under a PL5 promoter, with kanamycin selection). These two strains were used to study mycobacterial localization within *C. elegans* nematodes after bacterial infection. *M. marinum* cultures were grown at 32ºC standing in T25 tissue culture flasks. *E. coli* and *M. smegmatis* cultures were grown at 37ºC shaking in sterile disposable glass test tubes. *M. marinum* and *M. smegmatis* were grown in Middlebrook 7H9 media (Difco, Sparks, MD) supplemented with 0.5% glycerol, 10% albumin-dextrose complex (ADC) and 0.25% Tween 80 (M-ADC-TW), while *E. coli* was grown in Miller's Luria Broth (NPI, Mt. Prospect, IL).

II.3 (B) C. elegans *Maintenance and Synchronization*

N2 (Bristol, wild-type), KU25 [*pmk-1*(km25)], IG10 [*tol-1*(nr2033)], NU3 [*dbl-1*(nk3)], GR1307 [*daf-16*(mgDf50)], EU31 [*skn-1*(zu135)], JT366 [*vhp-1*(sa366)] and TP12 [*kaIs12*(col-19::GFP)] *C. elegans* strains were used in this study. The nematodes were grown and maintained on nematode growth media (NGM) plates using standard methods at room temperature (Brenner, 1974). The room temperature was regularly monitored and maintained at 19ºC to 21ºC. Synchronous cohorts of *C. elegans* were

obtained by lysing gravid nematodes using an alkaline bleach solution (Emmons et al., 1979). After removing the bleach solution and washing the embryos, they were stored in M9 buffer overnight to obtain L1 larvae. These L1 larvae were transferred onto NGM plates seeded with OP50 *E. coli* for growth of age-synchronized nematodes.

II.3 (C) C. elegans *Infection with Mycobacterial Cultures and Recovery*

Bacterial cultures were grown until they reached stationary phase of growth. 70 µl of *E. coli*, *M. smegmatis* or *M. marinum* were seeded on small tissue culture dishes (35x10 mm, Falcon), with NGM agar by spreading the bacterial cultures to cover $3/4^{th}$ of the infection plates. These seeded infection plates were placed at room temperature overnight to allow bacterial cultures to grow, equilibrate/stabilize and become ready for infection the next day. Three day old age-synchronized adult *C. elegans* were washed with ddH_20 to remove residue *E. coli* and transferred onto plates seeded with *E. coli, M. smegmatis or M. marinum*. Cohorts of *C. elegans* were infected for a period of 4, 24 or 48 hours to each individual bacterial strain. After the period of infection, the nematodes were transferred onto small NGM recovery plates with *E. coli* seeded in the center of each plate. 20 nematodes were incubated on each small recovery NGM plate and cohorts of 60 nematodes were used for each bacterial infection. Nematodes were counted daily and transferred onto fresh *E. coli* seeded plates every other day until experimental nematodes stopped laying eggs. They were then transferred every 3-4 days to avoid overgrowth of seeded *E. coli* until the nematodes reached senescence and died. The nematodes were considered dead if they were unresponsive to touch by the picker. Each bacterial infection experiment was repeated at least three times with 20, 40 or 60

nematodes, unless stated otherwise. *C. elegans* were incubated at room temperature (19ºC to 21ºC) for all experiments.

II.3 (D) Survival, Bagging and Morphological Characterization of C. elegans

C. elegans L1 larvae incubated on *E. coli* seeded NGM plates after synchronization were considered 0 days old. They were grown for three days at room temperature before subjecting them to bacterial infection. On day 4, they were recovered on to fresh *E. coli* seeded NGM plates and followed for survival and changes in morphology. Number of nematodes that died due to bagging of the adult nematode (where embryos hatch within the adult and bring about the death of the adult) on day 5 and 6 were counted. Nematodes that lost their dark pigmentation after bacterial infection were characterized as depigmented. Nematodes that were less than 2/3rd the length of a healthy nematode were characterized as having a shortened length. On day 6, depigmented and shorter nematodes were counted. Nematodes that died prior to 15 days were considered to have a shortened lifespan.

II.3 (E) Imaging of C. elegans *for Morphological Differences and Fluorescent Mycobacteria*

TP12 [*kaIs12*(col-19::GFP)] *C. elegans* expressing cuticular eGFP under the control of *col-19*, a member of the collagen superfamily, were infected with ψms23 (*M. smegmatis*::tdTomato) or ψmm91 (*M. marinum*::tdTomato). Infected *C. elegans* were mounted on a 3% agar pad with a thickness of ~ 1 mm. 15 µl of 5mM levamisole was added to immobilize the nematodes and keep the agar pad moist for imaging. 25mm round cover slips with a thickness of 0.17mm (#1.5) were placed on the agar pad to keep

C. elegans in place and allow imaging. Using a confocal microscope (Nikon A1R+/A1+) infected nematodes were imaged under differential interface contrast (DIC), and fluorescent filters (GFP and tdTomato) using a 10x objective. The nematodes were imaged at 4, 12, 18, 24 hours during infection, and 6, 24 hours post infection. 60 nematodes for each bacterial infection and time point were imaged. DIC images were used to identify patterns of morphological changes in cohorts nematodes with different bacterial infected. Morphological changes in *M. smegmatis* and *M. marinum* infected nematodes were compared to that of *E. coli* infected nematodes. Fluorescent imaging using GFP and tdTomato filters were used to identify the spread and colonization of *M. marinum* and *M. smegmatis* within *C. elegans* gut. The 60 nematodes imaged for each time point were randomly divided into three groups and mycobacterial fluorescent signals were visually quantified. Each nematode was arbitrarily divided in three segments (upper, middle, lower) and fluorescent bacteria were quantified in each segment.

II.3 (F) CFU Assays for Mycobacterial Load and Colonization of C. elegans

At 4, 12 and 24 hours during infection and 6 hours post-infection, 30 *C. elegans* were infected with wild-type *M. marinum* or wild-type *M. smegmatis* and transferred to 500 µl of M9 buffer with 0.05% Tween-20 in 1.5 ml microcentrifuge tubes. After briefly vortexing, they were spun down at 800 rpm for 15s and the supernatant was removed. These nematodes were washed 3x with 500ul of 1x PBS with 0.05% Tween-20 and resuspended in 600 µl of 1x PBS with 0.05% Tween-20; 100 µl of this suspension was plated to determine background levels of bacteria in serial dilutions. The 20

nematodes in each in 500 µl of 1x PBS with 0.05% Tween-20 were homogenized with a hand held motorized pestle for a total of 45s. After the nematodes were broken up releasing, the bacteria from their gut, they were vortexed on high and plated for CFU in serial dilutions. 20 µl spot plating was used in triplicate for each of the dilutions used. *M. smegmatis* was grown at 37°C and *M. marinum* was grown at 32°C.

II.3 (G) High-Resolution Confocal Imaging of C. elegans

Using a confocal microscope (Nikon A1R+/A1+) with spectral capability, 25 emission channels with a resolution of 6.0 nm were use to detect wavelengths of 500 to 640 nm. This wavelength range allowed detection of GFP (500-520 nm) and tdTomato (560-620 nm). Using a 40x oil immersion objective, TP12 nematodes infected with *E. coli* (OP50), ψms23 (*M. smegmatis*::tdTomato) or ψmm91 (*M. marinum*::tdTomato) were imaged during infection (4 and 24 hours) and post-infection (30 hours). The nematodes were immobilized with 15 µl of levamisole (5 mM) and the head (pharyngeal pump), mid-gut regions and lower-gut regions were imaged. About 15 nematodes were imaged at each time point for each infection with ψms23 and ψmm91 and about 5 nematodes were imaged for each time point that were infected with *E. coli*. Representative images are presented to evaluate differences in bacterial colonization and morphological changes in nematodes from each infection group.

II.3 (H) Transmission Electron Microscopy Imaging of C. elegans

C. elegans infected with bacteria were fixed, embedded, sectioned and imaged using previously described methods with slight modifications (Hall et al., 2012). At 4 and 24 hours during infection and 6 hours post-infection 20-30 *C. elegans* from each

group (*E. coli*, *M. smegmatis* and *M. marinum*) were obtained and washed two times with 500 µl of 1x M9 buffer. The nematodes were then immersed in a fixative solution with 2.5% glutaraldehyde, 2% paraformaldehyde and 0.1% (w/v) malachite green in a working buffer (0.1 HEPES, pH 7.4, containing 2 mM MgCl2). Using a PELCO BioWave® microwave the nematodes in the fixative solution were microwaved under vacuum at 100W for 10 mins and let stand for 3 mins. This microwave procedure was repeated and the specimens were placed at room temperature for 1 hour, followed by microwaving at 500W for 10s, pausing for 20 seconds and then microwaving for 10s. The nematodes were washed three times with 500 µl working buffer, followed by microwaving them for 1 minute after each wash. To improve contrast, the nematodes were post-fixed in 1% (w/v) osmium tetroxide with 1.5% (w/v) potassium ferricyanide in working buffer. They were microwaved at 100W for 2 minutes, followed by letting them stand for 2 minutes. This was repeated 4 times. The specimens were dehydrated by rinsing the samples with 50% acetone, 70% acetone, 90% acetone, and three times with 100% acetone. After each rinse, the specimens were microwaved at 150W for 1 minute. The specimens were then infiltrated with resin, Quetol 651-modified Spurr low viscosity epoxy resin, using 1:1 acetone:resin followed by 100% resin three times. They were microwaved at 200W for 4 minutes between each infiltration step. The specimens were transferred into embedding tubes and the resin was allowed to polymerize overnight at 60°C. Longitudinal sections were obtained from the embedded specimens and a JEOL 1200EX transmission electron microscope at an accelerated voltage of 100kV was used to image them.

II.3 (I) Macrophage Infection Mutant (MIM) M. marinum *Infection*

Previously described *M. marinum* mutants, *mimA-K, nrp, ppe24, sdhD, pks12, fadD29, fadD30* and *ppe53* were used for *C. elegans* infection to determine their extent of attenuation in (Mehta et al., 2006). We infected 3 day old adult N2 nematodes with these mutants for a period of 24 hours. Mutant strain cultures were grown until they were in stationary phase of growth (OD >1.2) and 70 µl of each were seeded on small NGM plates the day prior to infection as described above. Triplicates of 20 N2 worms (total of 60) were infected with each strain of *M. marinum*. After infection they were recovered and mortality rates were assessed at two days post infection (day 6). Three strains that displayed significant attenuation, mimA, mimG and mimI were complementation with the appropriate *Mtb* gene, mimA::Rv0246, mimG::Rv3242c and mimI::Rv1502 (Mehta et al., 2006). To confirm attenuation of *M. marinum* mutants in *C. elegans*, three strains complemented with their *Mtb* orthologs were infected into *C. elegans* and mortality rates were at compared two days post-infection (day 6). These experiments were performed at least twice to ensure reproducaibility.

II.3 (J) Statistical Analyses

Parametric two-tailed unpaired t-test statistical analyses were used to compare the means of different bacterial infection groups at distinct time points using GraphPad Prism software. Means, standard deviations and standard errors were calculated using GraphPad Prism software and Microsoft Excel spreadsheets. A non-parametric log-rank statistical method was used to determine the difference in survival for groups of *C. elegans* after infection, using an online application for survival analysis of lifespan assays found on http://sbi.postech.ac.kr/oasis (released on May 2009; last accessed on March 20th 2014) (Yang et al., 2011).

II.4 Results

II.4 (A) Pathogenic Mycobacteria Cause Mortality in C. elegans

Since infection of *C. elegans* by mycobacteria has not been previously documented, we investigated whether different mycobacterial species can infect and cause disease in these nematodes. We infected *C. elegans* with *E. coli*, *M. smegmatis*, a non-pathogenic mycobacterial species and *M. marinum*, pathogenic mycobacteria that prefer growth at temperatures similar to those preferred by nematodes. *C. elegans* were infected with *E. coli*, *M. smegmatis* or *M. marinum* for 4, 24 or 48 h (Figure 1A-D). At 24 and 48 h, nematodes infected with *M. marinum* had a significantly higher mortality rate when compared to those infected with *M. smegmatis* or *E. coli* (Figure 1C-D), but *M. smegmatis* displayed similar mortality rates to *E. coli* at all time points. Two days post-infection with *M. marinum* for 24 h, *C. elegans* display over 80% mortality,

whereas, when infected with *M. smegmatis*, they display <15% mortality (Figure 1C). The majority of nematode deaths occur due to an event seen under unfavorable conditions for *C. elegans*, described as bagging, where the gravid adult nematode is unable to lay eggs and egg hatching (viviparity) occurs within the worm, resulting in the death of the adult, but allowing survival of the progeny (Chen and Caswell-Chen, 2004; Seidel and Kimble, 2011). Consistent with these observations, bagging has been previously observed as a *C. elegans* response to bacterial infection (Mosser et al., 2011). Interestingly, even the <20% of surviving nematodes after *M. marinum* infection displayed morphological changes, including loss of pigmentation and shortening (Figure 2). Prolonged infection with *M. marinum* progressively increased the rate and total number of mortalities observed in *C. elegans*, but infection with *M. smegmatis* did not impact mortality in this manner, demonstrating that the mechanisms involved are specific to the pathogenic species. Overall, these observations suggest that mycobacterial virulence mechanisms play a role in *C. elegans* pathogenesis and these nematodes can be used as a novel virulence model for analysis of the molecular determinants involved in both the pathogen and host.

Figure 1. *C. elegans* Infected with *M. marinum* have a Higher Mortality Rate Compared to *M. smegmatis* or *E. coli*. (A) Experimental plan for the infection of *C. elegans* to *E. coli* (OP50), *M. smegmatis (Ms)* and *M. marinum (Mm)*. (B-D) 60 adult N2 (wild-type) nematodes each were infected with experimental bacterial strains for 4, 24 or 48 hours on day 3 as indicated by the area of the grey shaded region above. After recovering onto NGM plates seeded with OP50 nematode survival was measured. The long-rank method was used to compare survival of each infection group. *C. elegans* infected with *M. marinum* for 24 hours or more display a significantly higher rate of mortality as compared to *E. coli* or *M. smegmatis* infection. (B) Survival of N2 nematodes after 4 hours of infection. *Mm* and *Ms* Chi^2 statistic of 3.63 ($p = 0.0567$); *Mm* and *E. coli* Chi^2 statistic of 6.72 ($p = 0.0095$); *Ms* and *E. coli* Chi^2 statistic of 0.78 ($p = 0.3776$). (C) Survival of N2 nematodes after 24 hours of infection. *Mm* and *E. coli* Chi^2 statistic of 78.74 ($p < 0.0001$); *Ms* and *E. coli* Chi^2 statistic of 1.50 ($p = 0.2207$); *Mm* and *Ms* Chi^2 statistic of 57.19 ($p < 0.0001$). (D) Survival of N2 after 48 hours of infection. *Mm* and *Ms* Chi^2 statistic of 96.34 ($p < 0.0001$); *Mm* and *E. coli* Chi^2 statistic of 119.90 ($p < 0.0001$); *Ms* and *E. coli* Chi^2 statistic of 3.17 ($p = 0.0750$).

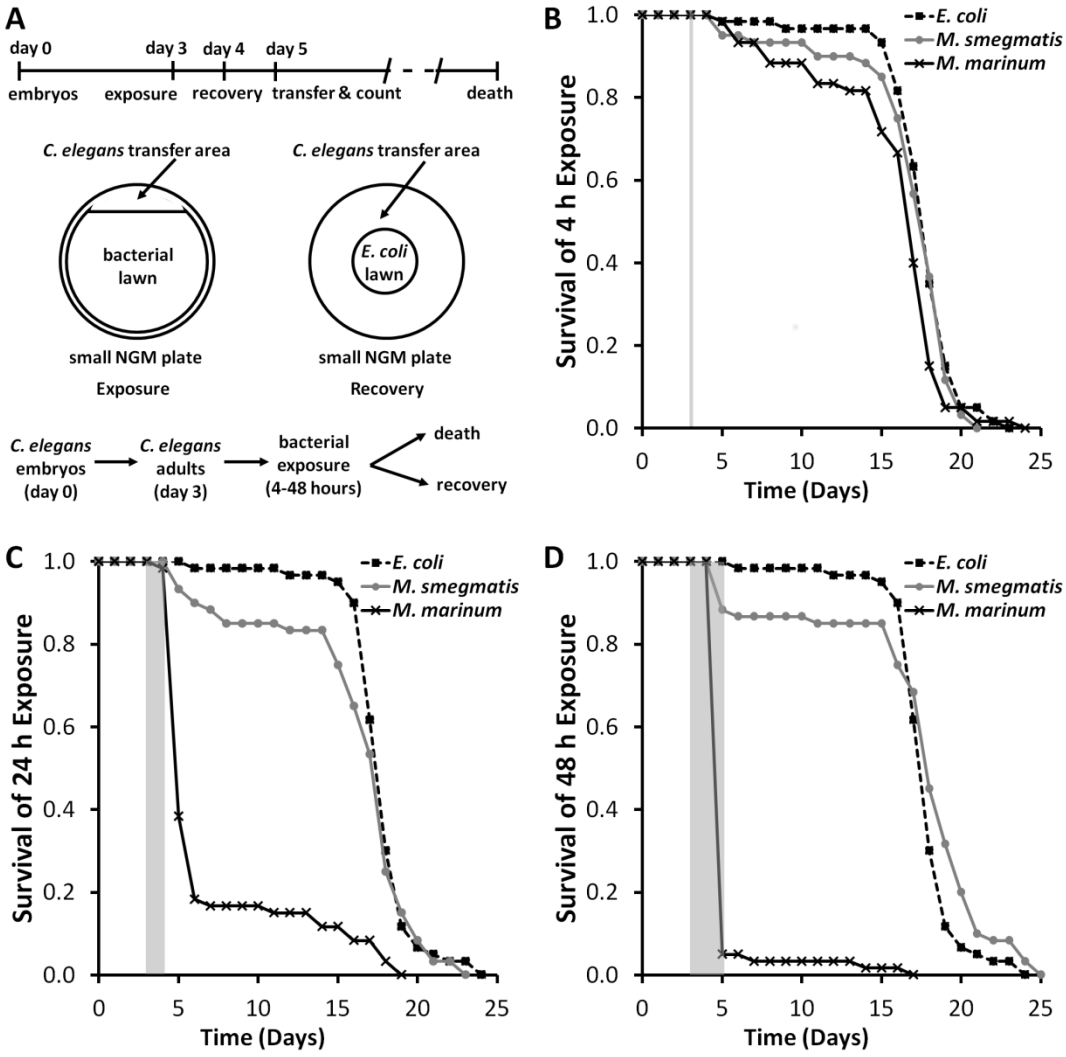
A
day 0
day 3
day 4
day 5
embryos
exposure
recovery
transfer & count
death
C. elegans transfer area
bacterial lawn
small NGM plate
Exposure
C. elegans transfer area
E. coli lawn
small NGM plate
Recovery
C. elegans embryos (day 0)
C. elegans adults (day 3)
bacterial exposure (4-48 hours)
death
recovery
B
Survival of 4 h Exposure
Time (Days)
E. coli
M. smegmatis
M. marinum
C
Survival of 24 h Exposure
Time (Days)
E. coli
M. smegmatis
M. marinum
D
Survival of 48 h Exposure
Time (Days)
E. coli
M. smegmatis
M. marinum

Figure 2. Morphological Changes in Wild-type (N2) *C. elegans* Infected with Bacteria. (A-D) 3 trials of 20 adult N2 nematodes each (total n = 60) were infected with *E. coli* (OP50), *M. smegmatis* (MC^2155) or *M. marinum* (ψmm1) for 24 hours, and physiological and morphological changes were characterized. P-values are shown comparing *E. coli* infection to *M. smegmatis* infection and *M. smegmatis* infection to *M. marinum* infection (unpaired t-test). (A) Mean (±SEM) number of nematodes that died 11 days post-infection (day 15), characterized as having a shortened lifespan. (B) Mean (±SEM) number of nematodes that bagged and died 2 days post-infection (day 6). (C-D) For each trial, percent depigmentation and shortened length were characterized for the remaining nematodes after initial mortality due to bacterial infection. (C) Mean (±SEM) number of nematodes with a loss of pigmentation at 2 days post-infection (day 6) was determined by a visible reduction in cuticular pigmentation are reported. (D) Mean (±SEM) number of nematodes with a length of less than $2/3^{rd}$ the lengths of a healthy adult nematode at 2 days post-infection are reported (day 6).

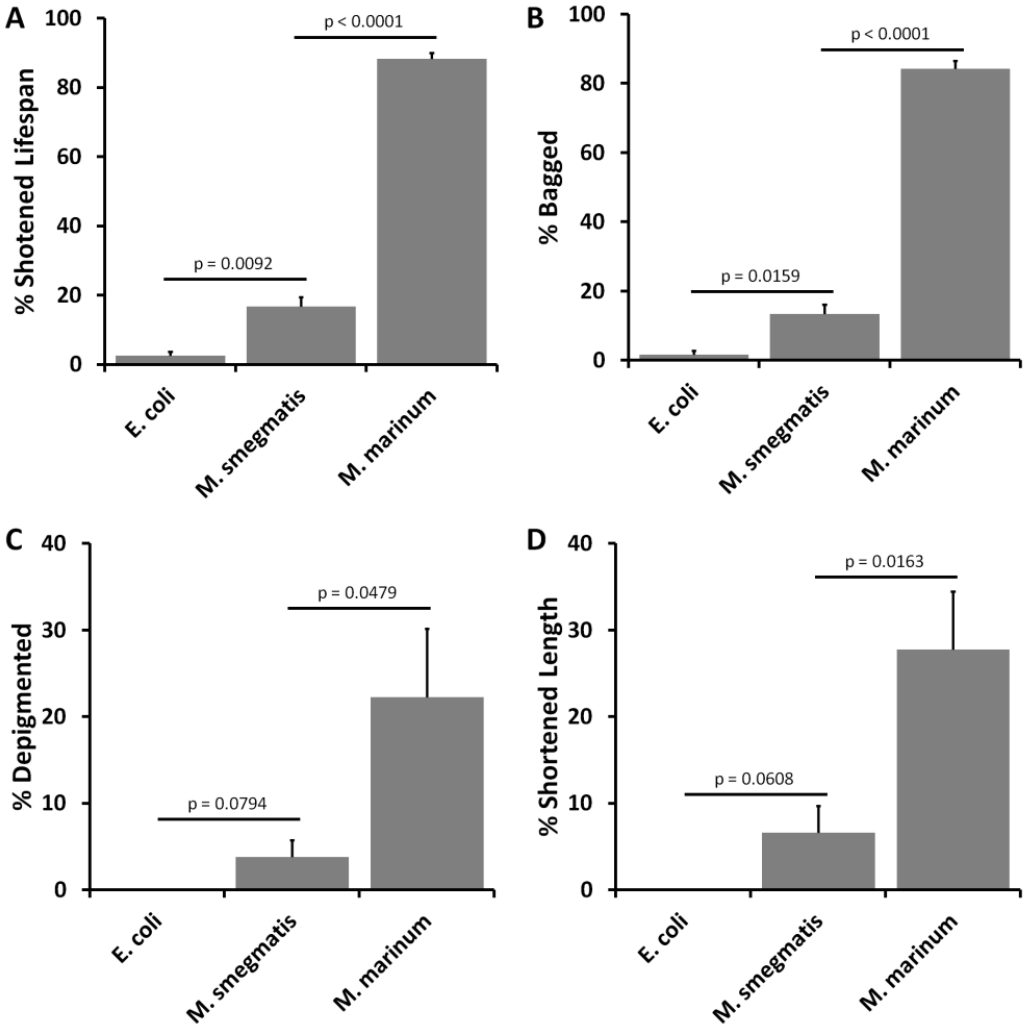
A
% Shotened Lifespan
100
80
60
40
20
0
p < 0.0001
p = 0.0092
E. coli
M. smegmatis
M. marinum
B
% Bagged
p < 0.0001
p = 0.0159
C
% Depigmented
40
30
20
10
0
p = 0.0479
p = 0.0794
D
% Shortened Length
p = 0.0163
p = 0.0608

II.4 (B) M. marinum *Cause Irreversible Morphological Changes in* C. elegans

In order to understand the process of mycobacterial pathogenesis in *C. elegans* during the 24 h infection with *M. marinum* and 24 h afterward (48 h total), nematodes were imaged by differential interference contrast (DIC) microscopy. Nematodes infected with both *M. marinum* and *M. smegmatis* displayed reduced pigmentation, disruptions in cellular arrangement and increased retention of embryos within gravid nematodes as compared to those infected with *E. coli*, the standard food source for *C. elegans* (Figure 3 and 4). During the 24 h infection period *E. coli* infected nematodes were healthy, did not lose their pigmentation and were able to lay eggs (Figure 3A-D and 4A-B). Interestingly, during the 24 h infection with *M. smegmatis*, although most nematodes lost pigmentation they regained pigmentation, cellular arrangement and were able to lay eggs by 6 h post-infection, demonstrating that the *M. smegmatis* induced morphological changes are reversible (Figure 3E-H and 4C-D). In contrast, nematodes infected with *M. marinum* experience irreversible morphological changes and are unable to lay eggs up to 24 h post-infection and, since only a few *C. elegans* remain, it was not be feasible to follow them further (Figure 3I-L and 4E-F). Over 80% of these nematodes died via bagging observed 24 hours post-infection (Figure 3L and 4F). Our results suggest that, while both *M. marinum* and *M. smegmatis* induce pathological changes in *C. elegans*, the immune response is able to defend the nematode from permanent damage due to *M. smegmatis*, but is ineffective at protecting nematodes from *M. marinum* infection. *M. marinum* causes permanent pathological changes or mortality, reminiscent of infections by pathogenic and non-pathogenic mycobacterial species in mammals.

Figure 3. TP12 *C. elegans* Infected with *M. marinum* Display Irreversible Morphological Changes. Differential interference contrast (DIC) Images of TP12 (*col-19*::GFP) nematodes infected with *E. coli* (OP50), *M. smegmatis* (ψms23) or *M. marinum* (ψmm91) for 24 hours and recovered on *E. coli* (OP50) seeded plates post-infection, display morphological changes. (A-D) *E. coli* infected nematodes are able to lay eggs and retain their dark pigmentation. (E-H) *M. smegmatis* infected nematodes experience a reversible retention of eggs and loss of pigmentation during infection, but regain their pigmentation and ability to lay eggs post-infection. (I-L) *M. marinum* infected nematodes experience an irreversible retention of eggs and loss of pigmentation during infection and are unable to recover post-infection. The majority of these nematodes undergo bagging, leading to death of the adult nematode. (K) *M. marinum* infected nematodes display egg retention and loss of pigmentation 6 hours post-infection. (L) The arrow points to an example of the "Bag of nematodes" event that occurs when embryos are hatched in utero of gravid nematodes.

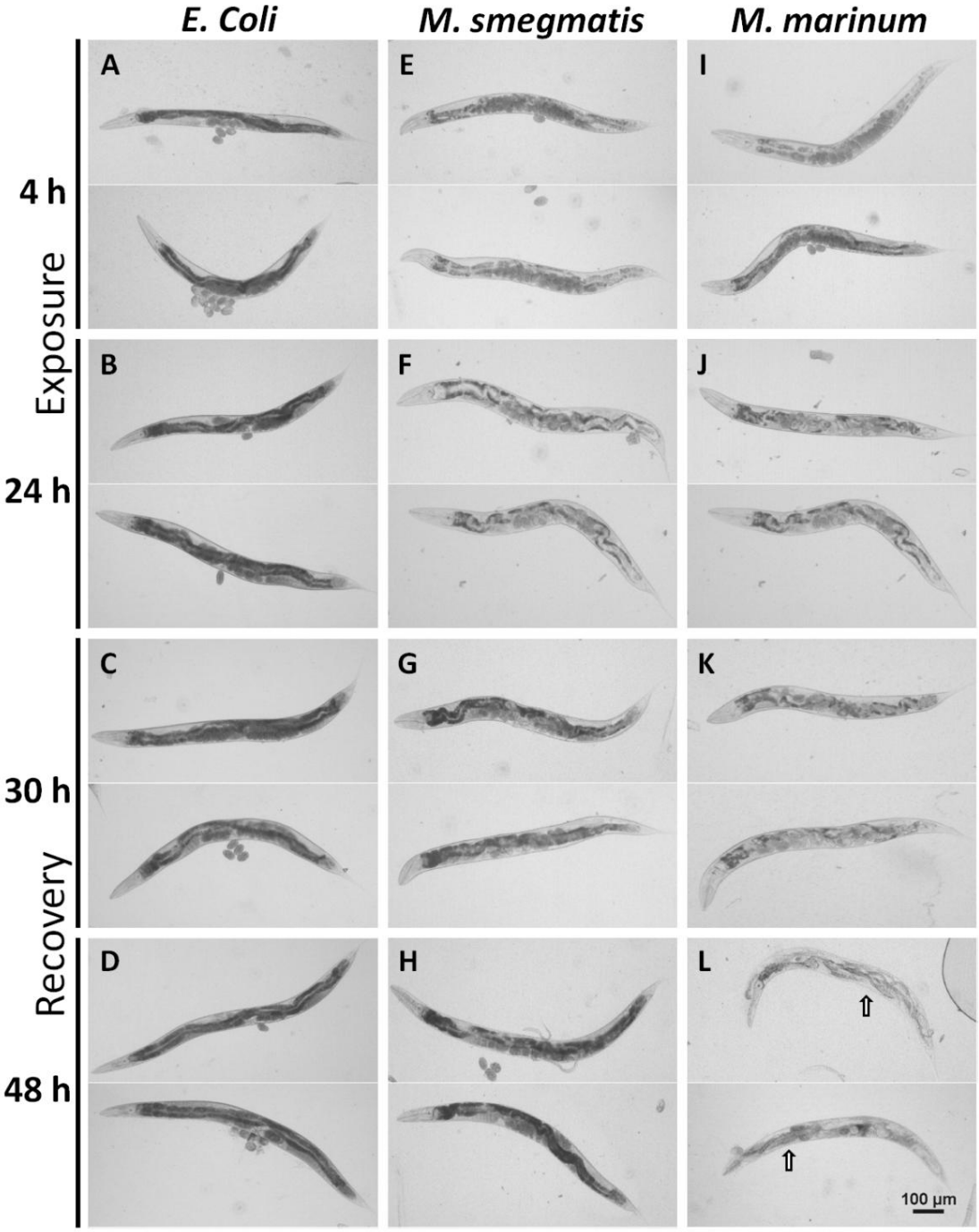
E. Coli
M. smegmatis
M. marinum
A
E
I
4 h
Exposure
B
F
J
24 h
C
G
K
30 h
Recovery
D
H
L
48 h
100 µm

Figure 4. N2 *C. elegans* Infected with *M. marinum* Display The Same Irreversible Morphological Changes. Differential interference contrast (DIC) Images of N2 (wild-type) nematodes infected with *E. coli* (OP50), *M. smegmatis* (MC^2155) or *M. marinum* (ψmm1) for 24 hours and recovered on *E. coli* (OP50) seeded plates post-infection display morphological changes. (A-B) *E. coli* infected nematodes are able to lay eggs and retain their dark pigmentation. (C-D) *M. smegmatis* infected nematodes experience a reversible retention of eggs and loss of pigmentation during infection, but regain their pigmentation and ability to lay eggs post-infection. (E-F) *M. marinum* infected nematodes experience an irreversible retention of eggs and loss of pigmentation during infection and are unable to recover post-infection. The majority of these nematodes undergo bagging, leading to death of the adult nematode. (E) *M. marinum* infected nematodes displaying a high rate of egg retention and loss of pigmentation at 24 hours of infection. (F) The arrow points to an example of the "Bag of nematodes" event that occurs when embryos are hatched in utero of gravid nematodes.

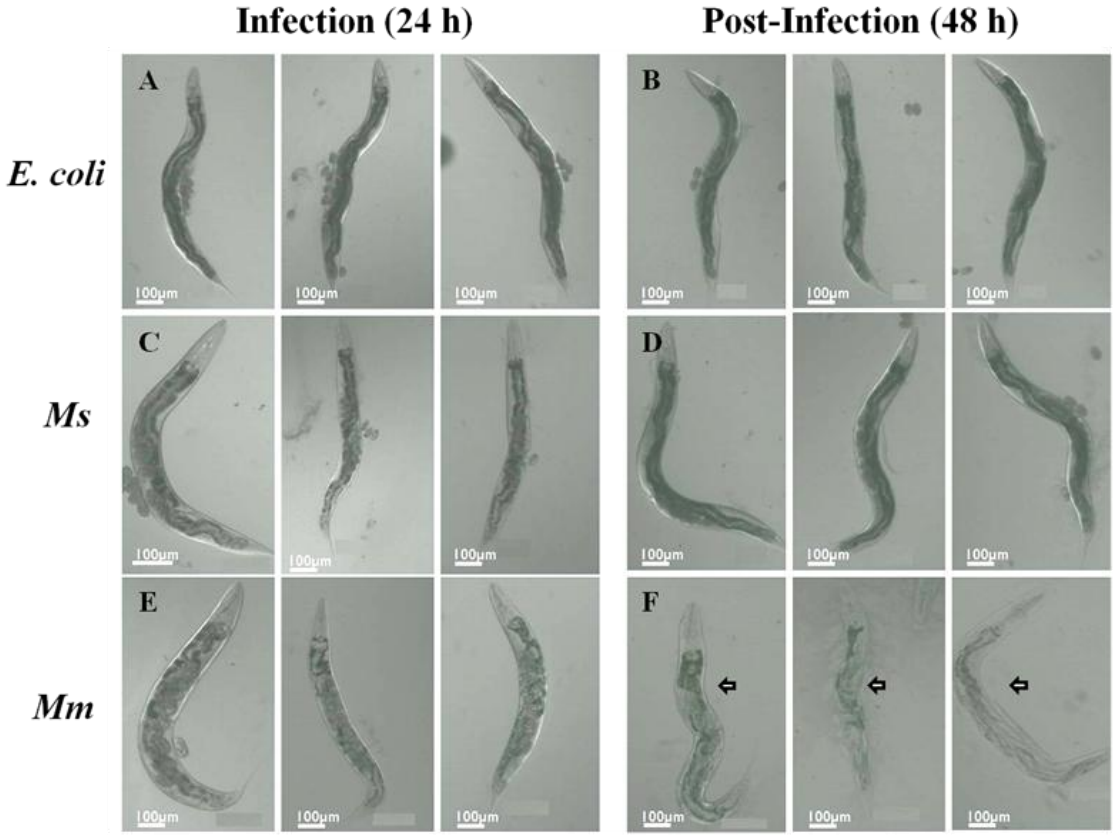

Bagging (⇦) – "Bag of worms" occur when embryos are retained in utero as an adult stress response to unfavorable environmental conditions.

Figure 5. TP12 *C. elegans* Infected with *M. marinum* Have a Higher Mortality Rate As Compared to *M. smegmatis* or *E. coli*. 60 adult TP12 nematodes were infected with *E. coli* (OP50), *M. smegmatis* (ψms23) or *M. marinum* (ψmm91) for 24 hours on day 3 as indicated by the area of the grey shaded region above. After recovering onto NGM plates seeded with OP50 nematode survival was measured. Survival of TP12 worms is similar to that of N2 worms infected with bacteria. The long-rank method was used to compare survival of each infection group. *M. marinum* (*Mm)* and *M. smegmatis (Ms)* Chi^2 statistic of 54.28 ($p < 0.0001$); *Mm* and *E. coli* Chi^2 statistic of 57.71 ($p < 0.0001$); *Ms* and *E. coli* Chi^2 statistic of 1.52 ($p = 0.2181$).

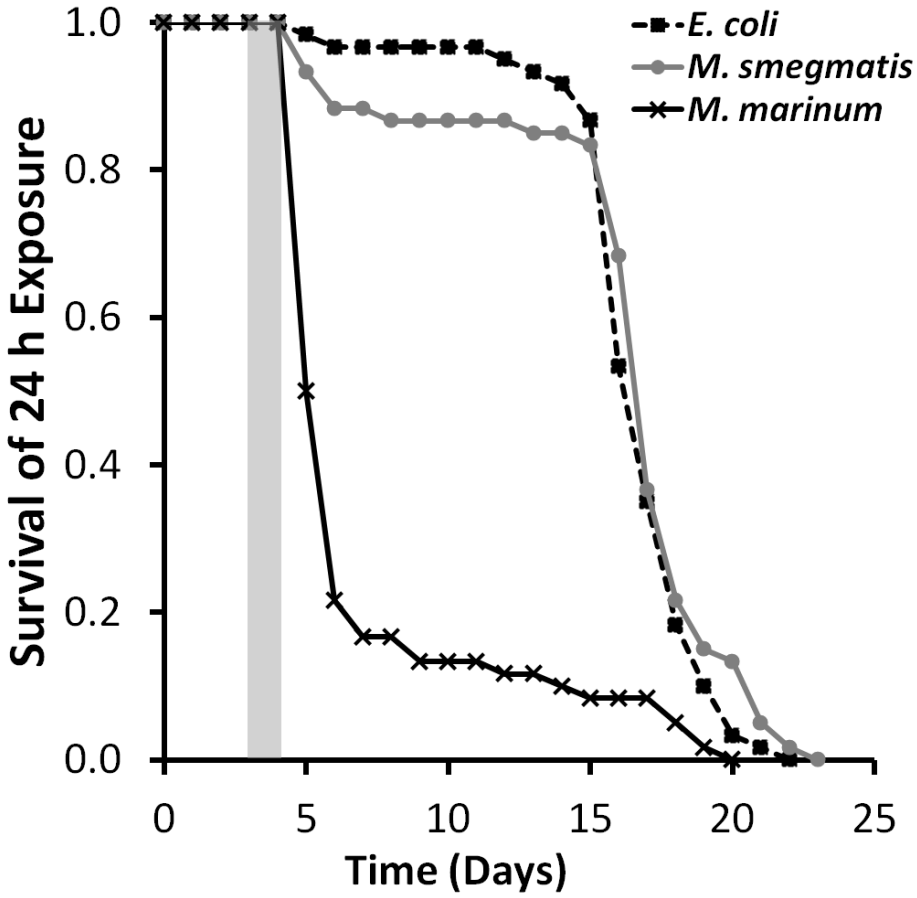

Figure 6. Morphological Changes in TP12 *C. elegans* Infected with Bacteria. (A-D) 3 trials of 20 adult TP12 nematodes (total n = 60) were infected with *E. coli* (OP50), *M. smegmatis* (MC^2155) or *M. marinum* (ψmm1) for 24 hours, and morphological changes were characterized. P-values are shown comparing *E. coli* infection to *M. smegmatis* infection and *M. smegmatis* infection to *M. marinum* infection (unpaired t-test). (A) Mean (±SEM) number of nematodes that died 11 days post-infection (day 15), characterized as having a shortened lifespan. (B) Mean (±SEM) number of nematodes that bagged and died 2 days post-infection (day 6). (C-D) For each trial, percent depigmentation and shortened length were determined for the remaining nematodes after initial mortality due to bacterial infection. (C) Mean (±SEM) number of nematodes with a loss of pigmentation 2 days post-infection (day 6), were determined by a visible reduction in cuticular pigmentation are reported. (D) Mean (±SEM) number of nematodes with a length of less than 2/3rd the length of a healthy adult nematode 2 days post-infection (day 6) are reported.

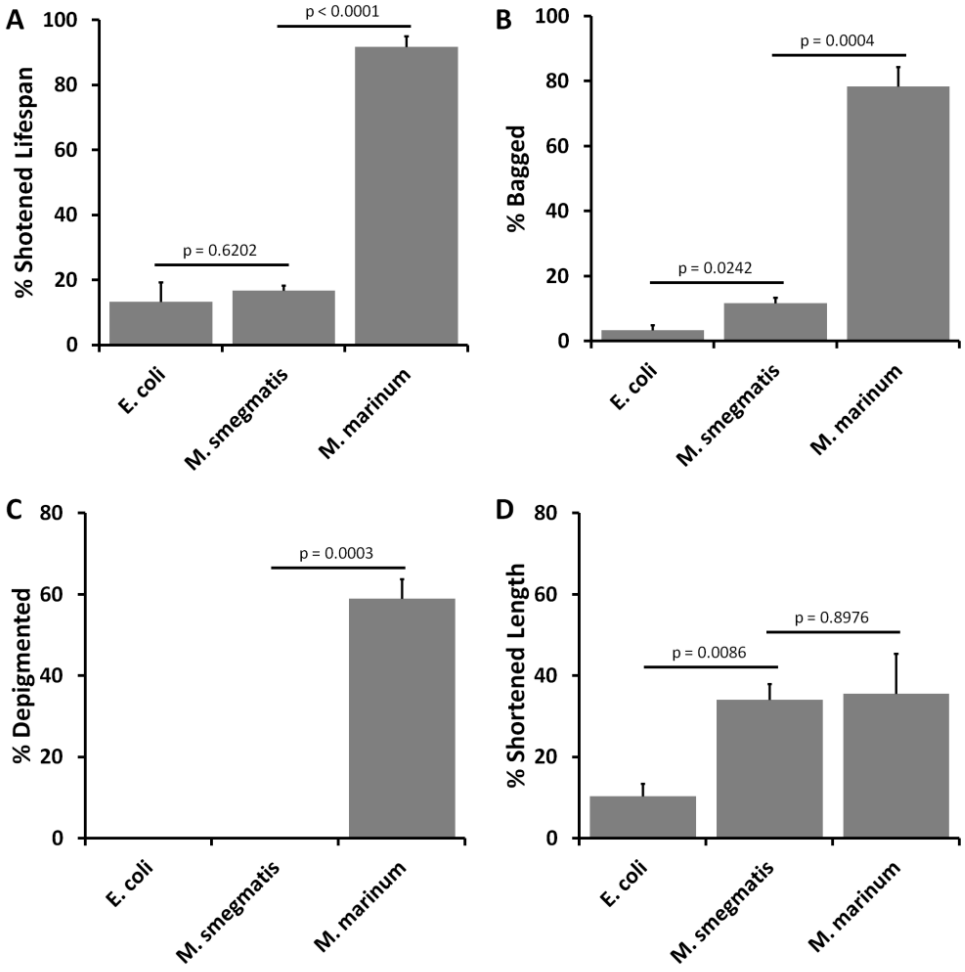

II.4 (C) M. marinum *Colonize* C. elegans *while* M. smegmatis *Does Not*

We infected fluorescent (GFP) *C. elegans* with fluorescently (tdTomato) tagged *M. marinum* and *M. smegmatis* (ψms23) and found that these fluorescently tagged strains produce similar morphological changes and mortalities to those observed with non-tagged *E. coli*, *M. smegmatis* and *M. marinum* (Figure 5 and 6), suggesting that the fluorescent markers themselves do not significantly impact mycobacterial interactions with *C. elegans*. We examined *C. elegans* at 4, 12, 18, 24, 30 and 48 h post-infection for 24 h. Fluorescent *M. marinum* and *M. smegmatis* are found in *C. elegans* as early as 4 hours into infection (Figure 7A, G). At 4 h post-infection >95% of nematodes were colonized by *M. marinum* in what appeared to be the gut; whereas, <30% displayed intact *M. smegmatis* within them (Figure 7 and 8). Apparently, *C. elegans* digests *M. smegmatis* in a similar manner to its food, *E. coli*, but *M. marinum* persists (Figure 8A-C). Quantitative analyses demonstrated that the number of intact *M. smegmatis* present in *C. elegans* was significantly less than *M. marinum* at all time points (Figure 8A-C and 9). We divided nematode images into three segments (upper, middle and lower) and found that the majority of *M. marinum* were within the pharyngeal and lower gut regions. Even at 6 hours post-infection, *M. smegmatis* was barely observable within nematodes (Figure 7E-F and 8A-C), while *M. marinum* persists, primarily within the pharyngeal and tail regions of the nematode (Figure 7K-L and 8A-C).

*W*e imaged infected *C. elegans* at 24 hours post-infection (48 h) and found that >50% of the *C. elegans* carried *M. marinum* (Figure 9A-C), while <5% of *M. smegmatis* infected nematodes had bacteria within them (Figure 9A-C). We confirmed our observations from fluorescent microscopy by plating the nematodes for colony forming units (CFU) at 4, 12, 24, 30 and 48 h post-infection. We consistently observed >2-fold higher levels of *M. marinum* CFU in *C. elegans* as compared *M. smegmatis* (Figure 8D). Since these experiments were carried out with fluorescently labeled bacteria, we confirmed these observations using unlabeled organisms and obtained nearly identical results, demonstrating that fluorescent protein expression is not responsible for the differences in phenotype between *M. smegmatis* and *M. marinum* (Figure 10). There was a dramatic decrease in *M. smegmatis* within nematodes as early as 6 h post-infection; whereas, *M. marinum* only modestly decreased by 6 h and persists even out beyond 24 h post-infection (Figure 8D and 10). Taken together, these data demonstrate that *M. marinum* colonizes and survives within *C. elegans* much better than *M. smegmatis*.

Figure 7. ***M. marinum*** **Accumulates Within** ***C. elegans*** **During Infection and Remains Within the Nematode Post-Infection.** TP12 (*col-19*::GFP) nematodes infected with ψmm91 and ψms23 were imaged at 4, 12, 18, 24, 30 and 48 hours during and post-infection. While *M. marinum* and *M. smegmatis* are both visible within infected nematodes, there is a significantly higher accumulation of *M. marinum* (G-L) as compared to nematodes infected with *M. smegmatis* (A-F). After infection, *M. smegmatis* is virtually absent from the nematodes (E-F), while *M. marinum* persists (K-L). *M. marinum* appears to mostly accumulate in the head (pharyngeal) and tail (lower gut) regions of infected nematodes.

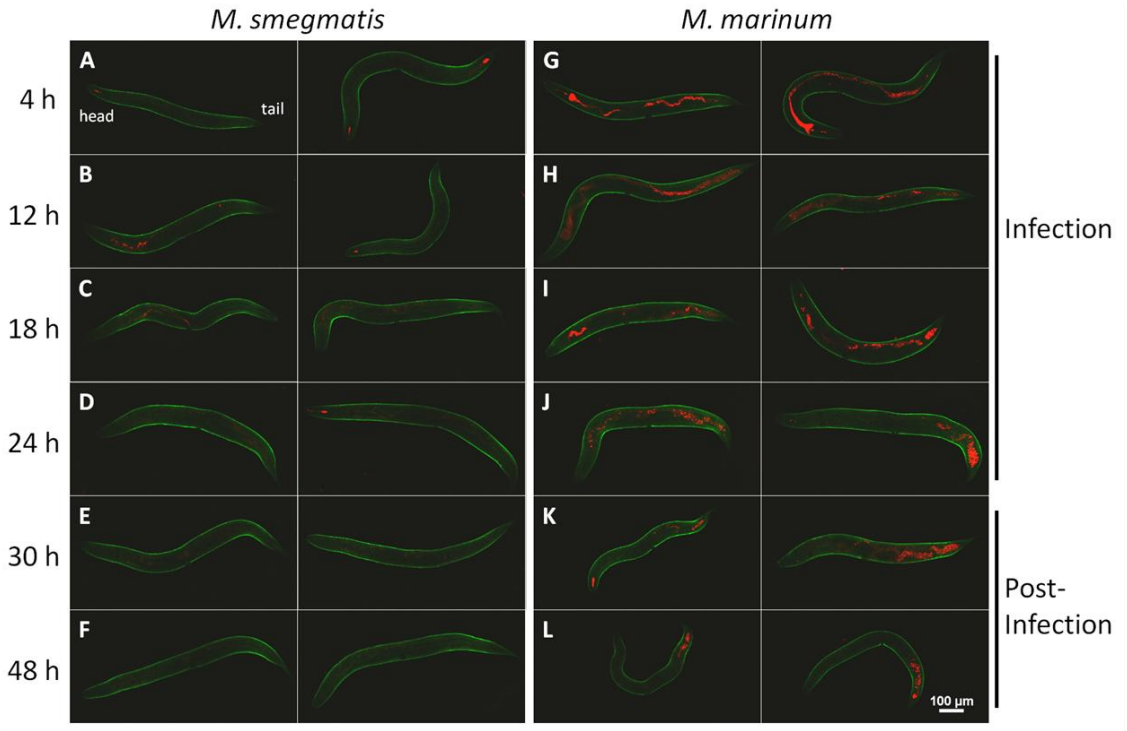

Figure 8. *M. marinum* is Better Able to Colonize Infected *C. elegans* Than *M. smegmatis.* TP12 nematodes infected with either *M. smegmatis* (ψms23) or *M. marinum* (ψmm91) for 24 hours were imaged and quantified at 4, 12, 18 and 24 hours during and post-infection (30 h and 48 h). 60 nematodes for each infection were quantified at each time point. They were randomly split into three groups of 20 for quantification. Each nematode was evaluated as three separate regions: upper, middle and lower. At each time point during and post-infection, significantly higher levels of *M. marinum* are present as compared to *M. smegmatis*. P-values between *M. smegmatis* and *M. marinum* at each time point are indicated (unpaired t-test). (A-C) Quantification of bacterial clusters in the upper, middle and lower regions of infected nematodes. *M. marinum* infected nematodes displayed significantly higher bacterial loads at each time point during and post-infection. (A) *C. elegans* with at least one cluster of mycobacteria in the upper, middle or lower segment of the nematode. (B) *C. elegans* with 4 or more clusters of mycobacteria in the upper, middle or lower segment of the nematode. (C) *C. elegans* with 11 or more clusters of mycobacteria in the upper, middle or lower segment of the nematode. (D) Colony forming units (CFU) of mycobacteria recovered from homogenized *C. elegans*. 20 to 30 nematodes homogenized using a hand-held motorized pestle at 4, 12, 24, 30 and 48 hours were plated. Nematodes at 4, 12 and 24 hours indicate the times during infection, while nematodes at 30 and 48 hours indicate the times 6 and 24 hours post-infection. *M. marinum* colonization of *C. elegans* was significantly higher than that by *M. smegmatis*. *M. smegmatis* was essentially cleared post-infection while *M. marinum* colonized the nematodes well.

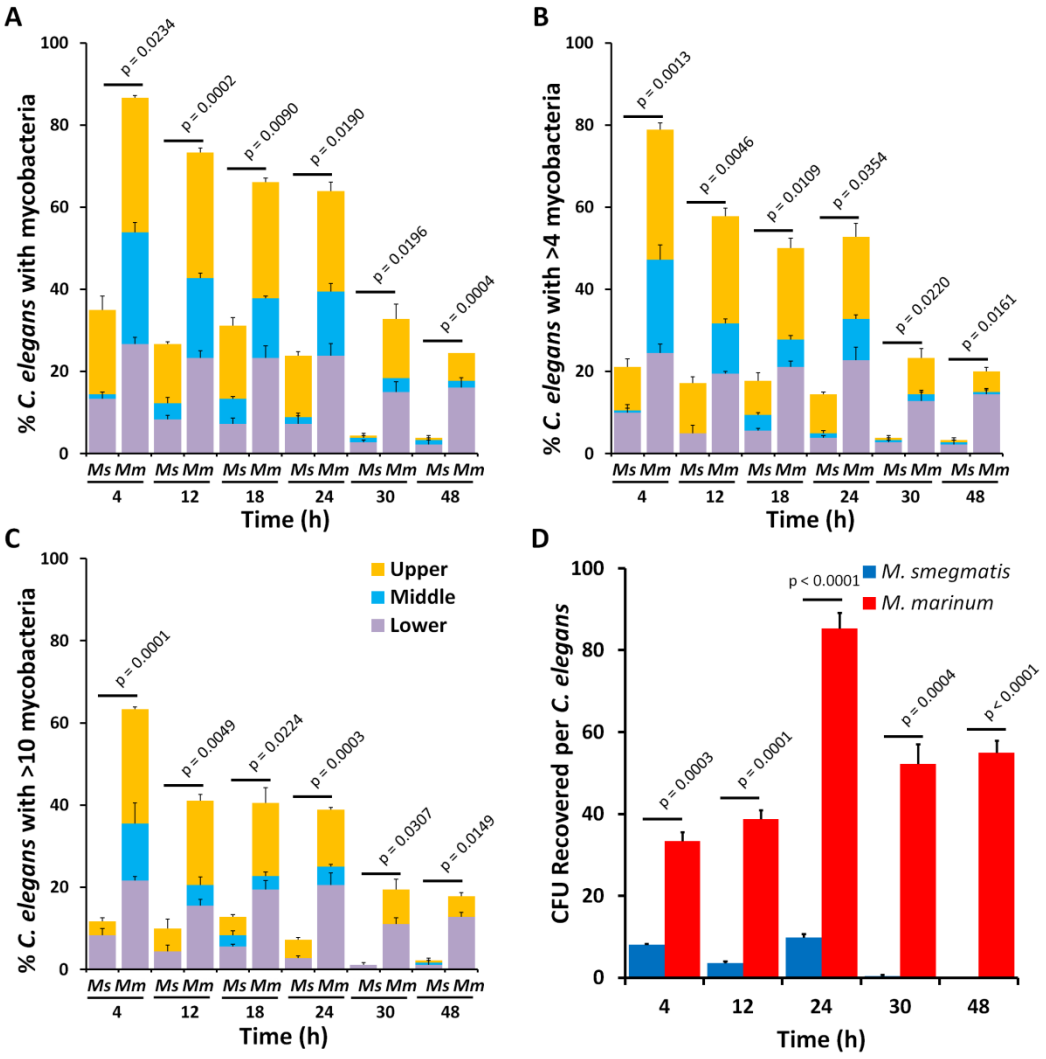
A
% C. elegans with mycobacteria
p = 0.0234
p = 0.0002
p = 0.0090
p = 0.0190
p = 0.0196
p = 0.0004
Ms Mm
4
12
18
24
30
48
Time (h)
B
% C. elegans with >4 mycobacteria
p = 0.0013
p = 0.0046
p = 0.0109
p = 0.0354
p = 0.0220
p = 0.0161
Time (h)
C
% C. elegans with >10 mycobacteria
Upper
Middle
Lower
p = 0.0001
p = 0.0049
p = 0.0224
p = 0.0003
p = 0.0307
p = 0.0149
Time (h)
D
CFU Recovered per C. elegans
M. smegmatis
M. marinum
p < 0.0001
p = 0.0003
p = 0.0001
p = 0.0004
p < 0.0001
Time (h)

Figure 9. Quantification of Bacterial Load Within *C. elegans*. TP12 nematodes infected with either *M. smegmatis* (ψms23) or *M. marinum* (ψmm91) for 24 hours were imaged and quantified at 4, 12, 18 and 24 hours during infection and post-infection (30 h and 48 h). 60 nematodes for each infection were quantified at each time point. They were randomly split into three groups of 20 each and quantified. Each nematode was characterized in three different regions: upper, middle and lower (figure 4). Quantification of bacterial load in the entire worm (A-C) and lower-segment of the worm (D-F) are compared to evaluate differences in localization. At each time point during and post-infection, significantly higher levels or *M. marinum* are present in nematodes as compared to *M. smegmatis*. P-values between *M. smegmatis* and *M. marinum* at each time point are provided (unpaired t-test). (A) Percent *C. elegans* with at least one fluorescent bacterial cluster within the nematode. (B) Percent *C. elegans* with 4 or more fluorescent bacterial clusters within the nematode. (C) Percent *C. elegans* with 11 or more fluorescent bacterial clusters within the nematode. (D) Percent *C. elegans* with at least one fluorescent bacterial cluster in the lower segment of the nematode. (E) Percent *C. elegans* with 4 or more fluorescent bacterial clusters in the lower segment of the nematode. (F) Percent *C. elegans* with 11 or more fluorescent bacterial clusters in the lower segment of the nematode.

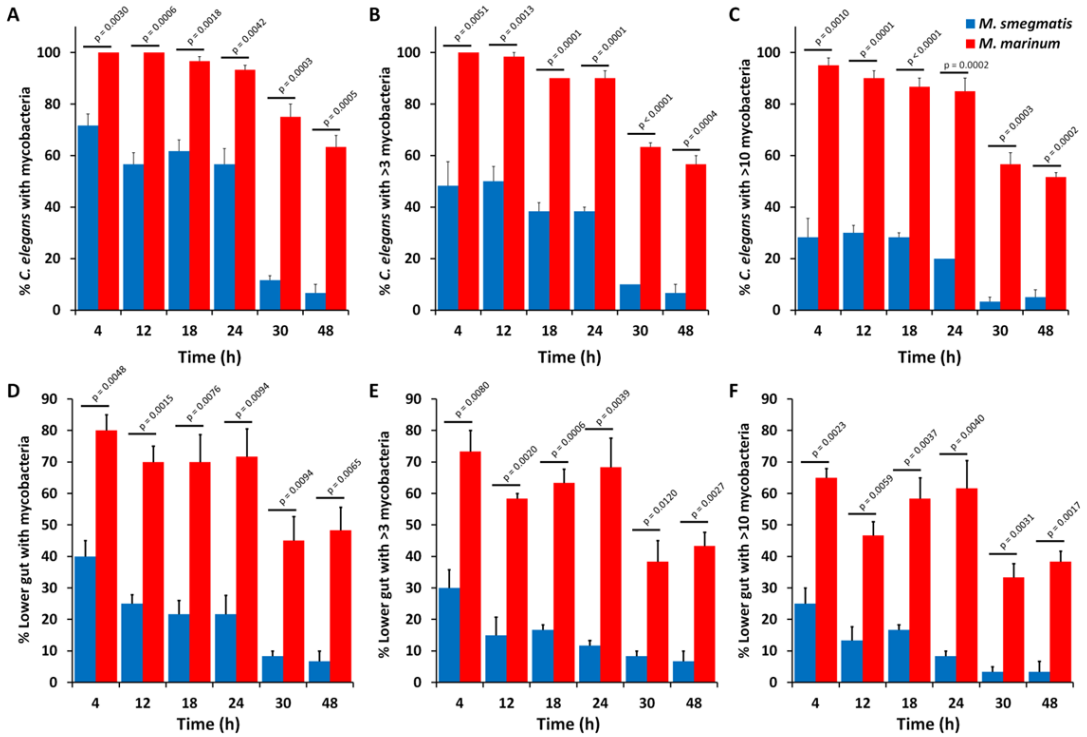

Figure 10. Bacterial Load in *C. elegans* (N2) Determined by Plating for CFU Displays High Levels of Colonization by *M. marinum*. Adult N2 nematodes infected with either *M. smegmatis* (MC^2155) or *M. marinum* (ψmm1) for 24 hours were homogenized and plated for colony forming units (CFU) at 4, 12 and 24 hours during infection and post-infection, 30 and 48 hours. 30 nematodes each were homogenized and plated for each time point except for *M. marinum* infected nematodes at 48 hours due to their high mortality rate. 20 worms were homogenized and plated for the 48 hour time point with *M. marinum*. P-values are shown for comparison of CFU recovered from *M. smegmatis* and *M. marinum* infection at each time point (unpaired t-test).

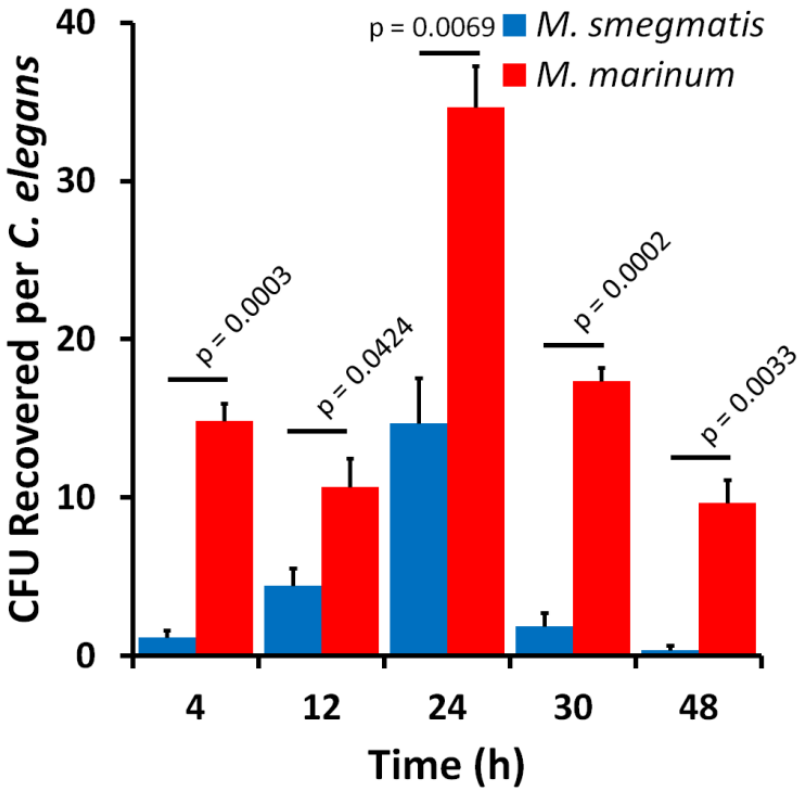

II.4 (D) M. marinum *Attach to the* C. elegans *Gut Epithelium and Colonize the Oro-Pharynx and Lower Gut*

In order to better understand the mechanism involved in maintenance of *M. marinum* within *C. elegans*, we imaged the course of infection out to 30 h using high resolution confocal microscopy. We were particularly interested in whether *M. marinum* were within the lumen of the gut, attached to the gut epithelium or had crossed the gut epithelial barrier and entered into host cells. We imaged the head, mid-gut and lower-gut regions of nematodes where accumulations of mycobacteria were observed. We found both *M. smegmatis* and *M. marinum* in the head at both 4 and 24 h post-infection, but at 30 h, when the bacteria are no longer present, *M. smegmatis* is mostly cleared, whereas, *M. marinum* is retained at high numbers. In general, *M. smegmatis* is not found within the mid-gut or lower gut regions at all, though some individual bacteria are sometimes observed. In contrast, *M. marinum* is observed within the mid-gut and lower-gut at moderate to high levels out to 30 h post-infection and particularly the lower gut had high numbers of bacteria at late time points (Figure 11).

Interestingly, nematodes infected with mycobacteria (both *M. smegmatis* and *M. marinum*) displayed a larger lumen in the lower gut region (Figure 11 I, L, O and R) by 24 h post-infection than nematodes infected with *E. coli* (Figure 12). We also observed the initial stages of bagging for nematodes infected with *M. marinum* (Figure 11K and Q) in contrast to those with *M. smegmatis* (Figure 11H and N). While these images revealed that a majority of *M. marinum* were in the lumen of the gut, they did not

definitively answer the question of whether persisting bacteria are attached to the gut epithelial lining.

We embedded, sectioned and imaged nematodes infected with *M. smegmatis* and *M. marinum* for 24 hours using a transmission electron microscopy (Figure 13). While *E. coli* infected nematodes displayed a smooth non-wrinkled cuticular surface, *M. smegmatis* and *M. marinum* infected *C. elegans* displayed a cuticle with numerous crevices (Figure 13 A-C). These indentations were mild in nematodes infected with *M. smegmatis* and extensive in those infected with *M. marinum* (Figure 13 B-C). Folding of the cuticle can be a result of a stress response in nematodes, most likely when exposed to mycobacteria that resulted in depigmentation and shortening of the nematode length (Figure 2 C-D, 3 and 4). In *C. elegans* infected with *M. smegmatis* we did not observe many intact bacteria, rather there was mostly digested debris in the gut lumen of the nematode (Figure 13 D). When occasional bacteria were present, *M. smegmatis* was not attached to the gut epithelium and remained in the lumen (Figure 13 E-F). *C. elegans* infected with *M. marinum* displayed attachment to the *C. elegans* gut epithelium (Figure 13 G-I). These observations help to explain the clearing of *M. smegmatis* from infected *C. elegans* post-infection, while *M. marinum* can colonize the gut of infected nematodes even 48 hours post infection.

Figure 11. High Resolution Confocal Images Show *M. marinum* Persist Within the Oro-Pharynx and Lower Gut of *C. elegans* Adult TP12 nematodes infected with either *M. smegmatis* (ψms23) or *M. marinum* (ψmm91) were imaged at 4 and 24 hours during infection and 6 hours post-infection (30 hour). The head, mid-gut and lower-gut regions of about 15 TP12 nematodes each at 4, 24 and 30 hour were imaged by confocal microscopy. A 40x oil-immersion objective and a digital zoom of 2.5x was used (effective magnification 100x). A spectral filter for excitation wavelengths of 500-640nm was used. (A-C) Nematodes after 4 hours of infection with *M. smegmatis* (*Ms*). (D-F) Nematodes after 4 hours of infection with *M. marinum* (*Mm*). (G-I) Nematodes after 24 hours of infection with *Ms*. (J-L) Nematodes after 24 hours of infection with *Mm*. (M-O) Nematodes 6 hours post-infection by *Ms*. (P-R) Nematodes 6 hours post-infection by *Mm*.

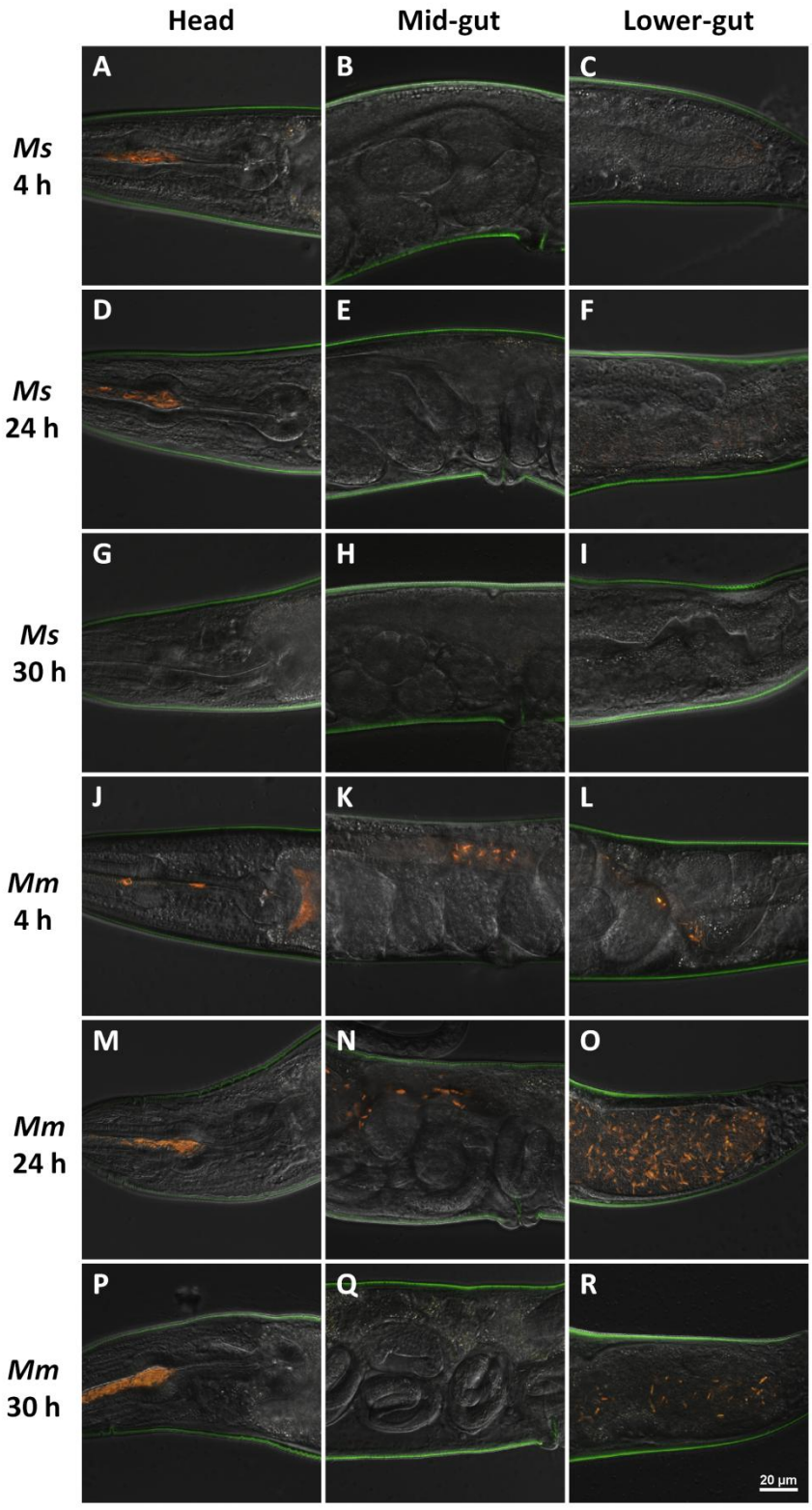
Head
Mid-gut
Lower-gut
Ms
4 h
Ms
24 h
Ms
30 h
Mm
4 h
Mm
24 h
Mm
30 h
A
B
C
D
E
F
G
H
I
J
K
L
M
N
O
P
Q
R
20 µm

Figure 12. Morphological Characteristics of *C. elegans* (TP12) Infected with *E. coli* (OP50). Adult TP12 nematodes infected with *E. coli* (OP50) were imaged at 4 and 24 hours during infection and 6 hours post-infection (30 hour), for comparison with nematodes infected with mycobacteria for 24 hour (Figure 11). The head, mid-gut and lower-gut regions of five TP12 nematodes each at 4, 24 and 30 hour were imaged by confocal microscopy. A 40x oil-immersion objective and a digital zoom of 2.5x was used (effective magnification 100x). A spectral filter for excitation wavelengths of 500-640nm was used. (A, D, G) Head regions of nematodes displaying the oral canal and the pharyngeal pump. The shaded area beneath the pharyngeal pump is due to darker pigmentation of the nematodes. (B, E, H) Mid-gut region of the nematodes displaying fertilized ova in a row, close to the vulva. The ova are in early stages of embryonic cell division. The lining of the gut is partly obstructed by the opaque dark pigmentation seen in healthy adult nematodes. (C, F, I) Lower-gut region of the nematodes displaying the tail end of the nematodes and the anal opening. The lumen of the lower gut is narrow, similar to the mid-gut lumen region.

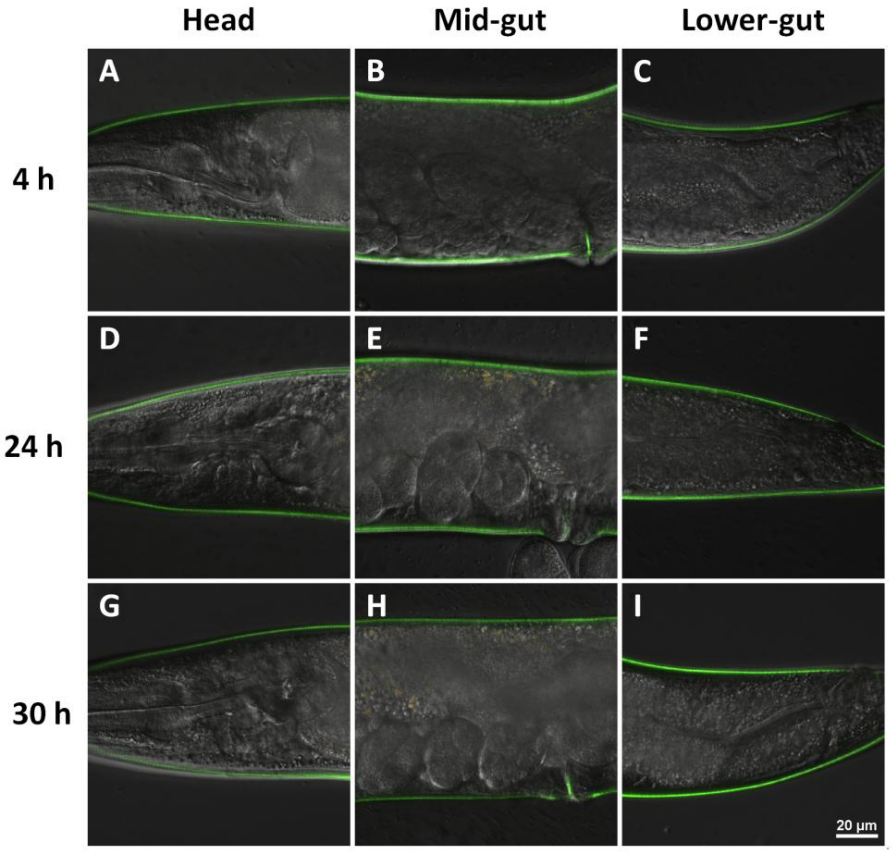

Figure 13. *M. marinum* are Attached to the Gut Epithelium of Infected *C. elegans*. Transmission Electron Microscopy (TEM) of *C. elegans* infected with *E. coli*, *M. smegmatis* and *M. marinum* after 24 hours. (A) Cuticle of *C. elegans* infected with *E. coli* remains smooth and show no signs of contraction. (B) Cuticle of *C. elegans* infected with *M. smegmatis* show slight contraction and small crevices (black arrow). (C) Cuticle of *C. elegans* infected with *M. marinum* show extensive contraction and crevices (black arrow) leading to shortening of the nematode. (D-F) *C. elegans* infected with *M. smegmatis* showed no attachment to the gut epithelium (arrow head), but rather remained in the gut lumen when present. (G-I) *C. elegans* infected with *M. marinum* displayed frequent attachment of *M .marinum* to the *C. elegans* gut epithelium.

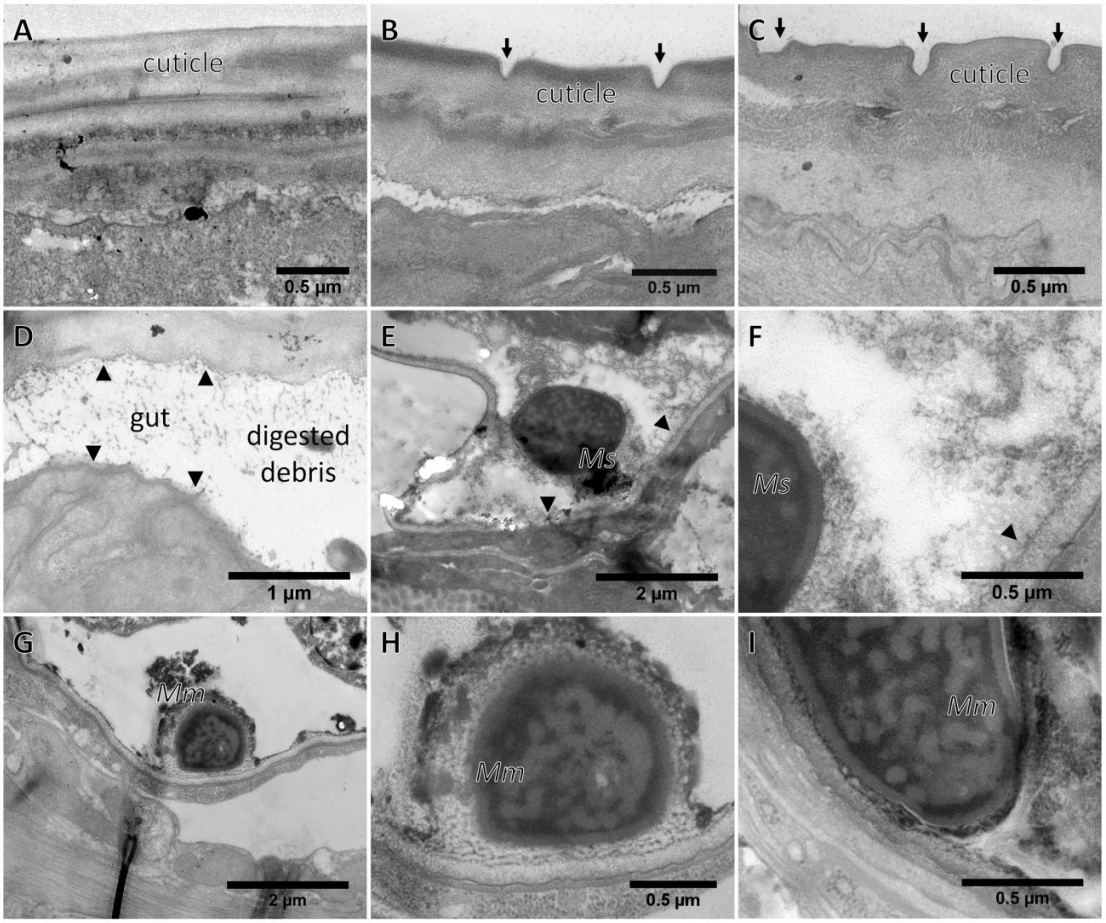

II.4 (E) C. elegans *Provide a Novel Virulence Model for* M. marinum

We recently identified several *M. marinum* mutants that are defective for their ability to infect and grow within mammalian macrophages (Mehta et al., 2006). This set of mutants was used to examine whether *C. elegans* could be used to evaluate whether *M. marinum* genes play a role in pathogenesis for nematodes. We screened 18 *M. marinum* mutants for virulence in *C. elegans*, as measured by survival of the nematodes post-infection (Figure 14). The majority of the *M. marinum* mutants produced less nematode mortality than wild type, but only 44% (8) of the mutants reached the significance cutoff of $p < 0.05$. Three of these mutants, *mimA*, *mimG* and *mimI* were complemented with the appropriate full-length wild-type gene and we demonstrated that complementation results in restoration of the ability to kill *C. elegans*, confirming that these genes are involved in *C. elegans* pathogenesis (Figure 15). Our results indicate that *C. elegans* can be used as a host for study of *M. marinum* pathogenesis and detailed analysis of its virulence mechanisms.

Figure 14. *C. elegans* Infected With Mutants of *M. marinum* Have Reduced Mortality Rates. (A-D) Survival of wild-type (N2) nematodes infected with mutants of *M. marinum*, two days post infection (day 6). Three trials of 20 nematodes (total n = 60) each were infected with the mutant strains and survival assessed on day 6. The survival rates of *C. elegans* infected with each mutant were compared *C. elegans* infected with wild-type *M. marinum* and p-values are shown (unpaired t-test). (A-D) Mean (±SEM) of *C. elegans* relative survival after infecting with *M. marinum* mutants.

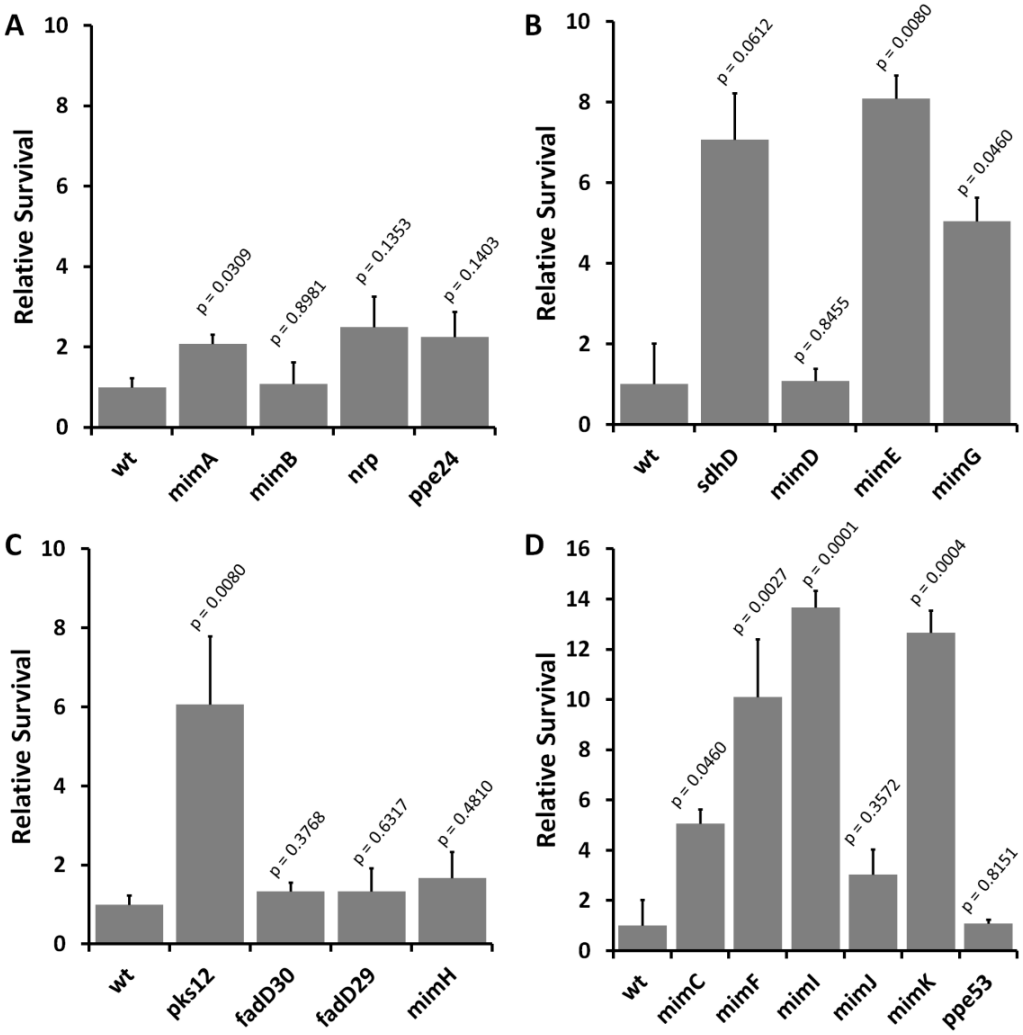

Figure 15. *C. elegans* Infected with Complemented Mutant Strains of *M. marinum*. Three *M. marinum* mutants were complemented by introducing their *Mtb* orthologs gene (Mehta et al., 2006). Three mutants, *mimA*, *mimG* and *mimI* and their complemented strains were compared in *C. elegans* infection assays to confirm that the observed phenotype is due to the mutated gene. The complementing genes were introduced in a low copy number plasmid vector, pJDC89. Adult N2 nematodes were infected with each respective *M. marinum* strain for 24 hours and mortality was assessed two days post-infection (day 6). P-values are shown comparing the mutants and their respective complemented clones. This experiment was repeated twice. All complemented *M. marinum* strains were significantly more virulent compared to their respective mutants.

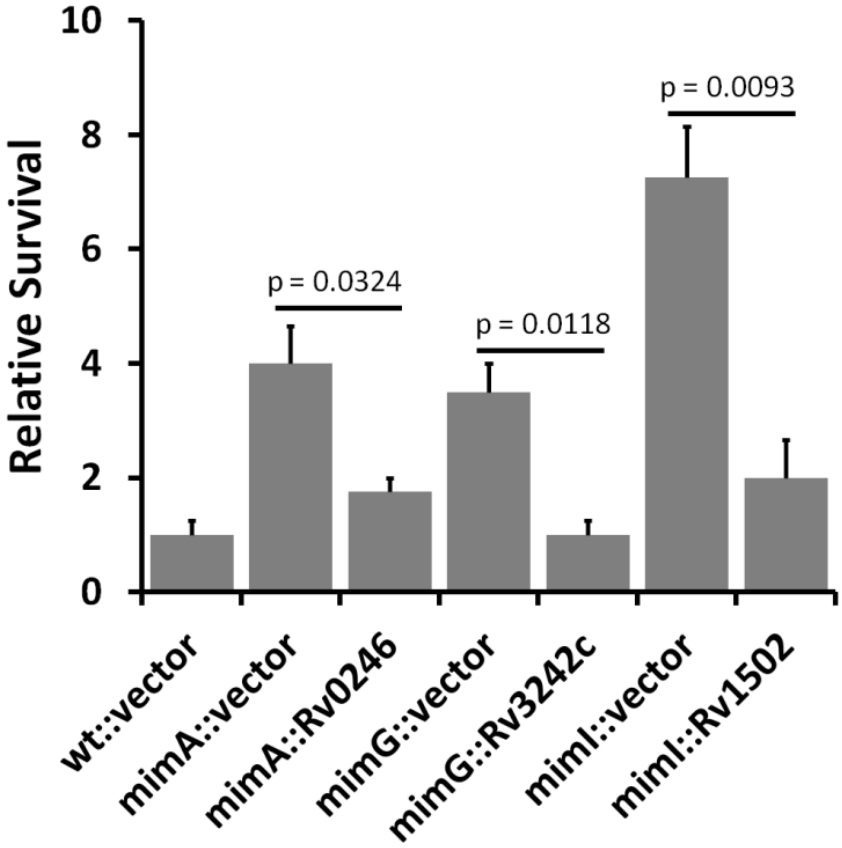

II.5 Discussion

Mtb is a successful human pathogen that has evolved the ability to use multiple strategies to evade and modulate the host immune system, even frequently establishing chronic infections. Understanding *Mtb* pathogenesis is important to develop interventions that can address the global problem of TB currently affecting about 2 billion people worldwide and resulting in over 2 million deaths annually (Dye et al., 1999). The study of *Mtb* has been facilitated by use of *Mycobacterium marinum*, as a model system (Deng et al., 2011; Stinear et al., 2008; Tobin and Ramakrishnan, 2008). *M. marinum* has an optimal growth temperature of $<33^{o}$C making *Mtb* model hosts, such as mice and guinea pigs, very useful for analysis of skin infections, but less so for pulmonary infections (Balasubramanian et al., 1994; Clark and Shepard, 1963a; McMurray, 2001; Shi et al., 2011). *C. elegans* is a valuable model for study of host innate immune responses because of its well characterized genetics and the availability of extensive molecular tools, making it possible to perform an array of genetic analyses (Ashrafi et al., 2003; Juang et al., 2013; Kim et al., 2005; Tabach et al., 2013; Taylor and Dillin, 2013; Wilkins et al., 2005).

We infect *C. elegans* with *M. marinum* and show that pathogenic *M. marinum* cause mortality in nematodes. *C. elegans* has not been used to study the pathogenesis of *M. marinum* previously. However a group of researchers screened several bacteria in the same study for potential *C. elegans* pathogens and *M. marinum* was one of the pathogenic bacteria that they tested. They did not observe an increase in mortality of *C.*

elegans infected with *M. marinum* (Couillault and Ewbank, 2002). There were a number of differences in the experimental methods use that likely explain the difference in the results, for example they used *C. elegans* L4 larvae for infection while we used gravid adult nematodes. In our own study we found that it was important to use controlled conditions for infections to reduce variability in results obtained. The consistency of data obtained in our study in multiple *C. elegans* strains and mutants argues that *M. marinum* is pathogenic for adult nematodes.

In examination of *C. elegans* for the study the pathogenesis due to bacterial infections there are several important readouts that allow evaluation of virulence mechanisms. They include mortality, attachment to epithelium, colonization of the gut epithelium, invasion of the gut epithelium, toxin-mediated killing and adhesive biofilm like structures on cuticle (Hodgkin et al., 2000; Jansen et al., 2002; Jansson et al., 1984; Kurz et al., 2003; Maadani et al., 2007; Moy et al., 2004; Park et al., 2002; Sem and Rhen, 2012; Tan et al., 1999). In the case of our *C. elegans* model for *M. marinum* pathogenesis, we used the outcomes of mortality, bagging, depigmentation, shortening of length and colonization of the gut epithelium. Readouts such as depigmentation and bagging overlap with phenotypes commonly observed in *C. elegans* stress responses, as might be expected for bacterial infections.

Our data suggest that *C. elegans* is a very useful model for study of *M. marinum* virulence mechanisms. We characterized the ability of *M. marinum* to persist within the gut of the nematode and also attach to the gut epithelium. These observations provide the foundation that could allow us to further characterize bacterial ligands involved in

pathogenesis as well as the *C. elegans* receptors involved. This new virulence model allowed identification of 8 *M. marinum* mutants that are attenuated for *C. elegans* infection. We can now use this *C. elegans* model to screen for *M. marinum* genes that are important in colonization, evaluate the general applicability of these genes to pathogenesis in mammals and dissect their mechanisms of action from the perspective of both the host and pathogen.

CHAPTER III

CHARACTERIZATION OF THE PUTATIVE VIRULENCE GENE REGULATOR *LUXR1* (MMAR_1239) IN *MYCOBACTERIUM MARINUM*

III.1 Summary

Several mycobacterial species are human pathogens with the ability to evade their host's immune system and establish successful acute and chronic infections. *Mycobacterium tuberculosis (Mtb)* is the causative agent of tuberculosis. *M. marinum* is another pathogenic mycobacterial species that causes a granulomatous skin infections in humans and a chronic tuberculosis-like disease in fish and amphibians. *M. marinum* is often used to study *Mtb* pathogenesis, since it is easily manipulated under BSL-2 safeguards and has a shorter generation time (5 hours vs. 20 hours). Many pathogenic mycobacteria, including *M. marinum* are able to persist within granulomas in their host, despite a significant immune response. Similarly, mycobacteria can form biofilms, which may play an important role in pathogenesis, making treatment and sterilization of granulomatous lesions more difficult. We have recently identified an *Mtb* gene, designated Rv3295 (*Mtb luxR1*) that has high similarity to *tetR* and luxR transcriptional regulators found in many bacterial species and often play a role in virulence gene regulation. The *Mtb luxR1* gene is very similar to *tetR*-related genes in other pathogenic mycobacteria, such as *M. marinum* (86% identity over 220 amino acids), and is less similar to *tetR*-related genes in non-pathogenic species, such as *M. smegmatis* (30% identity over 100 a.a.). In *M. marinum*, this gene was designated MMAR_1239 when the

M. marinum gene sequence was annotated (*Mm luxR1*). In order to understand the potential role of this gene in virulence, we constructed an insertion mutation in *luxR1* and one of the surrounding genes thought to be in an operon with *luxR1*. The locus containing *luxR1* was also evaluated for operon structure to determine the genes that are co-transcribed. *In vitro* host cell infection assays were used to determine the function of these genes during infections with host cells. Mutant and wild-type *M. marinum* strains were compared for differences in virulence. The *Mm-luxR1* mutant displayed attenuated virulence in a macrophage infection assays and a *C. elegans* infection assay. This study provides insight into the role of *luxR1* in pathogenesis of *M. marinum*.

III.2 Introduction

Several Gram positive and Gram negative bacteria including *Vibrio* species have a Lux operon that plays a role in modulating virulence factors (Schauder et al., 2001). An analogous pathway that is induced in *Streptomyces* in response to changes in their environment has been identified and characterized (Takano, 2006). *Streptomyces* are phylogenetically closely related to *Mycobacterium*, and protein orthologs of *Streptomyces* genes in mycobacteria have been studied to evaluate whether they have similar roles using LuxR proteins from *Vibrio* species and *Streptomyces griseus* to search for similar genes in mycobacteria, we identified several orthologs of the *luxR* gene. Of these potential *luxR* genes, one gene, Rv3295 in *Mtb* (*Mtb-luxR1*) and MMAR_1239 in *M. marinum* (*Mm-luxR1*) was of particular interest due to the presence of highly similar conversed domains and its absence in avirulent mycobacterial species.

Rv3295 and MMAR_1239 are predicted to produce 221 and 224 amino acid (a.a.) regulatory proteins respectively. These proteins have a DNA binding domain (TetR_N) and an AcrR domain, similar to the LuxR in *Vibrio harveyi* (205 a.a.) and ArpA in *Streptomyces griseus*. Rv3295 is also of particular interest among other potential LuxR analogs identified because our laboratory found that an Rv3295 *M. tuberculosis* mutant reduced infectivity for macrophages and is less virulent in a mouse model as compared to wild type (wt) *M. marinum*. Since Rv3295 has a potential role in mycobacterial virulence, we examined the function of *luxR1* in *M. marinum*. *M. marinum* is a close relative to *M. tuberculosis* and is a useful model organism for study of *M. tuberculosis* genetics and pathogenesis (Stinear et al., 2008; van der Sar et al., 2004b). We used *M. marinum* as model to study the ortholog of the *Mtb-luxR1* gene, *Mm-luxR1* and characterized its role in pathogenesis of *M. marinum* infections.

Mtb has many regulatory proteins with regions that have similarity to the LuxR protein motif. When comparing these *Mtb* LuxR analogs to LuxR in *Vibrio fischeri*, *Vibrio harveyi*, and ArpA in *Streptomyces griseus*, we found that 10 of them have an amino acid identity score of over 35% were selected as candidate LuxR regulators. Most of these genes have a LuxR-HTH (helix-turn helix) DNA binding domain, similar to that of *V. fischeri* (Figure 16 A). Two genes (Rv3295 and Rv3557c) have TetR DNA binding domains similar to *V. harveyi* and *S. griseus.* These two mycobacterial genes also have an AcrR DNA-binding transcriptional regulatory domain similar to that of *V. harveyi* and *S. griseus* (Figure 16 A). Phylogenic relationships suggest that Rv3295 and Rv3557c are different from the *Mtb* LuxR homologs and similar to *V. harveyi* gene (Figure 16 B).

Figure 16 Protein Motif Similarities Between Mycobacterial LuxR Proteins and LuxR Proteins of Related Bacteria. (A) Comparison of conserved domains of LuxR analogs in *Mtb* as compared to *Vibrio* and *Streptomyces griseus*, having over 35% identity in amino acid sequence (a.a.). (B) Phylogenic relationship between the luxR analogs in (A). A BLAST analysis on the NCBI website for genes was used to compare these genes of interest.

(A)

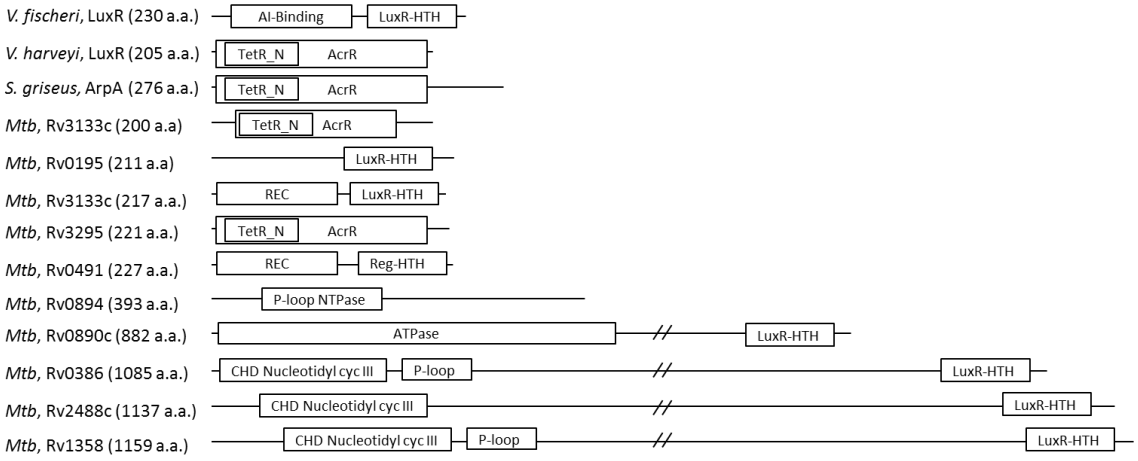

(B)

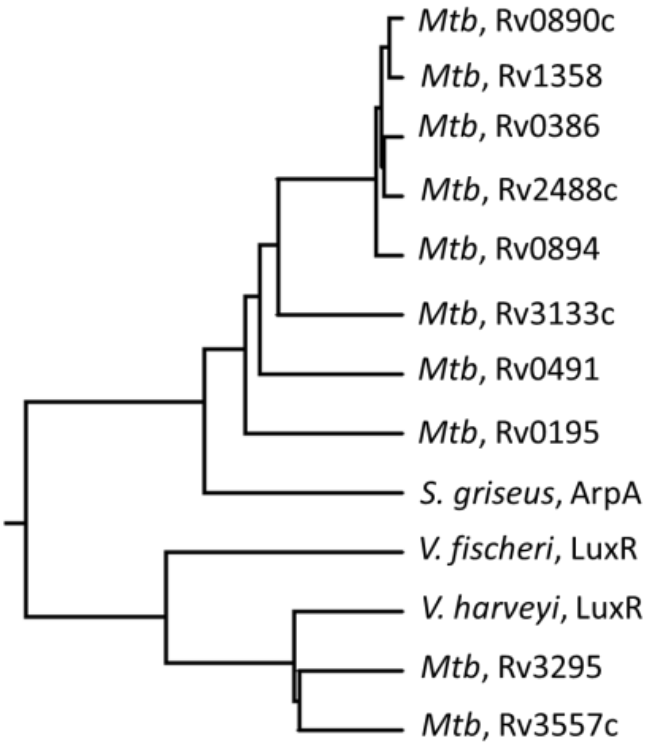

Figure 17 Phylogenic Relationships Between LuxR1 Proteins in Various Mycobacterial Species (A) Phylogenic relationship between orthologs of *Mm-luxR1* with at least 75% a.a. identity when the regulatory domain was compared (last 161 a.a.). (B) Phylogenic relationship between several mycobacteria, *Vibrio* and *S. griseus*, showing that Rv3295, *Mtb luxR1* is closely related to pathogenic strains and less so to *M. smegmatis*. A BLAST analysis on the NCBI website for genes was used to compare these genes of interest.

(A)

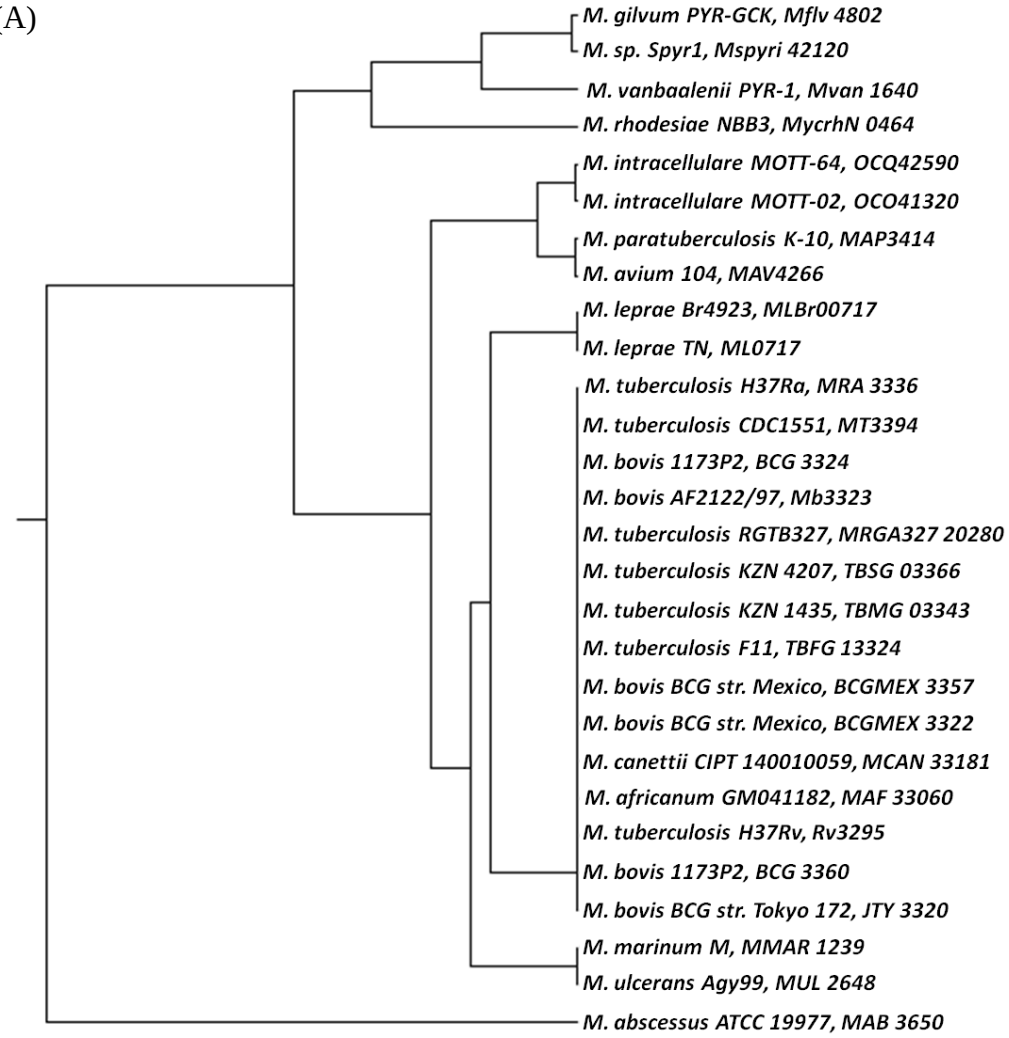
M. gilvum PYR-GCK, Mflv 4802
M. sp. Spyr1, Mspyri 42120
M. vanbaalenii PYR-1, Mvan 1640
M. rhodesiae NBB3, MycrhN 0464
M. intracellulare MOTT-64, OCQ42590
M. intracellulare MOTT-02, OCO41320
M. paratuberculosis K-10, MAP3414
M. avium 104, MAV4266
M. leprae Br4923, MLBr00717
M. leprae TN, ML0717
M. tuberculosis H37Ra, MRA 3336
M. tuberculosis CDC1551, MT3394
M. bovis 1173P2, BCG 3324
M. bovis AF2122/97, Mb3323
M. tuberculosis RGTB327, MRGA327 20280
M. tuberculosis KZN 4207, TBSG 03366
M. tuberculosis KZN 1435, TBMG 03343
M. tuberculosis F11, TBFG 13324
M. bovis BCG str. Mexico, BCGMEX 3357
M. bovis BCG str. Mexico, BCGMEX 3322
M. canettii CIPT 140010059, MCAN 33181
M. africanum GM041182, MAF 33060
M. tuberculosis H37Rv, Rv3295
M. bovis 1173P2, BCG 3360
M. bovis BCG str. Tokyo 172, JTY 3320
M. marinum M, MMAR 1239
M. ulcerans Agy99, MUL 2648
M. abscessus ATCC 19977, MAB 3650

(B)

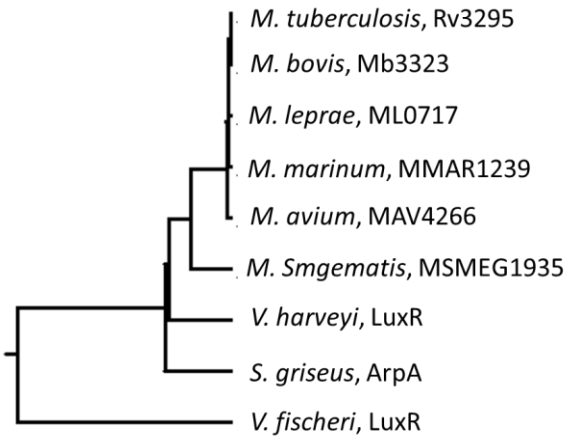
M. tuberculosis, Rv3295
M. bovis, Mb3323
M. leprae, ML0717
M. marinum, MMAR1239
M. avium, MAV4266
M. Smgematis, MSMEG1935
V. harveyi, LuxR
S. griseus, ArpA
V. fischeri, LuxR

Both Rv3295 and Rv3557c have orthologs across different mycobacterial species. However, Rv3295 is mainly present in pathogenic strains of mycobacteria (Figure 17 A). *M. smegmatis* is a non-pathogenic mycobacteria and the closest ortholog to Rv3295 in this organism had only a 31% identity in a.a. On the contrary, Rv3557c has a 75% identical ortholog in *M. smegmatis*. These observations suggest that Rv3295 is potentially important in virulence of mycobacteria. We designated Rv3295 *Mtb-luxR1*, and examined the role of this gene in virulence using *M. marinum* as a model (*Mm-luxR1*).

Our laboratory examined an *Mtb-luxR1* insertion (Mariner transposon) mutant obtained from the Johns Hopkins School of Medline's TARGET mutant library to determine the *luxR1* gene's role in virulence and pathogenesis by *Mtb*. We complemented the *Mtb-luxR1* mutant with a multi-copy vector constitutively expressing the *luxR1* gene. When *Mtb-wt* and *Mtb-luxR1*mutant were grown in nutrient rich 7H9 media with glycerol as the carbon source, there was no difference in their growth rates (Figure 18 A). This indicates that the *Mtb-luxR1* gene does not play an important role in the growth of the *Mtb* under nutrient rich conditions. However, *Mtb-wt* and the *Mtb-luxR1* mutant were transformed with an overexpressing *luxR1* gene, they were able to extend their log phase and out-grow *Mtb-wt* and the *Mtb-luxR1* the mutant (Figure 18 A). This supports our hypothesis that the *Mtb-luxR1* gene plays a role in coordinating the transition from log phase of growth to stationary phase, but the primary role is not likely to be in nutrient rich conditions.

Figure 18. Growth Rate of *Mtb-luxR1* Mutant Compared to *Mtb-wt* in Media and in Macrophages. (A) Growth of *Mtb-wt*, *Mtb-luxR1* mutant, *Mtb-wt*–overexpressing *luxR1* and *Mtb-luxR1* mutant-complemented strains in Middlebrook 7H9 liquid media with ADC and glycerol. (B) Survival and growth of *Mtb-wt* and the *Mtb-luxR1* mutant in unstimulated J774A.1 macrophages.

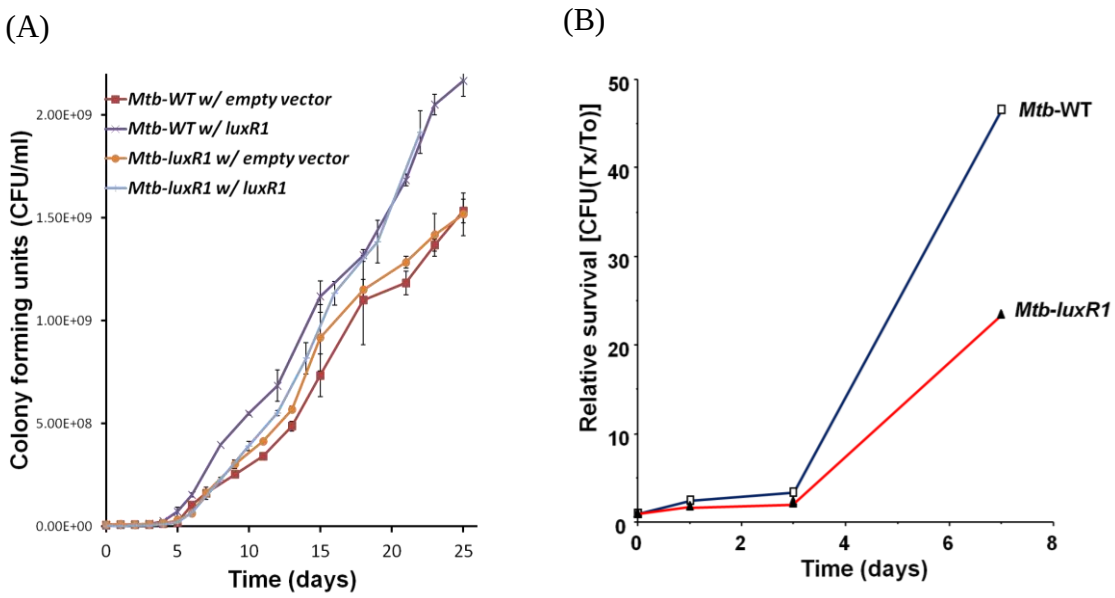

Murine macrophage cell lines can be useful for analysis of mycobacterial virulence mechanisms, including *M. marinum* (El-Etr et al., 2004; Subbian et al., 2007a). Such assays measure the ability of mycobacteria to adhere, associate, enter and survive within host cells. The *Mtb-luxR1* mutant does not display a significant difference in adherence, association or entry as compared to wild type. However, the *Mtb-luxR1* mutant displays nearly a 2-fold reduction in survival as compared to *Mtb-wt* (Figure 18 B). These observations suggest that nearby *Mtb-luxR1* gene contributes to the survival of *Mtb* in macrophages, which are one of the primary cells involved in controlling mycobacterial infections (Scherr et al., 2009; Yoshida et al., 2009).

These data suggest that the *Mtb-luxR1* gene contributes to the increased virulence and pathogenicity of *Mtb* by promoting intracellular survival in macrophages. However, the mechanisms involved by promoting survival remain unclear and their impact on pathogenesis overall has not yet been examined. In order to facilitate more detailed characterization, we used *M. marinum* as a model to more carefully dissect the role of this gene in virulence and pathogenicity.

III.3 Experimental Procedures

III.3 (A) Bacteria Growth Conditions

A wild-type clinical isolate of *M. marinum*, stain M (Ramakrishnan, 1997), was used in our studies. *M. marinum* cultures were grown at 32ºC standing in T25 tissue culture flasks. *M. marinum* were grown in Middlebrook 7H9 media (Difco, Sparks, MD)

supplemented with 0.5% glycerol, 10% albumin-dextrose complex (ADC) and 0.25% Tween 80 (M-ADC-TW).

III.3 (B) Characterization of Mm-luxR1 *Operon*

Total RNA was extracted at specific stages of growth (log phase and stationary phase) from *Mm wt*. Using *Mm-luxR1* and adjacent gene-specific primers, and intergenic primers for each of these genes, cDNA was made by reverse-transcriptase PCR. Using qPCR, transcript levels of each gene and the presence of the intergenic regions were determined. cDNA was also used as a template to carry out PCR reactions for each gene and across the corresponding intergenic region including both open reading frames to assay for the absence or the presence of a common transcript. Each set of gene-specific primers acted as a control for the expression levels of that gene. 16s rRNA was used as a positive control (house-keeping gene), for the cDNA synthesis and qPCR process. 16s rRNA was also used to assess whether the total RNA sample were contaminated with genomic DNA. After the formation of cDNA with gene specific primers, PCR was used to amplify each of the individual genes in the MMAR_1237-1241 region and their intergenic regions.

III.3 (C) Gene Expression Analysis of Mm-luxR1 *Gene Locus*

Mm-wt was grown to log (OD 0.2) and stationary phase (OD 1.2) and total RNA was extracted using a Trizol based extraction method. The RNA was treated with DNase to remove any residual genomic DNA contamination. Four biological replicates of RNA were obtained at each stage of growth. These RNA samples were analyzed for purity and their concentrations determined using a NanoDrop machine and a Bioanlyser. Using a

primer set specific for the *Mm-luxR1* gene (less than 200bp), cDNA was synthesized for each of the RNA replicates at each of the two growth conditions. 16s rRNA was used as a positive control (house-keeping gene). The cDNA copies of *Mm-luxR1* and 16s rRNA were used as templates to be quantitatively amplified using real-time PCR (qPCR).

III.3 (D) Construct Insertion Mutants of Mm-luxR1 *Gene Locus*

The *Mm-luxR1* insertion mutants were constructed using allelic exchange, as described previously (Parish and Stoker, 2000). The *Mm-luxR1* gene (675 bp) and about 1000 bp each of the left and right flanking regions were amplified using polymerase chain reaction (PCR). This PCR product was then subjected to transposon mutagenesis with a kanamycin resistant (KanR) marker. Using a set of appropriate restriction sites, *Mm-luxR1* gene with KanR insertion was ligated into an *E. coli* plasmid (pGoal19). The plasmid, pGoal19 has the *lacZ* gene, sucrose sensitive marker, sacB and an *E. coli* origin of replication. Once the *Mm-luxR1* gene with KanR was ligated with the vector, the ligation was used to transform competent *E. coli* (XL1-Blue) and select for blue colonies. Blue *E. coli* colonies were restriction mapped and sequenced to demonstrate the presence of the *Mm-luxR1* gene and to identify recombinant plasmids with KanR insertions within the *Mm-luxR1* gene. The recombinant plasmid carrying the mutated *Mm-luxR1* gene (KanR insertion) was introduced into *M. marinum* using a two-step homologous recombination process, as described previously (El-Etr et al., 2004). The pGoal19 plasmid lacks a mycobacterial origin of replication and KanR can only be maintained in *M. marinum* if the plasmid recombines into the *M. marinum* chromosomal DNA by homologous recombination. At this stage blue *M. marinum* colonies were

selected in the presence of X-gal and kanamycin. Blue colonies were allowed to undergo a second round of intra-chromosomal homologous recombination that releases the plasmid leaving only the KanR insertion in the *Mm-luxR1* gene. The resulting white colonies in the presence of X-gal, kanamycin and 10% sucrose were selected for more detailed characterization. *Mm-luxR1* insertion mutants were confirmed by PCR using specific primers for the mutant and wt genes and sequencing.

III.3 (E) Complement Mutants of Mm-luxR1 *Gene Locus*

To ensure that the phenotype observed is due to loss of a functional *Mm-luxR1* gene, complement gene clones, both single copy and multiple copy, were constructed. We used PCR to clone the *Mm-luxR1* gene with its promoter region into complementation vectors. Using appropriate restriction digestions and ligation, the resulting PCR product was inserted into plasmids with an appropriate selection marker. The single copy plasmids have an integrase gene and will ensure that the plasmid is chromosomally inserted. The multi-copy plasmid has a mycobacterial origin of replication and will be maintained in *M. marinum* episomally. These mutants and their complementing strains were then evaluated in virulence and pathogenicity assays. As a control for the resistnace markers and other genes on the plasmid, the *Mm-luxR1* mutant and the *Mm-wt* were transformed with the empty plasmid vector.

III.3 (F) Characterize Growth of Mm-luxR1 *Gene Locus Mutants*

M. marinum wild-type, *Mm-pcd* mutant, *Mm-luxR1* mutant, and *Mm-luxR1* complemented strains were grown in nutrient rich Middlebrook Albumin Dextrose Complex (MADC) media at 32°C. The starting density for each culture was an OD_{600} of

0.2. T75 tissue culture flasks were used to grow 35 ml standing cultures. They were shaken twice a day for the duration of the experiment. At each time point, an aliquot was used to measure and dilations plated to determine CFU. 10 µl spot plating was used in triplicate and three serial dilutions were plated per sample. Growth was monitored until an OD_{600} of >1.5, where *M. marinum* reaches the stationary phase of growth. CFUs were counted 5 to 7 days after plating and the plates were incubated at 32°C.

III.3 (G) Assays for Colony Morphology and Sliding Motility of Mm-luxR1 *Mutant*

Using stock cultures of *M. marinum* wild-type, *Mm-pcd* mutant, *Mm-luxR1* mutant, Middlebrook media agar plates were spotted with bacteria to determine colony morphology or the agar was stabbed with an inoculating stick carrying bacteria for sliding motility assays. For colony morphology assays, 1.5% agar plates were used. For sliding motility assays 0.3% agar plates with low glycerol (0.2%) were used. The plates were incubated at 32°C up to 10 days for both colony morphology and sliding motility assay.

III.3 (H) Biofilm Formation Assays

A crystal violet *in vitro* assay has been described for staining biofilms formed by *M. avium* and we used a similar method in our own studies (Carter et al., 2003). Using a 96 well plate the different *M. marinum* strains (*Mm-wt, Mm-luxR1* mutant, and *Mm-luxR1* mutant complemented) were grown for up to 12 days and mycobacteria that were tightly attached to the walls of the 96-well plate were stained using the crystal violet. This method determines the amount of biofilm formed at the bottom and walls of the 96 well plate. Biofilm formation was measured at days 2, 5, 9 and 12. A second biofilm

assay was carried out using these *Mm* strains. In this assay, bacterial cultures were grown in a 24-well plate with sterile acid-washed glass beads. On top of the glass beads a cover slip was placed to allow *M. marinum* to form a biofilm. At specific time points the cover slips were carefully removed and the mycobacterial biofilm structures were heat fixed. They were stained with a red dye for dead bacterial cells and imaged under a confocal microscope.

III.3 (I) Macrophage Cell Infection Assays

A J774A.1 murine macrophage cell line was used for macrophage infection assays. They were cultured and maintained at 37^{o}C. Prior to infection with *M. marinum*, they were incubated at 32^{o}C for 1 hour. Unstimulated macrophages were grown to about 80% confluency and then transferred into 24-well plates (~2.5 x 10^{6} cells/ml) and incubated for 24 hours. Using a multiple of infection (MOI) of 10 J774.A1 cells were infected separately with *Mm-wt*, *Mm-luxR1* mutant and the *Mm-luxR1* complement. For the association assay, J774A.1 cells were infected with *M. marinum* for about 30s and then washed with 1x PBS several times, warmed to 30^{o}C. For adherence assays, the macrophages were first fixed by formaldehyde and infected with *M. marinum* for about 30 minutes, and then washed with 1x PBS. Similar to the cell association assay, an entry assay was done where the pathogens were allowed 30 minutes to enter macrophages. For the survival assay, J774A.1 cells were infected for 30 minutes and then followed over time (4h, 8h, 16h, 24h, and 30h) to determine intercellular macrophage survival of the *Mm-luxR1* mutant as compared to *Mm-wt*. The numbers of *M. marinum* in each of the

assays were determined by plating them on Middlebrook agar plates and counting CFUs for each sample at each time point.

III.3 (J) C. elegans *Infection Assays*

M. marinum wild-type, *Mm-pcd* mutant, *Mm-pcd* complement strain, *Mm-luxR1* mutant, and *Mm-luxR1* complement strain were used for *C. elegans* infections. We infected 3 days old adult N2 nematodes with these strains for a period of 24 hours. *M. marinum* cultures were grown until they reached stationary phase (OD >1.2) and 70 µl of each were seeded on small NGM plates the day prior to infection. Triplicates of 20 N2 worms (total 60) were infected with each *M. marinum* strain. After infection they were recovered on *E. coli* containing plates and mortality rates were assessed two days post-infection (day 6).

III.3 (K) C. elegans *Competitive Infection Assays*

M. marinum wild-type, *Mm-pcd* mutant and *Mm-luxR1* mutant expressing either tdTomato or mCherry were used for *C. elegans* infection to determine the dynamics of competitive infections in *C. elegans*. We infected 3 day old adult TP12 nematodes for a period of 24 hours. We used individual cultures (wild-type and mutant separately) and 1:1 ratio of mixed wild-type and mutant cultures for both the *Mm-pcd* mutant and the *Mm-luxR1* mutant in separate experiments. *M. marinum* cultures were grown until they reached stationary phase (OD >1.2) and 70 µl of each were seeded on small NGM plates the day prior to infection as described above. During the course of infection ~10 worms were obtained for times points of 4h, 24h and 30h (6h post-infection) and imaged using confocal microscopy.

III.3 (L) Statistical Analysis

Student's t-tests were used to compare the means for experimental groups of two. ANOVA (analysis of variance) were used to compare the means of multiple groups. The t-test analyses were used to compare differences between wt and mutant data at a given time point. ANOVA were used to compare groups such as wt, mutant, complemented mutant, and overexpressing mutant, over the course of several time points. Statistical analyses were performed with the help of Microsoft EXCEL statistical tools and Prism GraphPad software.

III.4 Results

III.4 (A) Mm-luxR1 *Gene is Co-transcribed with* Mm-pcd *and MMAR_1241 Genes*

luxR genes are usually expressed as a part of operons (*lux* operons) (Dunlap, 1999). Since we made insertional mutations in *Mm-luxR1,* it is important to determine whether other genes are co-transcribed with the *luxR1* gene. This information will indicate whether the *Mm-luxR1* is a part of an operon and if polar effects on surrounding genes might be responsible for functions that might be attributed to *Mm-luxR1* gene. Determining the genes that are co-transcribed with *luxR1* gene also helps with design of appropriate complementation strategies for the mutant *Mm-luxR1* gene. In *M. marinum*, *luxR1* is the third gene of five genes that are close together and thought to be transcribed in the same direction (Figure 19 A). The first gene is a hypothetical gene denoted by an open reading frame (ORF) with no known function. The second is a piperidine-6-carboxilic acid dehydrogenase (pcd) shown to be involved in the biosynthesis of

cephamycin C via α-aminoadipic acid in *M. avium* and *Streptomyces* species (Malmberg et al., 1993; Yamazaki et al., 2006). The fourth and fifth genes are an ATP-dependent helicase and an endonuclease, respectively. When cDNA is obtained from *M. marinum* at lag phase, we observed the transcription of the intergenic regions between MMAR_1239, MMAR_1240 and MMAR_1241 (Figure 19 B). Therefore, we predict a common transcript for genes MMAR_1241, *Mm-pcd* and *Mm-luxR1* (Figure 19 C), but different transcripts for MMAR_1238, MMAR_1239 and MMAR_1242.

III.4 (B) Mm-luxR1 *Gene Expression Increases during Lag Phase of Growth*

To characterize the expression profile of the *Mm-luxR1* gene we first examined expression at different phases of growth. We used qPCR and determined the transcript levels of *Mm-luxR1* during log phase (OD = 0.2) and lag phase (OD = 1.2) of growth. While *Mm-luxR1* was expressed both during the log and lag phase there were significantly higher levels ($p<0.0001$) of *Mm-luxR1* expression during the lag phase than during log phase (Figure 20).

Figure 19. Characterization of *Mm-luxR1* Operon Structure (A) Genes MMAR_1241 to MMAR_1237 can potentially be part of an operon, since they are located adjacent to each other and are transcribed in the same direction. Primers were used to amplify ~200bp intergenic regions from inside each gene into the next to determine the presence of a common transcript. The positions of each primer set are shown on the map. (B) PCR products of intragenic regions and intergenic regions of genes MMAR_1241 to MMAR_1237 using chromosomal DNA on RNA as the template. (C) Predicted *luxR1* operon with common transcript.

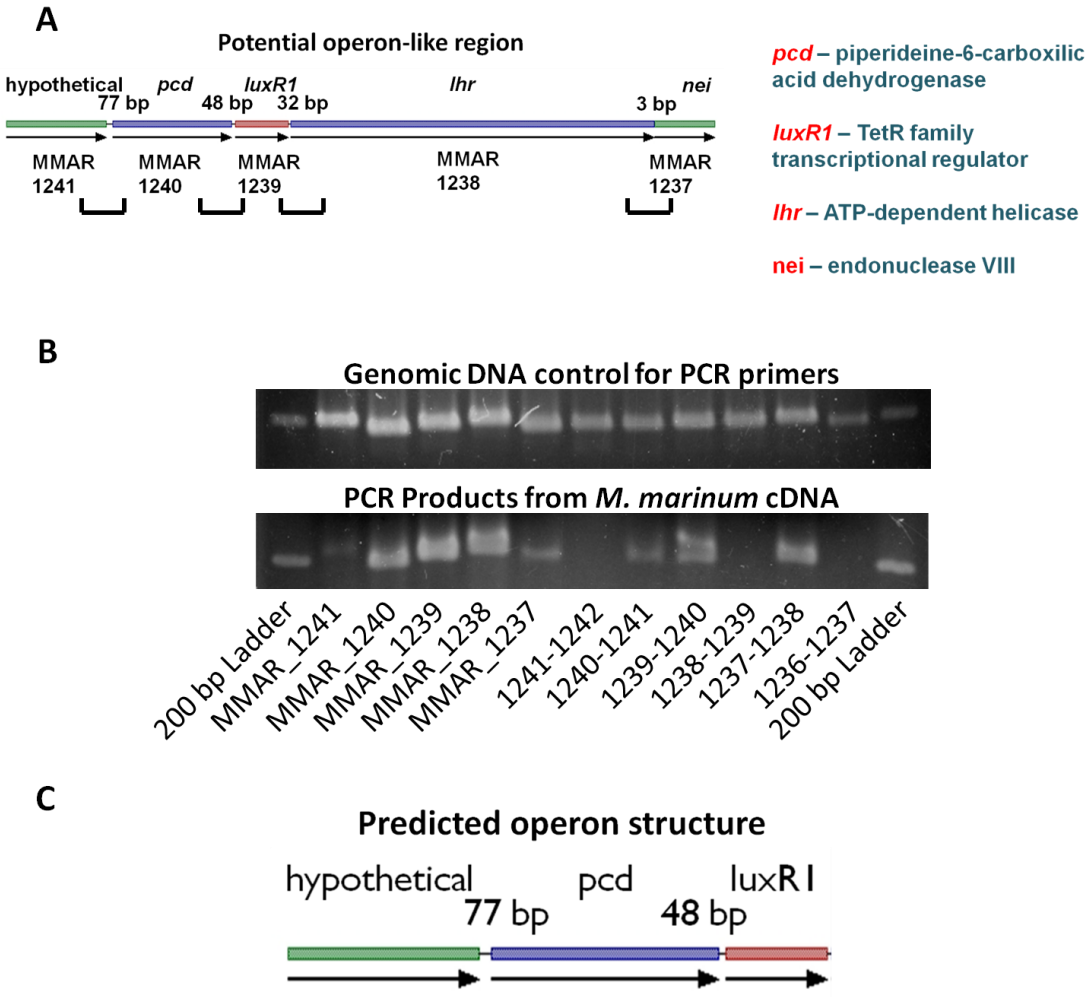

Figure 20. Gene Expression Levels of *Mm-luxR1* at Log-phase and Lag-phase of Growth. (A) Transcript levels of *Mm-luxR1* gene relative to 16s rRNA during log phase and lag phase. The results are the average of 4 biological replicates. (B) Relative transcript levels of *Mm-luxR1* during lag phase divided by the transcription levels during the log phase.

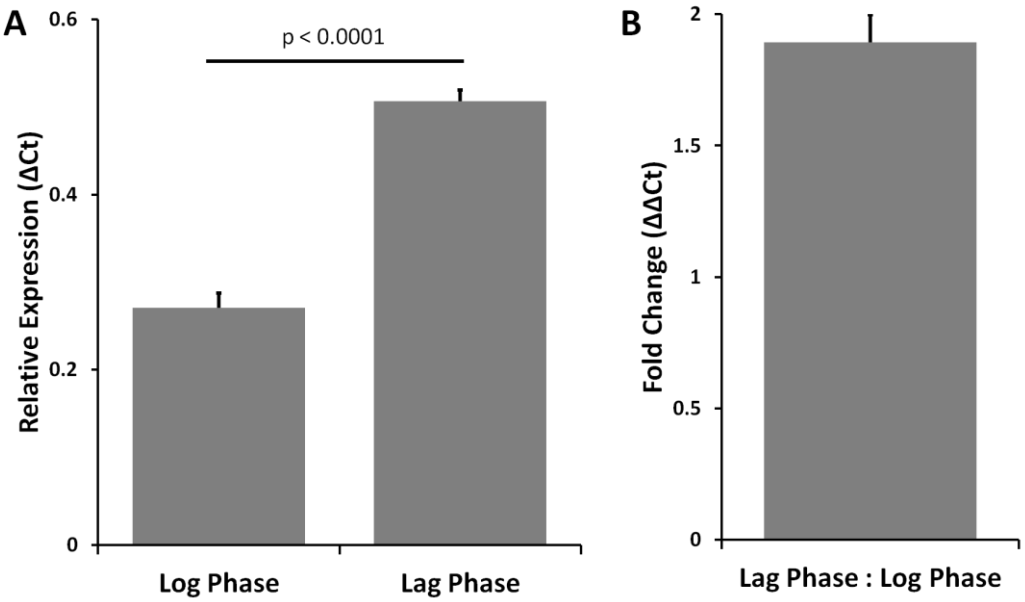

III.4 (C) Mm-luxR1 *Gene Locus Mutants Have an Increased Growth Rate in Nutrient-Rich Media*

We created two insertion mutants for genes *Mm-luxR1* and *Mm-pcd* in the *luxR1* operon (Figure 21). We also complemented these two insertion mutants in order to ensure that secondary mutations are not responsible for the phenotype of the *Mm-luxR1* mutant. Complement clones were created to control for differences in gene copy number. Both single copy and muti copy vectors for the mutated gene. We were interested in identifying if the *Mm-luxR1* gene plays a role in bacterial growth in laboratory media. When grown at 32°C, the *Mm-luxR1* mutant displays a significantly higher growth rate after 4-6 days of growth as compared to *Mm-wt* and the *Mm-luxR1* single copy complemented clone ($p < 0.01$) (Figure 22B).

The *Mm-pcd* mutant also displayed a significantly higher growth rate at 32°C after 4-6 days of growth as compared to *Mm-wt* ($p < 0.01$) (Figure 22 D). Interestingly there were no differences in growth rate of the either of the mutants (*Mm-luxR1* or *Mm-pcd*) as compared to *Mm-wt* when growth was measured using OD_{600} (Figure 22 A and C) and only by CFU. Possibly, this observation suggests that although the same number of cells are made in the wild type, some portion of those cells are unable to form colonies, whereas, the mutants can form colonies more effectively at higher OD (later stationary phase). This suggests that at higher ODs the *Mm-luxR1* and *Mm-pcd* mutants are better able to form colonies in nutrient rich media than *Mm-wt*. These observations indicate that the luxR1 gene locus may play a role in producing viable but not culturable *M. marinum* in nutrient rich growth media.

Figure 21. Confirmation of *Mm-luxR1* and *Mm-pcd* Mutants. (A) Schematic representation of insertional mutagenesis strategy for *Mm-luxR1* and *Mm-pcd* genes using a transposon with a kanamycin resistance marker. (B) Map of primer positions used for confirmation of insertion mutants. Right and left arms were amplified from the insertion to the gene. The entire gene was amplified to show larger product with each insertion. (C) Gel electrophoresis for confirmation of *Mm-luxR1* and *Mm-pcd* insertional mutants.

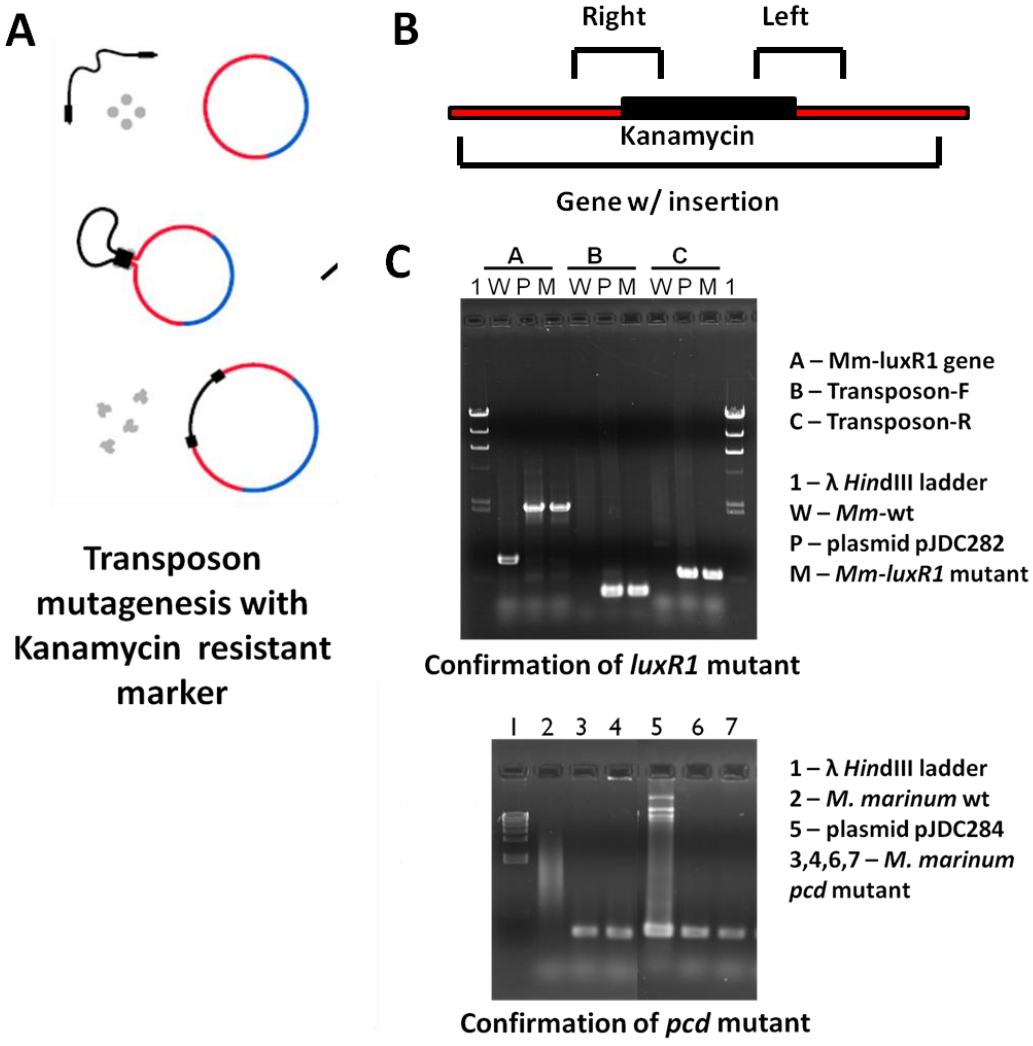

Figure 22. Growth of *Mm-luxR1* and *Mm-pcd* Mutants in Nutrient-Rich Media.
Growth of *M. marinum* strains in MADC media at 32°C. (A) Growth of *Mm-wt*, *Mm-luxR1* mutant and *Mm-luxR1* single-copy complement measured with OD_{600}. (B) Growth of *Mm-wt*, *Mm-luxR1* mutant and *Mm-luxR1* single-copy complement measured by plating for CFU. (C) Growth of *Mm-wt* and *Mm-pcd* mutant measured with OD_{600}. (D) Growth of *Mm-wt* and *Mm-pcd* mutant measured by plating for CFU.

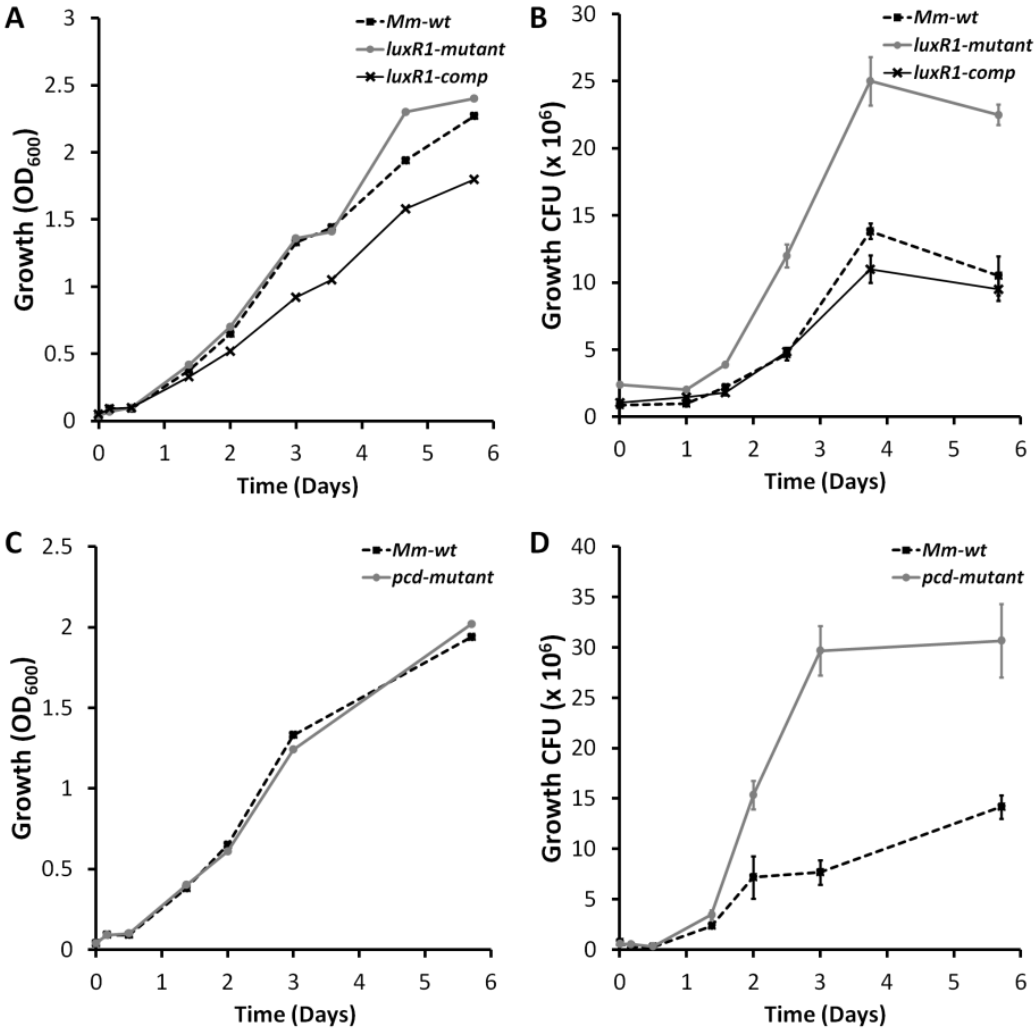

III.4 (D) Mm-luxR1 *and* Mm-pcd *Mutants Display Differences in Colony Size and Morphology as Compared to* Mm-wt

Since the *Mm-luxR1* gene product is a potential transcriptional regulator, we were interested in identifying whether thes genes it regulates play a role in production of surface structures or characteristics that would impact colony morphology. We plated *Mm-wt*, *Mm-pcd* and *Mm-luxR1* on MADC agar plates and incubated them at 32°C for 10 days (Figure 23). We did not observe a significant difference in the colony surface (smooth vs. rough) for either of the mutants as compared to *Mm-wt*. However, the *Mm-luxR1* mutant produced colonies that were slightly smaller than the *Mm-wt* colonies (Figure 23 J and L).

We cultured *Mm-wt*, *Mm-pcd* mutant and *Mm-luxR1* mutant in liquid MADC media at 32°C for 6 days until they reached lag phase and imaged them under a confocal microscopy. We looked at small colony and large colony morphologies to evaluate whether differences in colony morphology impacted mycobacterial aggregation or clumping (Figure 24). We observed that *Mm-wt* colonies and clumps were more spread out and less dense (Figure 24 A, D, G and J). *Mm-pcd* mutant colonies were more dense and not as spread out as *Mm-wt* (Figure 24 B, E, H and K). In contrast, *Mm-luxR1* mutant colonies and clumps were very dense and clumped a great deal (Figure 24 C, F, I L) as compared to *Mm-wt*. These observations suggest that the *Mm-luxR1* mutant and the *Mm-pcd* mutant differ from *Mm-wt* in characteristics that impact colony morphology and clumping in culture.

Figure 23. Colony Morphology of *Mm-wt, Mm-pcd* Mutant and *Mm-luxR1* Mutant
(A-F) Colony morphology for *Mm-wt*, *Mm-pcd* mutant and *Mm-luxR1* mutant inoculated by spot plating 10 µl of culture on an MADC agar plate and grown for 10 days at 32°C. (G-L) Colony morphology for of *Mm-wt*, *Mm-pcd* mutant and *Mm-luxR1* mutant inoculated by stabbing the agar with an inoculum on an MADC agar plate and grown for 10 days at 32°C.

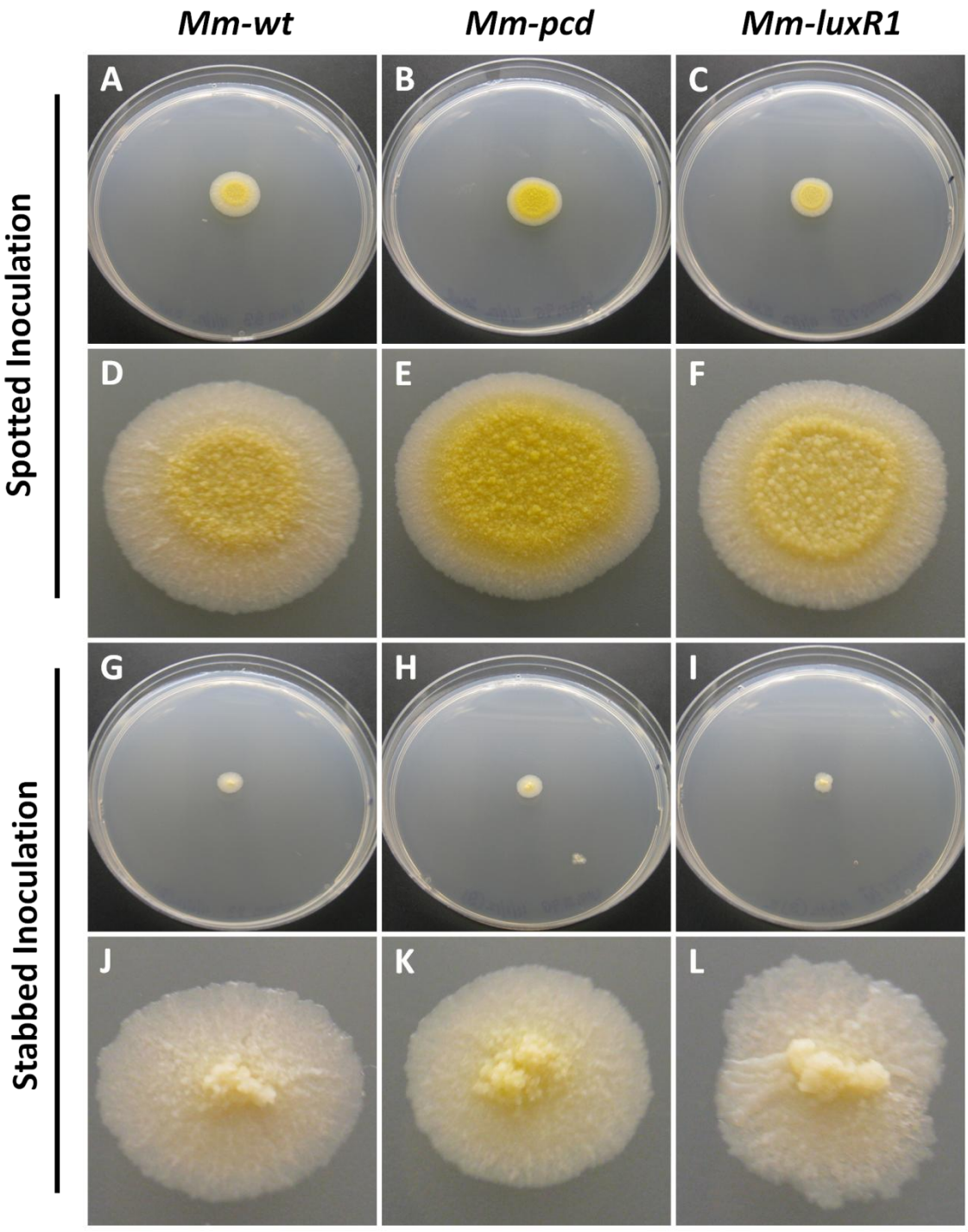
Mm-wt
Mm-pcd
Mm-luxR1
Spotted Inoculation
Stabbed Inoculation
A
B
C
D
E
F
G
H
I
J
K
L

Figure 24. Morphology and Clumping of *M. marinum* in Liquid Medium
(A-C) Clumps of *Mm-wt*::tdTomato (A), *Mm-pcd* mutant::tdTomato (B) and *Mm-luxR1* mutant::tdTomato (C) from active cultures grown in MADC media for 6 days (OD_{600} 1.0) at 32°C. (D-F) Small colony of *Mm-wt*::mCherry (D), *Mm-pcd* mutant::mCherry (E) and *Mm-luxR1* mutant::mCherry (F) from active cultures grown in MADC media for 6 days (OD_{600} 1.0) at 32°C. (G-I) Clumped bacteria from *Mm-wt*::tdTomato (G), *Mm-pcd* mutant::tdTomato (H) and *Mm-luxR1* mutant::tdTomato (I) cultures grown in MADC media for 6 days (OD_{600} 1.0) at 32°C. (J-L) Small clumps of *Mm-wt*::mCherry (J), *Mm-pcd* mutant::mCherry (K) and *Mm-luxR1* mutant::mCherry (L) from active cultures grown in MADC media for 6 days (OD_{600} 1.0) at 32°C.

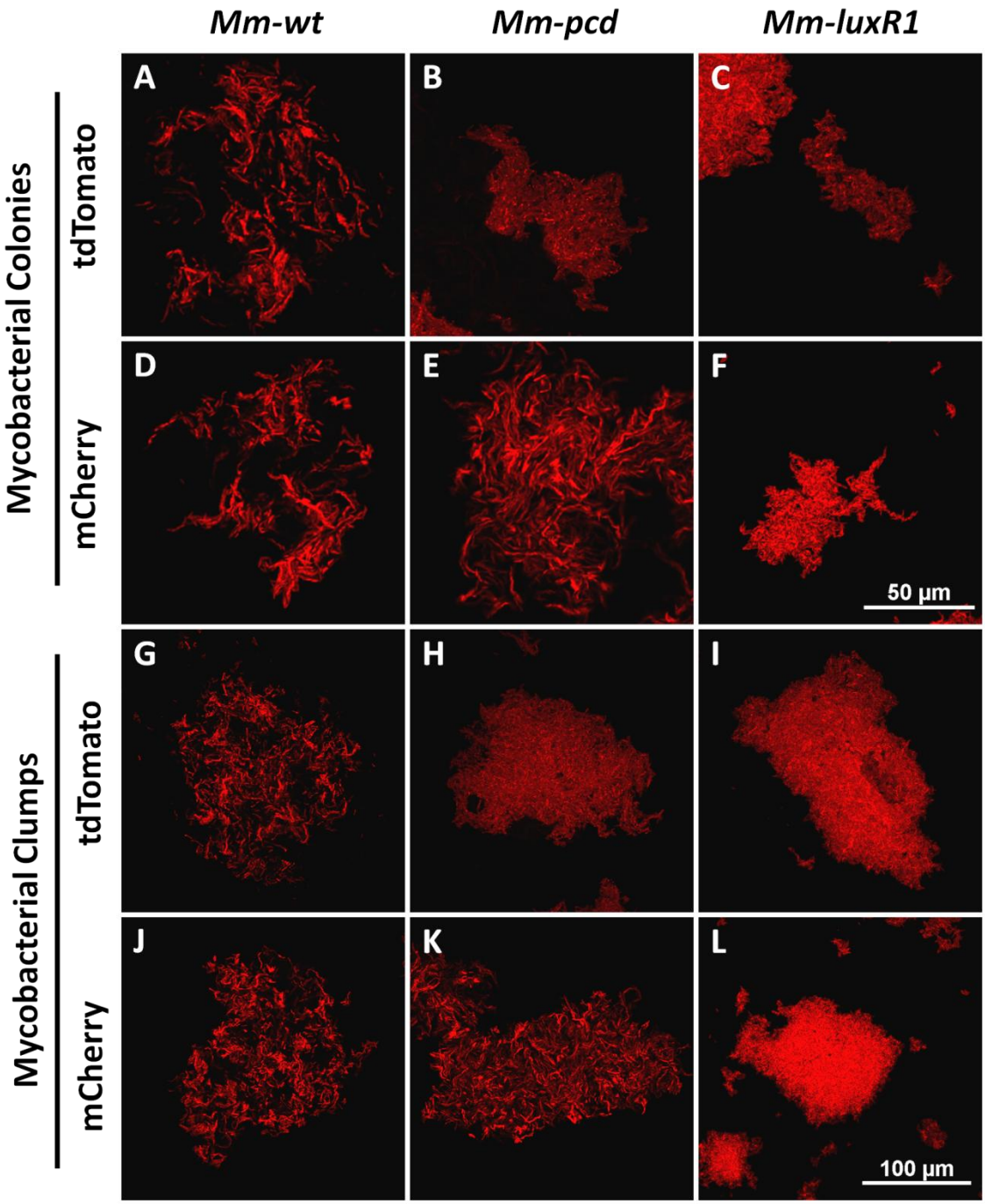
Mm-wt
Mm-pcd
Mm-luxR1
Mycobacterial Colonies
tdTomato
mCherry
Mycobacterial Clumps
tdTomato
mCherry
A
B
C
D
E
F
G
H
I
J
K
L
50 µm
100 µm

To further investigate the reduced colony sizes observed for *Mm-pcd* mutant and *Mm-luxR1* we performed motility assays (Figure 25). Using a lower percentage of agar (0.3%) and lower percentage of carbon source (0.2% glycerol), we cultured the *Mm-pcd* mutant and *Mm-luxR1* mutant at 32°C for 10 days. We followed the motility of the samples during days 5, 8 and 10. Mortality is a measurement of the ability of the bacteria to spread to areas with higher nutrient content. Mycobacteria with an intact ability or enhanced ability to spread on a surface will have larger colony sizes on a motility assay indicating the involvement of our genes of interest.

Compared to *Mm-wt* we observed a reduction in motility of the *Mm-pcd* mutant (Figure 25 N). The *Mm-luxR1* mutant had a much higher reduction in its ability as compared to *Mm-wt* (Figure 25 O). These observations suggest that the *Mm-luxR1* gene regulates gene important for surface characteristics that impact motility and spread.

Figure 25. Sliding Motility Assays for *Mm-wt, Mm-pcd* Mutant and *Mm-luxR1* Mutant. Sliding motility assays were done on 0.3% agar MADC plates with 0.2% glycerol and grown for 10 days. (A-I) Sliding motility of *Mm-wt*, *Mm-pcd* mutant and *Mm-luxR1* mutant inoculated by spot plating 10 µl. (J-O) Sliding motility of *Mm-wt*, *Mm-pcd* mutant and *Mm-luxR1* mutant inoculated by stabbed inoculation. (G, M) *Mm-wt* formed large colonies by sliding motility. (H, N) *Mm-pcd* mutant formed condensed colonies with intermediate levels of sliding motility. (I,O) *Mm-luxR1* mutant formed smaller condensed colonies.

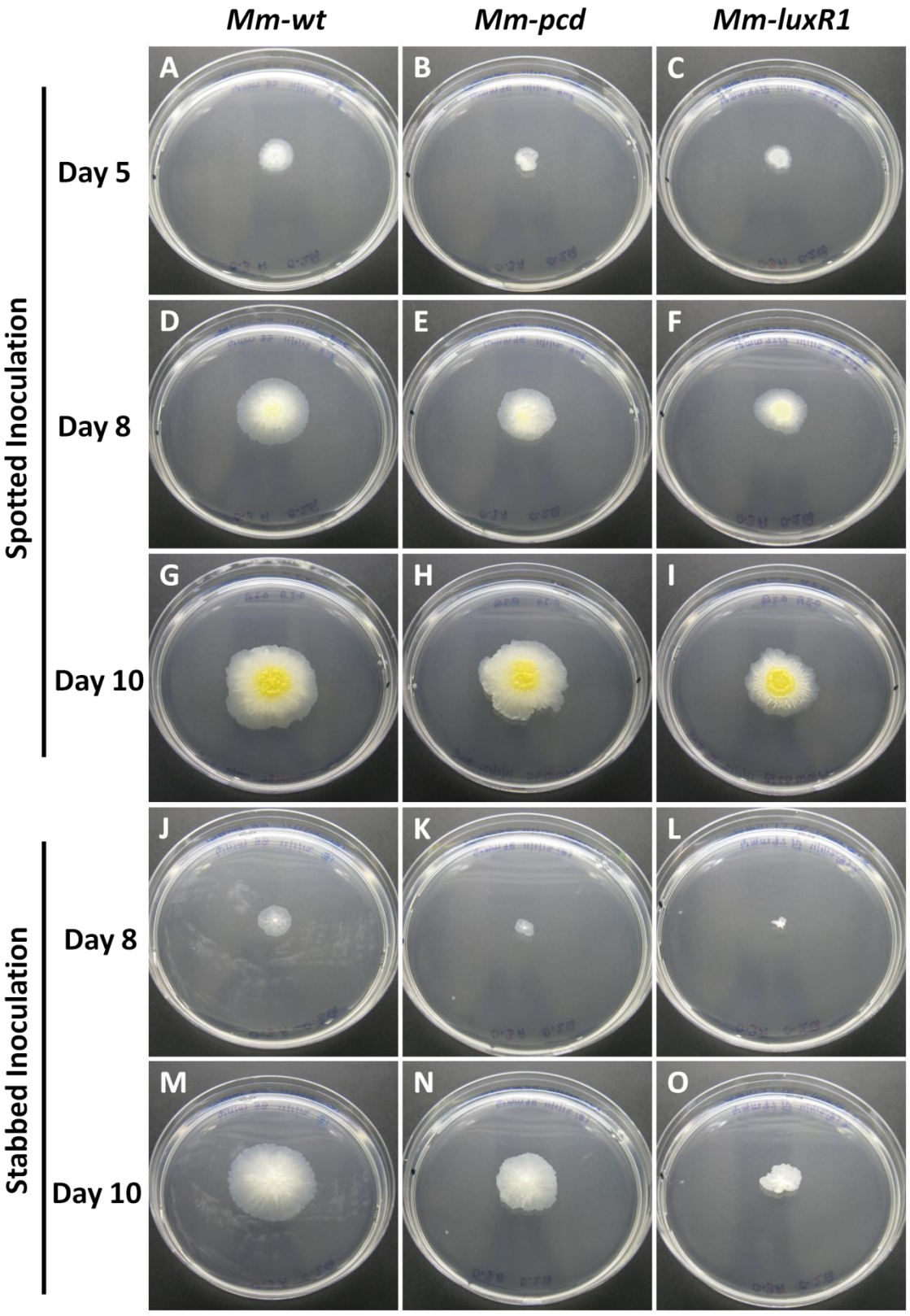
Mm-wt
Mm-pcd
Mm-luxR1
Spotted Inoculation
Day 5
Day 8
Day 10
Stabbed Inoculation
Day 8
Day 10
A
B
C
D
E
F
G
H
I
J
K
L
M
N
O

III.4 (E) Mm-luxR1 *Gene Locus Mutants Display an Increase in Biofilm Formation*

In mycobacterial pathogens and other pathogens such *Pseudomonas aeruginosa*, biofilms have been associated with virulence mechanisms and pathogenesis (Dong et al., 2012; Harjai et al., 2014). Biofilms are also associated with function of *luxR* regulators in pathogens such as *Vibrio harveyi* (Kadirvel et al., 2014). Also, the *pcd* gene has been shown to be important in biofilm formation in *M. avium* (Wu et al., 2009; Yamazaki et al., 2006). Therefore we looked at the impact of *Mm-luxR1* on biofilm formation. In our crystal violet assay, we observed an increase in biofilm formation in the *Mm-luxR1* mutant as compared to *Mm-wt* when grown in minimal media at room temperature and at 32°C ($p < 0.001$) (Figure 26 C and D). There was also an increase in biofilm formation in nutrient rich media when the culture was grown at 32°C (Figure 26 B). There was no difference in biofilm formation between the *Mm-pcd* mutant and *Mm-wt* when cultured in nutrient rich media at room temperature.

Figure 26. *Mm-luxR1* Mutant Displays Increased Biofilm Formation in the Crystal Violet Assay. (A) Intensity of crystal violet absorbance in *Mm-wt*, *Mm-luxR1* mutant and *Mm-luxR1* complemented clone cultures grown in nutrient rich MADC media at room temperature. (B) Intensity of crystal violet absorbance in *Mm-wt*, *Mm-luxR1* mutant and *Mm-luxR1* complemented clone cultures grown in nutrient rich MADC media at 32°C. (C) Intensity of crystal violet absorbance in *Mm-wt*, *Mm-luxR1* mutant and *Mm-luxR1* complemented clone cultures grown in minimal media at room temperature. (D) Intensity of crystal violet absorbance in *Mm-wt*, *Mm-luxR1* mutant and *Mm-luxR1* complemented clone cultures grown in minimal media at 32°C. After 12 days of incubation *Mm-luxR1* mutant displays increased biofilm formation.
* $p<0.05$, ** $p<0.01$ as compared to *Mm-wt*.

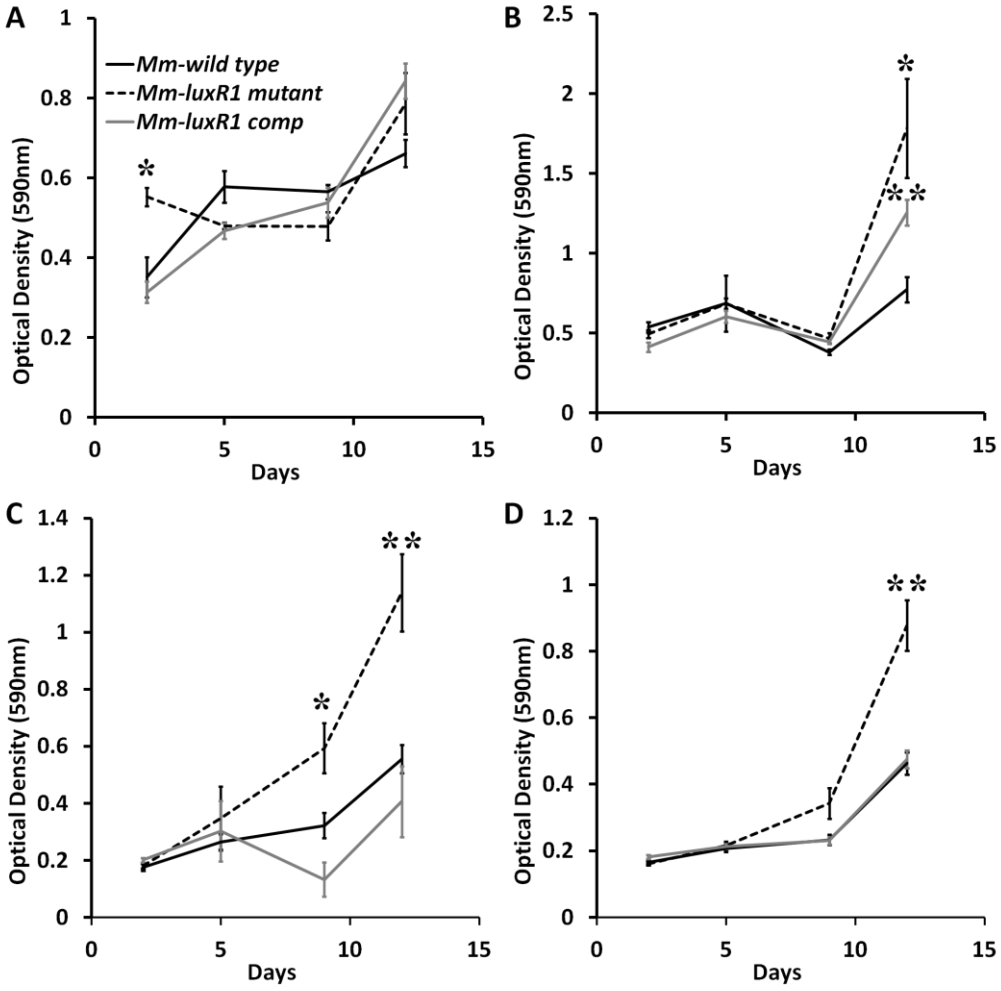

We observed a similar result for the *Mm-pcd* mutant. There is an increase in biofilm formation for the *Mm-pcd* mutant as compared to *Mm-wt* when grown in minimal media at room temperature and at 32°C ($p < 0.001$) (Figure 27 C and D). There was no difference in biofilm formation between *Mm-pcd* mutant and *Mm-wt* when cultured in nutrient rich MADC media (Figure 27 A and B). Therefore, our results suggest that *luxR1* modulates biofilm formation in *M. marinum*.

We also performed a glass bead biofilm assay for the *Mm-luxR1* mutant and *Mm-pcd* mutant and compared them to *Mm-wt* (Figure 28 and 29). The *Mm-luxR1* mutant showed a significantly higher level of biofilm formation in both MADC and minimal media (Figure 28 B, E) as compared to *Mm-wt* (Figure 28 A, D) and the *Mm-luxR1* complemented clone (Figure 28 C, F) ($p < 0.01$) (Figure 28 G and H). Similarly, we observed significantly higher levels of biofilm formation in the *Mm-pcd* mutant in MADC media as compared to *Mm-wt* (Figure 29 B, E and G). However, *Mm-pcd* mutant did not show a significant difference in biofilm formation as compared to *Mm-wt* in minimal media (Figure 29 B, E and H). Our crystal violet and glass bead assay results suggest that the *Mm-luxR1* gene plays a role in *M. marinum* biofilm formation than *Mm-pcd*.

Figure 27. *Mm-pcd* Mutant Displays an Increase in Biofilm Formation in the Crystal Violet Assay. (A) Intensity of crystal violet absorbance in *Mm-wt*, *Mm-pcd* mutant and *Mm-pcd* complemented clone cultures grown in nutrient rich MADC media at room temperature. (B) Intensity of crystal violet absorbance in *Mm-wt*, *Mm-pcd* mutant and *Mm-pcd* complemented clone cultures grown in nutrient rich MADC media at 32°C. (C) Intensity of crystal violet absorbance in *Mm-wt*, *Mm-pcd* mutant and *Mm-pcd* complemented clone cultures grown in minimal media at room temperature. (D) Intensity of crystal violet absorbance in *Mm-wt*, *Mm-pcd* mutant and *Mm-pcd* complemented clone cultures grown in minimal media at 32°C. After 12 days of incubation *Mm-pcd* mutant displays an increased in of biofilm formation when grown in minimal media.

* $p<0.05$, ** $p<0.01$ as compared to *Mm-wt*.

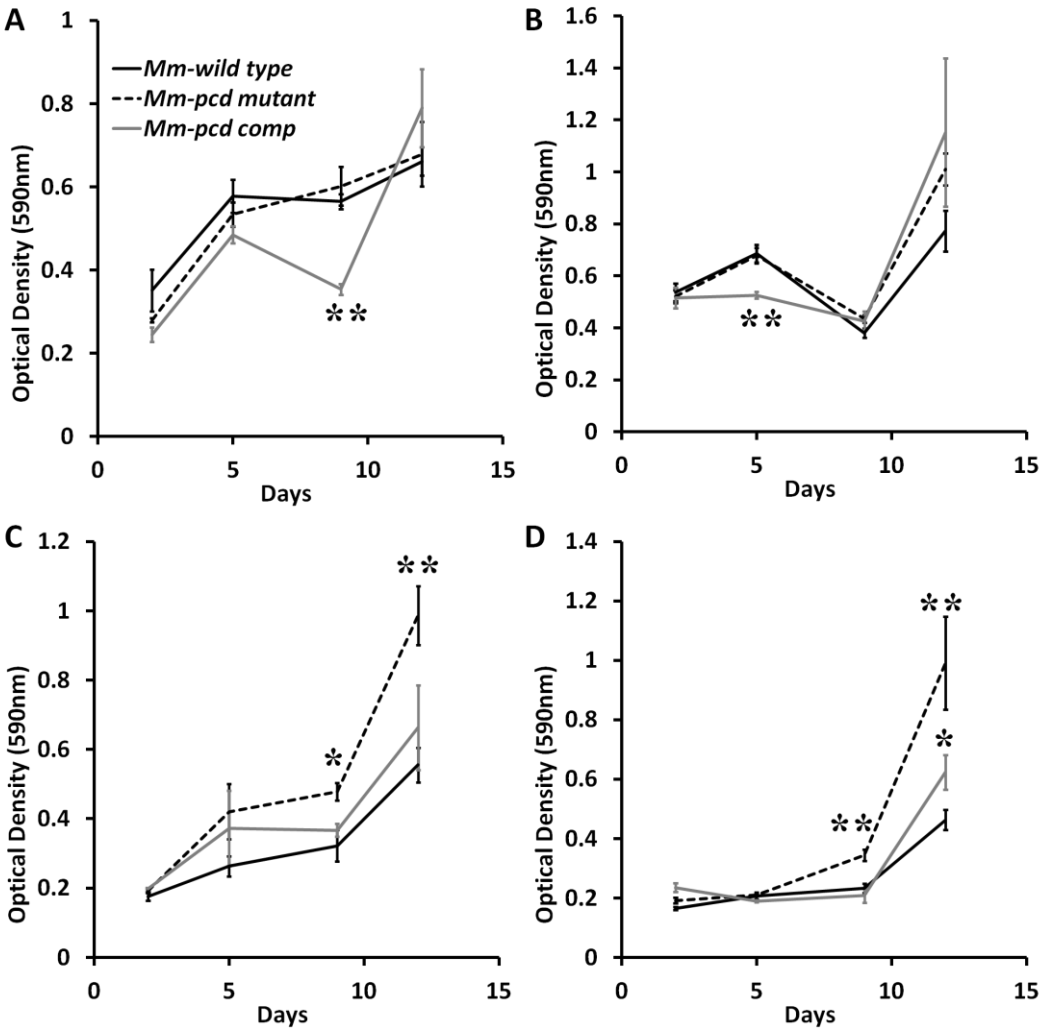

Figure 28. *Mm-luxR1* Mutant Displays an Increase in Biofilm Formation in a Glass Bead Biofilm Assay. (A-F) Biofilms were heat fixed, stained with propidium iodide and imaged using confocal microscopy. (A-C) *Mm-wt*, *Mm-luxR1* mutant and *Mm-luxR1* complemented clone biofilms formed on cover slips grown in MADC media at 32°C. (D-F) *Mm-wt*, *Mm-luxR1* mutant and *Mm-luxR1* complemented clone biofilms formed on cover slips grown in minimal media at 32°C. (G-H) Fluorescence Intensities were quantified using ImageJ software. (G) Mean ± SEM of biofilm intensity of 4 different samples of *Mm-wt*, *Mm-luxR1* mutant and *Mm-luxR1* complemented clone grown in MADC media at 32°C. *Mm-luxR1* mutant produced significantly more biofilm. (H) Mean ± SEM of biofilm intensity of 4 different samples of *Mm-wt*, *Mm-luxR1* mutant and *Mm-luxR1* complement grown in minimal media at 32°C. *Mm-luxR1* mutant produced significantly more biofilm.
** $p<0.01$ as compared to *Mm-wt*.

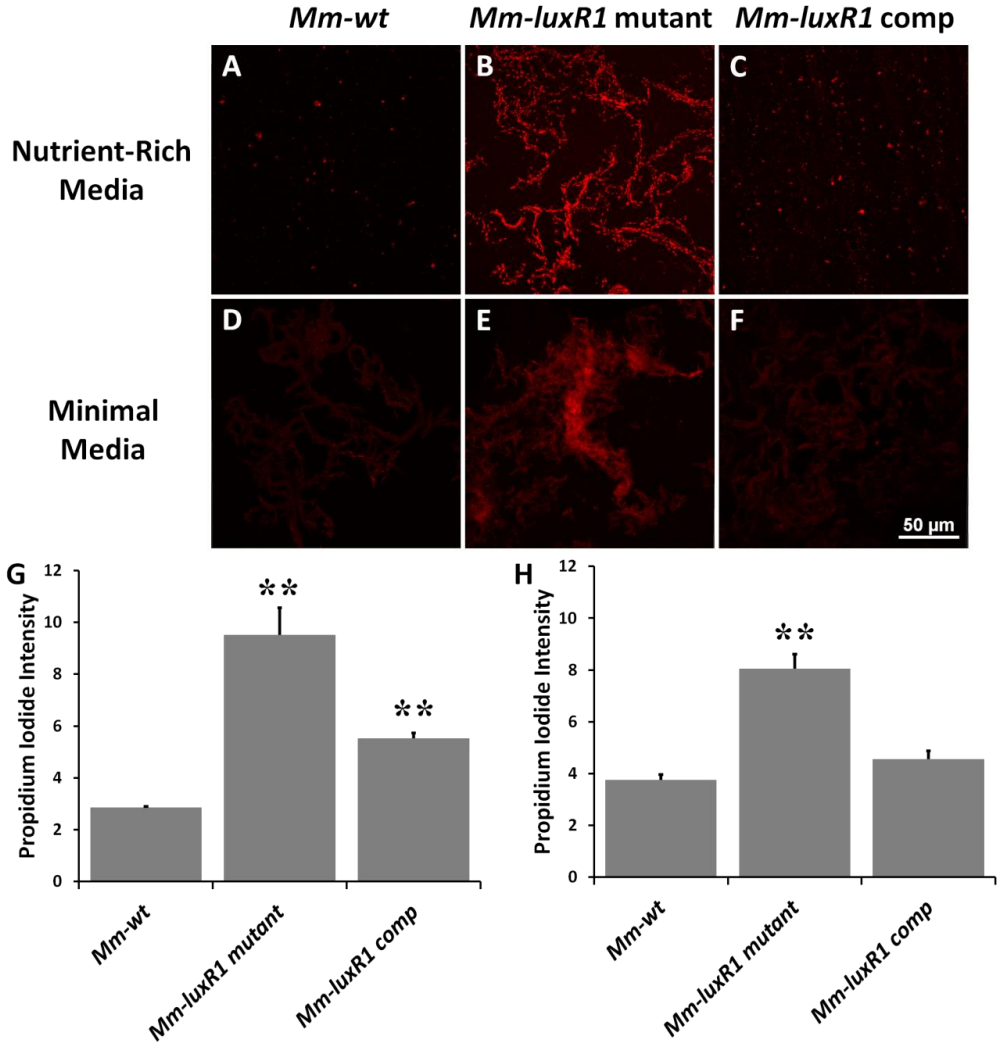

Figure 29. *Mm-pcd* Mutant Shows an Increase in Biofilm Formation in a Glass Bead Biofilm Assay. (A-F) Biofilms were heat fixed, stained with propidium iodide and imaged using a confocal microscope. (A-C) *Mm-wt, Mm-pcd* mutant and *Mm-pcd* complemented clone biofilms formed on cover slips grown in MADC media at 32°C. (D) *Mm-wt, Mm-pcd* mutant and *Mm-pcd* complemented clone biofilms formed on cover slips grown in minimal media at 32°C. (G-H) Fluorescence Intensities were quantified using ImageJ software. (G) Mean ± SEM of biofilm intensity of 4 different samples of *Mm-wt*, *Mm-pcd* mutant and *Mm-pcd* complemented clone grown in MADC media at 32°C. *Mm-pcd* mutant produced significantly more biofilm. (H) Mean ± SEM of biofilm intensity of 4 different samples of *Mm-wt*, *Mm-pcd* mutant and *Mm-pcd* complement grown in minimal media at 32°C.
* $p<0.05$ as compared to *Mm-wt*.

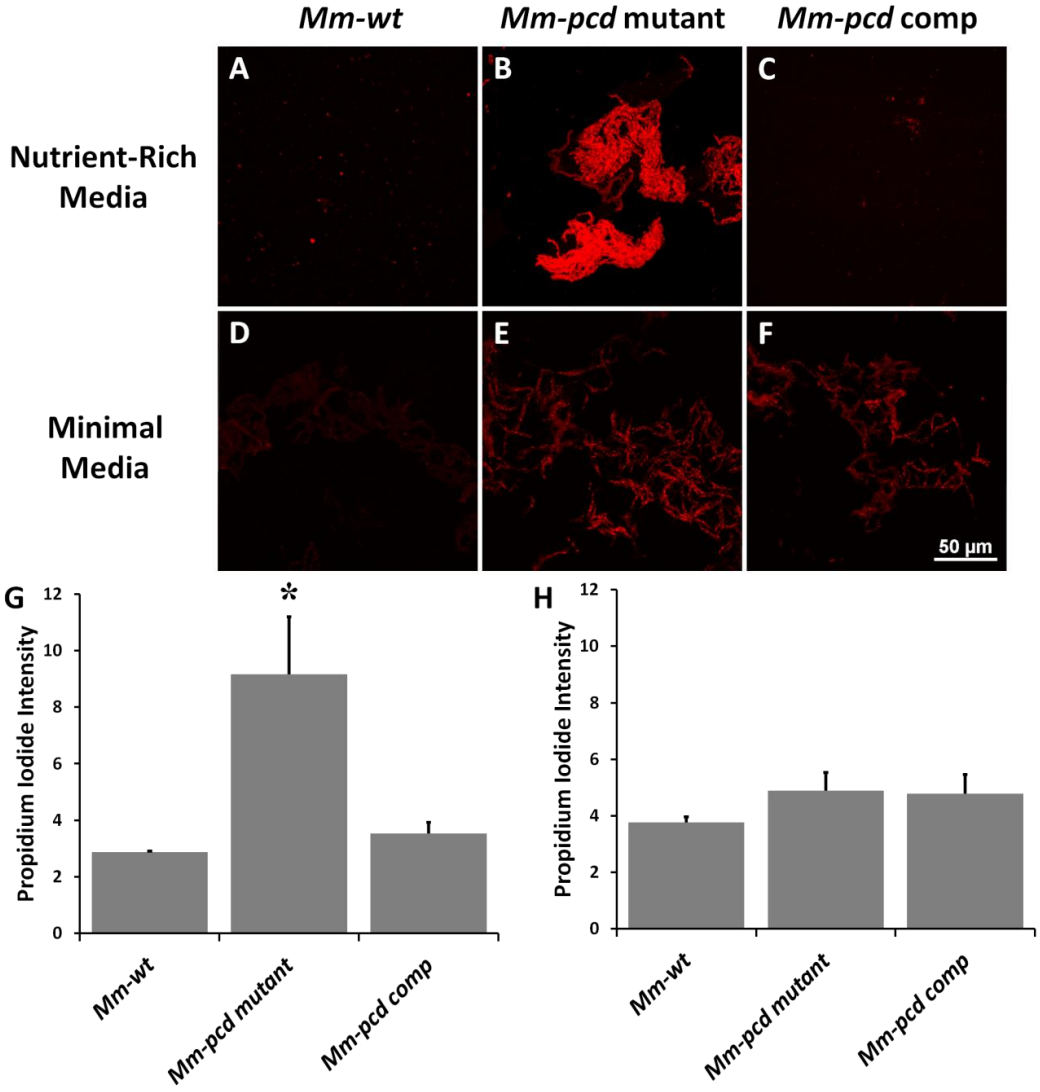

III.4 (F) Mm-luxR1 *Mutant is Defective in Macrophage Cell Entry*

Macrophages commonly encounter and phagocytose pathogenic mycobacteria. Parasitism of these cells occurs in a few distinct steps: association, adherence, entry and intracellular growth (Cosma et al., 2003). We used J774A.1 murine macrophages to examine each of these steps using the *Mm-luxR1* mutant and *Mm-wt*. We did not observe any significant differences in association and adherence for the *Mm-luxR1* mutant as compared to *Mm-wt* (data not shown). However, we did observe a significant decrease in entry into macrophages for the *Mm-luxR1* mutant as compared to the *Mm-wt* ($p = 0.0005$) and the *Mm-luxR1* complemented clone ($p = 0.0003$) (Figure 30). We also observed a reduction in intracellular growth in the *Mm-luxR1* mutant as compared to *Mm-wt*. These macrophage infection assays suggest that the *Mm-luxR1* gene is involved in *M. marinum* virulence through its role in macrophage infection.

Figure 30. *Mm-luxR1* Mutant Displays Attenuation in Macrophage Cell Entry
Macrophages (J774A.1) infected with multiplicity of infection (MOI) of 1 bacterium per cell of *Mm-wt*, *Mm-luxR1* mutant and *Mm-luxR1* complemented clone. Entry measured by percent amikacin resistant after 30 minutes. Percent entry is relative to number of bacteria inoculated into wells. *Mm-luxR1* mutant had a significantlyreduced macrophage entry as compared to *Mm-wt* (p=0.0005) and *Mm-luxR1* complemented clone (p=0.0003). Entry of *Mm-wt* and *Mm-luxR1* complemented clone display similar levels of entry (p=0.0952).

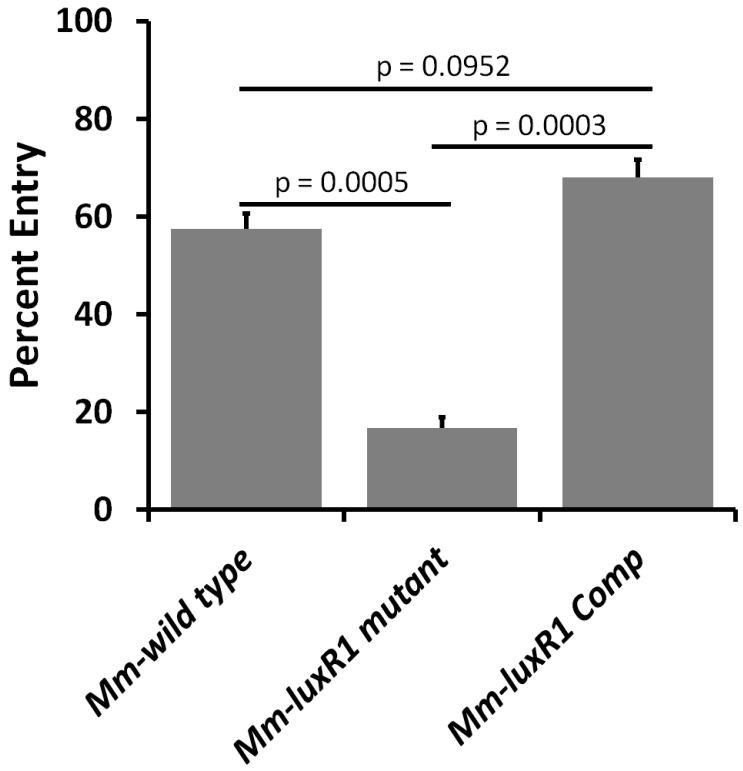

III.4 (G) Mm-luxR1 *Mutant is Attenuated in* C. elegans *Infection*

After finding that the *Mm-luxR1* gene impacts macrophage infection, we were interested in evaluating the behavior of the *Mm-luxR1* mutant in *C. elegans*. We infected *C. elegans* with *M. smegmatis*, *Mm-wt*, *Mm-luxR1* mutant, *Mm-pcd* mutant and their complemented clone strains (Figure 31). At two days post-infection we observed significant reduction of *C. elegans* mortality due to the *Mm-luxR1* mutant as compared to *Mm-wt* ($p = 0.0253$) (Figure 31 A). *C. elegans* infected with the *Mm-luxR1* mutant had over a 2-fold increase in survival as compared to *C. elegans* infected with *Mm-wt*. The *Mm-luxR1* complemented clone and the *Mm-luxR1* overexpressing strain had similar virulence in *C. elegans* as compared to *Mm-wt*. When the *Mm-pcd* mutant was used to infect *C. elegans*, it did not show attenuation as compared to *Mm-wt* ($p = 0.1481$) (Figure 31 B). Therefore, our *C. elegans* infection assays suggests that the *Mm-luxR1* gene is an important virulence factor in the *C. elegans* model, while *Mm-pcd* gene is not.

Figure 31. *Mm-luxR1* Mutant Displays Attenuation in the *C. elegans* Model of Infection. (A-B) Survival of wild-type (N2) nematodes infected with *luxR1* mutant in *M. marinum*, two days post-infection (day 6). Three trials of 20 nematodes (total n = 60) each were infected with the *luxR1* mutant and survival assessed on day 6. The survival rates of *C. elegans* infected with each *M. marinum* mutant were compared *C. elegans* infected with wild-type and p-values are shown (unpaired t-test). (A) Mean (±SEM) of *C. elegans* relative survival after infection with *Mm-wt*, *Mm-luxR1* mutant, *Mm-luxR1* complemented clone and *Mm-luxR1* over-expressing strain. *Mm-luxR1* mutant is significantly attenuated (p = 0.0253) in *C. elegans* as compared to *Mm-wt*. (B) Mean (±SEM) of *C. elegans* relative survival after infection with *Mm-wt*, *Mm-pcd* mutant, *Mm-pcd* complemented clone I (complemented with *pcd*) and *Mm-pcd* complemented clone II (complemented with *pcd* and *luxR1*). *Mm-pcd* did not display attenuation in *C. elegans*.

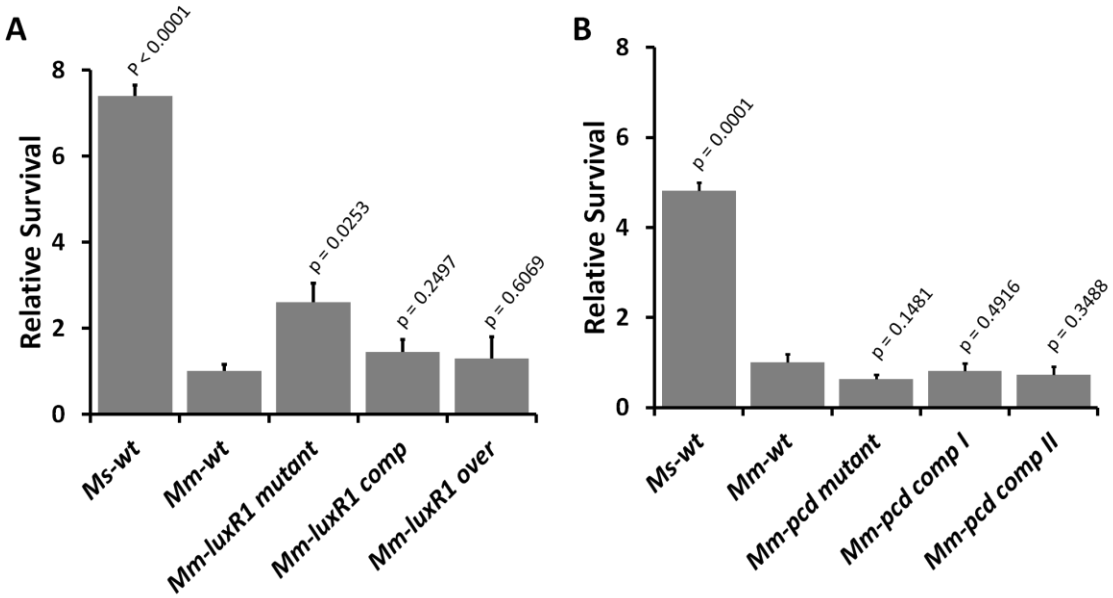

III.4 (H) Mm-luxR1 *Attenuation is Rescued When* C. elegans *is Co-Infected with* Mm-*Wild-type*

After finding that the *Mm-luxR1* gene is an important virulence factor in *C. elegans,* we examined the dynamics of *C. elegans* infection by mixed *M. marinum* culture of the *luxR1* mutant and wt. We used *M. marinum* strains tagged with two different fluorescent proteins, tdTomato and mCherry and performed competition assays in *C. elegans*. We infected *C. elegans* with *Mm-wt* and *M. marinum* mutant separately and with mixed cultures in parallel to evaluate competition in the same population of nematodes. We compared the *Mm-wt* and *Mm-pcd* mutant and found that they display colonization of the lower gut of *C. elegans,* even 6 hours post infection (Figure 32 P and Q, 33 P and Q). These observations support the *pcd* mutant is not attenuated in *C. elegans* (Figure 31 B). In both the competitive infection with *Mm-wt* and *Mm-pcd* mutant and infection by each strain alone, we observe colonization of the lower gut by these strains, even 6 hours post-infection (Figure 32 R and 33 R).

We infected *C. elegans* with *Mm-wt* and *Mm-luxR1* mutant and found that, while *Mm-wt* displayed colonization of the *C. elegans* lower gut (Figure 34 J, M, P and 35 J, M, P), the *Mm-luxR1* mutant did not show colonization of the *C. elegans* lower gut 6 hours post-infection (Figure 34 K, N, Q and 35 K, N, Q). These observations support the conclusion the *Mm-luxR1* mutant is significantly attenuated in *C. elegans* as compared to *Mm-wt* (Figure 31 A). When *Mm-wt* and *Mm-luxR1* mutant were co-infected into *C. elegans*, we observed rescue of the *Mm-luxR1* mutant and colonization of the *C. elegans* lower gut 6 hours post-infection (Figure 34 L, O, R and 35 L, O, R). This result indicates that either the function of *Mm-luxR1* gene can be complemented in trans by the *Mm-wt*; or infection with *Mm-wt* modulates the host response to allow the *Mm-luxR1* mutant to colonize the lower gut. These observations open new avenues of investigation into the function of *luxR1* and the *C. elegans* model needs to be further analyzed to better understand the mechanisms of susceptibility/resistance involved in colonization by *M. marinum*.

Figure 32. *Mm-wt* (tdTomato) vs. *Mm-pcd* Mutant (mCherry) Competitive Infections Show Co-colonization of the *C. elegans* Oro-Pharynx and Lower Gut.
Adult TP12 (*col-19*::GFP) nematodes infected with ψmm141 (*Mm-wt*::tdTomato), ψmm144 (*Mm-pcd* mutant::mCherry), or 1:1 mixed infection of ψmm141: ψmm144 were imaged at 4 and 24 hours during infection and 6 hours post-infection (30 hour). The head and lower-gut regions of 10 TP12 nematodes each at 4, 24 and 30 hour were imaged using confocal microscopy. A 40x oil-immersion objective and a digital zoom of 2.5x was used (effective magnification 100x). A spectral filter for excitation wavelengths of 500-640 nm was used, spectrally unmixed and colors chosen for the wavelength corresponding to each mycobacterial strain, ψmm141 (yellow) and ψmm144 (pink). (A-C) Nematode oro-pharynx after 4 hours of infection with ψmm141 (*Mm-wt*::tdTomato), ψmm144 (*Mm-pcd* mutant::mCherry) or both. (D-F) Nematode oro-pharynx after 24 hours of infection with ψmm141, ψmm144 or both. (G-I) Nematode oro-pharynx 6 hours post-infection. (J-K) Nematode lower gut after 4 hours of infection with ψmm141 (*Mm-wt*::tdTomato), ψmm144 (*Mm-pcd* mutant::mCherry) or both. (D-F) Nematode lower gut after 24 hours of infection to ψmm141, ψmm144 or both. (G-I) Nematode lower gut 6 hours post-infection. (P) *C. elegans* lower gut remained colonized with *Mm-wt* (tdTomato) 6 hours post-infection (yellow). (Q) *C. elegans* lower gut remained colonized with *Mm-pcd* (mCherry) 6 hours post-infection (pink). (R) *C. elegans* lower gut remained colonized with both *Mm-wt* (tdTomato) and *Mm-pcd* (mCherry) 6 hours post-infection (yellow & pink).

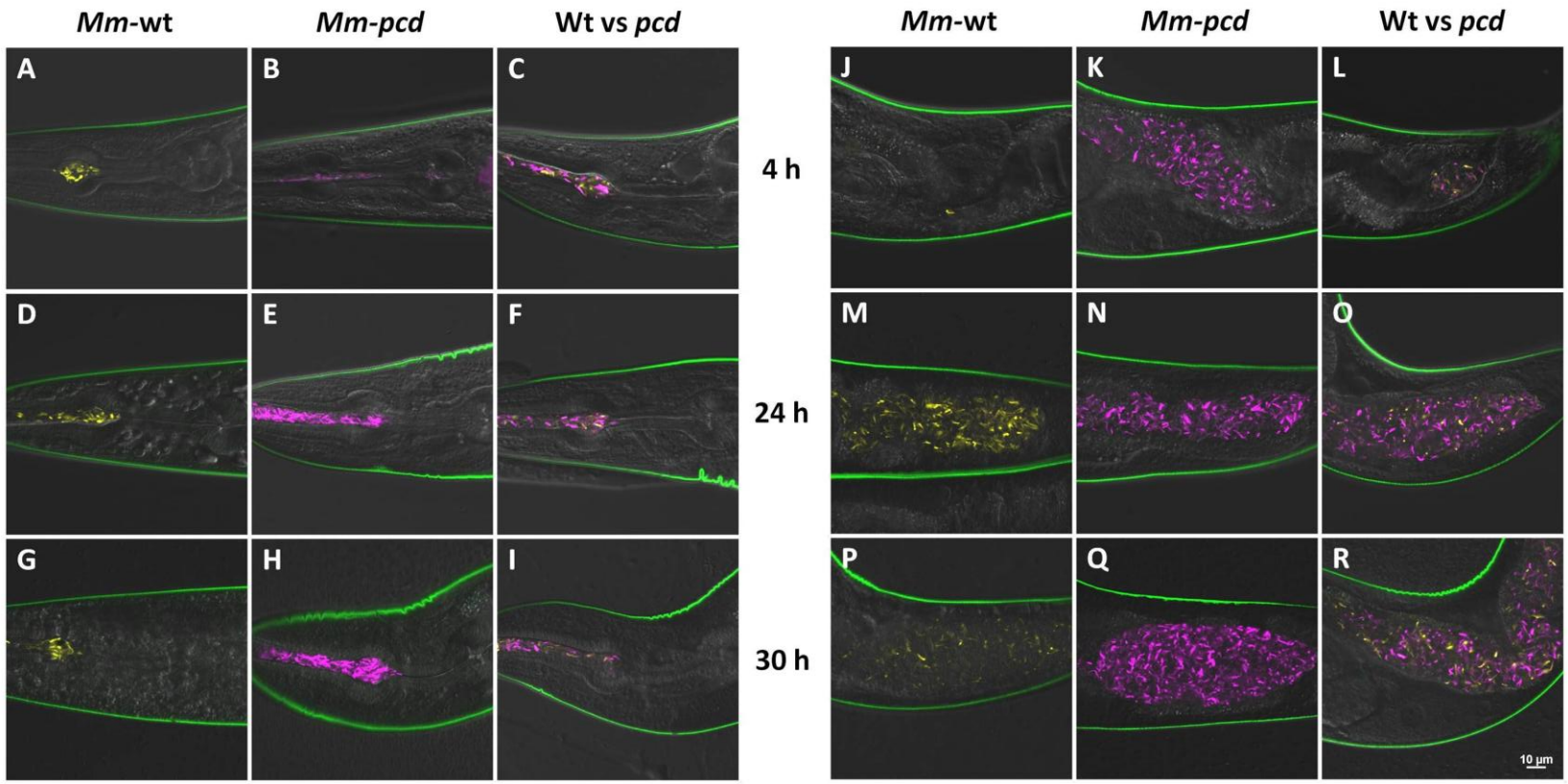

M. marinum wild-type vs. *pcd* mutant

M. marinum wild-type vs. *pcd* mutant

Figure 33. *Mm-wt* (mCherry) vs. *Mm-pcd* Mutant (tdTomato) Competitive Infections Show Co-colonization of the *C. elegans* Oro-Pharynx and Lower Gut.
Adult TP12 (*col-19*::GFP) nematodes infected with ψmm142 (*Mm-wt*::mCherry), ψmm143 (*Mm-pcd* mutant::tdTomato), or 1:1 mixed infection of ψmm142: ψmm143 were imaged at 4 and 24 hours during infection and 6 hours post-infection (30 hour). The head and lower-gut regions of 10 TP12 nematodes each at 4, 24 and 30 hour were imaged using confocal microscopy. A 40x oil-immersion objective and a digital zoom of 2.5x was used (effective magnification 100x). A spectral filter for excitation wavelengths of 500-640 nm was used, spectrally unmixed and colors chosen for the wavelength corresponding to each mycobacterial strain, ψmm142 (red) and ψmm143 (light blue). (A-C) Nematode oro-pharynx after 4 hours of infection with ψmm142 (*Mm-wt*::mCherry), ψmm143 (*Mm-pcd* mutant::tdTomato) or both. (D-F) Nematode oro-pharynx after 24 hours of infection with ψmm142, ψmm143 or both. (G-I) Nematode oro-pharynx 6 hours post-infection. (J-K) Nematode lower gut after 4 hours of infection with ψmm142 (*Mm-wt*::mCherry), ψmm143 (*Mm-pcd* mutant::tdTomato) or both. (D-F) Nematode lower gut after 24 hours of infection with ψmm142, ψmm143 or both. (G-I) Nematode lower gut 6 hours post-infection. (P) *C. elegans* lower gut remained colonized with *Mm-wt* (mCherry) 6 hours post-infection (red). (Q) *C. elegans* lower gut remained colonized with *Mm-pcd* (tdTomato) 6 hours post-infection (light blue). (R) *C. elegans* lower gut remained colonized with both *Mm-wt* (mCherry) and *Mm-pcd* (tdTomato) 6 hours post-infection (red & light blue).

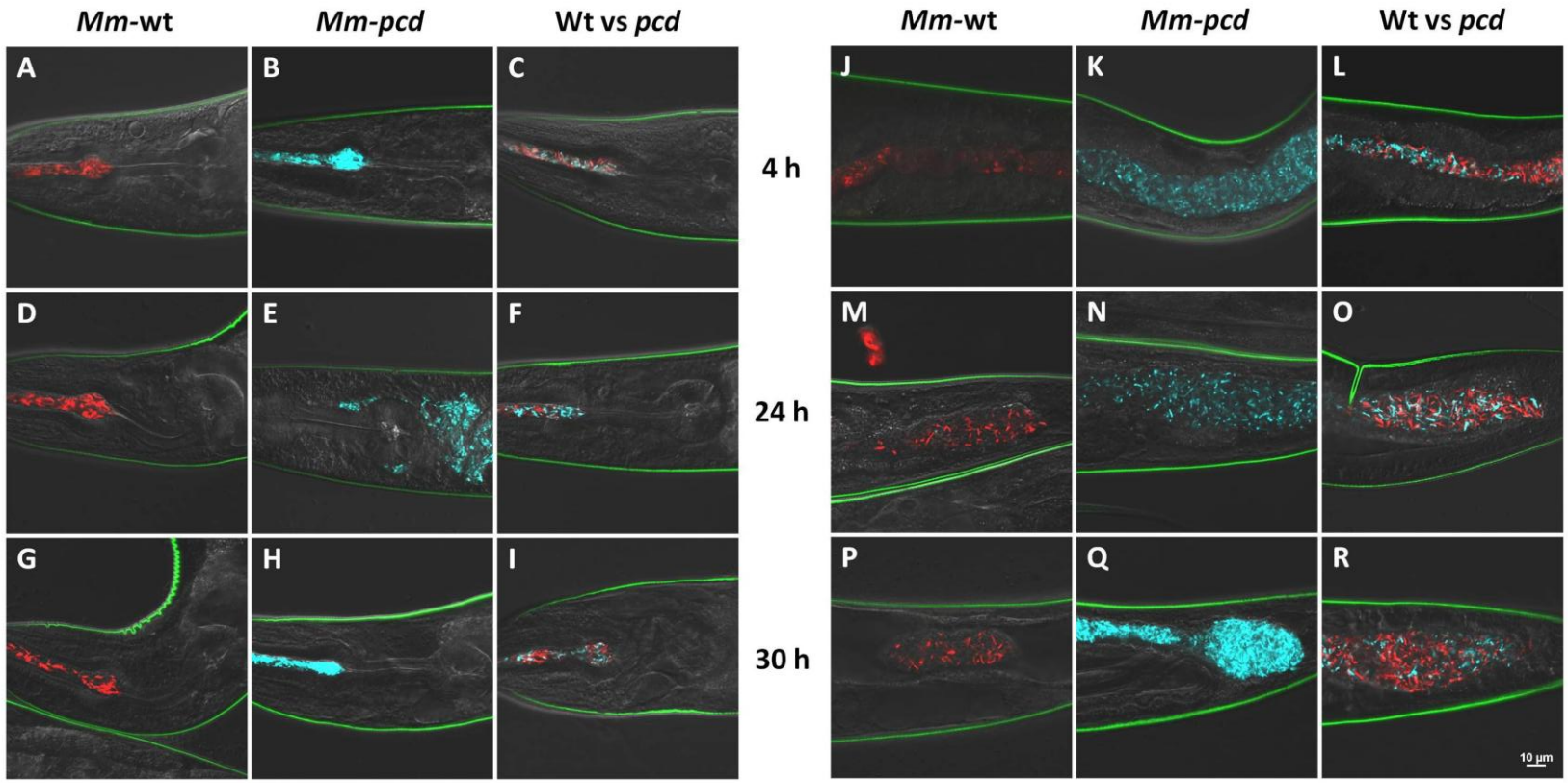

M. marinum wild-type vs. *pcd* mutant

M. marinum wild-type vs. *pcd* mutant

Figure 34. *Mm-wt* (tdTomato) vs. *Mm-luxR1* Mutant (mCherry) Competitive Infections Rescue Attenuation of *luxR1* and Increase Colonization. Adult TP12 (*col-19*::GFP) nematodes infected with ψmm141 (*Mm-wt*::tdTomato), ψmm146 (*Mm-luxR1* mutant::mCherry), or 1:1 mixed infection of ψmm141: ψmm146 were imaged at 4 and 24 hours during infection and 6 hours post-infection (30 hour). The head and lower-gut regions of 10 TP12 nematodes each at 4, 24 and 30 hour were imaged using confocal microscopy. A 40x oil-immersion objective and a digital zoom of 2.5x was used (effective magnification 100x). A spectral filter for excitation wavelengths of 500-640 nm was used, spectrally unmixed and colors chosen for the wavelength corresponding to each mycobacterial strain, ψmm141 (yellow) and ψmm146 (red). (A-C) Nematode oro-pharynx after 4 hours of infection with ψmm141 (*Mm-wt*::tdTomato), ψmm146 (*Mm-luxR1* mutant::mCherry) or both. (D-F) Nematode oro-pharynx after 24 hours of infection with ψmm141, ψmm146 or both. (G-I) Nematode oro-pharynx 6 hours post-infection. (J-K) Nematode lower gut after 4 hours of infection with ψmm141 (*Mm-wt*::tdTomato), ψmm146 (*Mm-luxR1* mutant::mCherry) or both. (D-F) Nematode lower gut after 24 hours of infection with ψmm141, ψmm146 or both. (G-I) Nematode lower gut 6 hours post-infection. (P) *C. elegans* lower gut remained colonized with *Mm-wt* (tdTomato) 6 hours post-infection (yellow). (Q) *C. elegans* lower gut shows reduced levels of colonization with *Mm-luxR1* (mCherry) 6 hours post-infection (red). (R) *C. elegans* lower gut shows much higher level of colonization with *Mm-luxR1* (mCherry) 6 hours post-infection (red), essentially rescuing its attenuation phenotype.

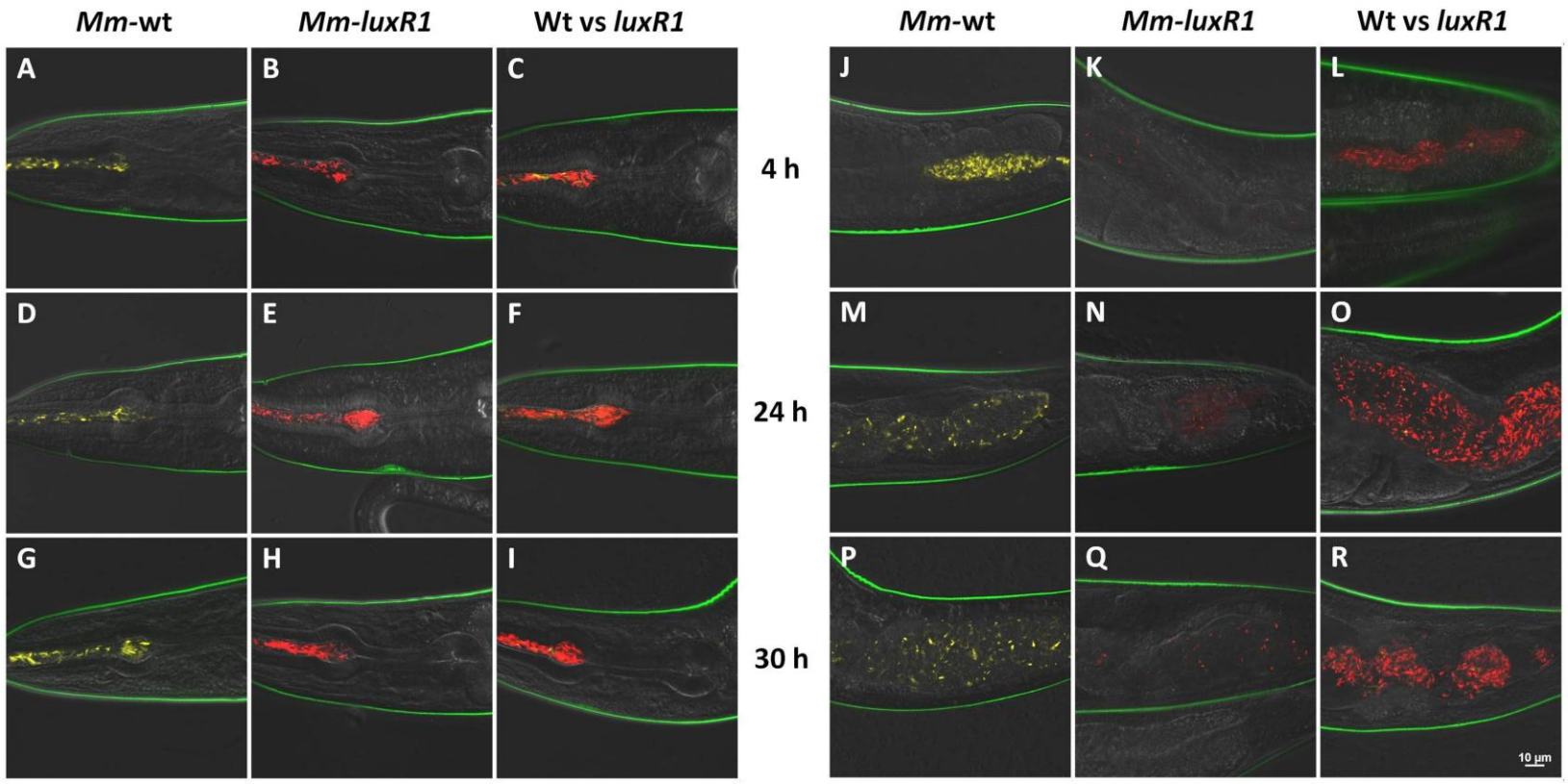

M. marinum wild-type vs. *luxR1* mutant

M. marinum wild-type vs. *luxR1* mutant

Figure 35. *Mm-wt* (mCherry) vs. *Mm-luxR1* Mutant (tdTomato) C**ompetitive Infections Rescue Attenuation of *luxR1* and Increase Colonization.** Adult TP12 (*col-19*::GFP) nematodes infected with ψmm142 (*Mm-wt*::mCherry), ψmm145 (*Mm-luxR1* mutant::tdTomato), or 1:1 mixed infection of ψmm142: ψmm145 were imaged at 4 and 24 hours during infection and 6 hours post-infection (30 hour). The head and lower-gut regions of 10 TP12 nematodes each at 4, 24 and 30 hour were imaged using confocal microscopy. A 40x oil-immersion objective and a digital zoom of 2.5x was used (effective magnification 100x). A spectral filter for excitation wavelengths of 500-640 nm was used, spectrally unmixed and colors chosen for the wavelength corresponding to each mycobacterial strains, ψmm142 (red) and ψmm145 (blue). (A-C) Nematode oro-pharynx after 4 hours of infection with ψmm142 (*Mm-wt*::mCherry), ψmm145 (*Mm-luxR1* mutant::tdTomato) or both. (D-F) Nematode oro-pharynx after 24 hours of infection with ψmm142, ψmm145 or both. (G-I) Nematode oro-pharynx 6 hours post-infection. (J-K) Nematode lower gut after 4 hours of infection with ψmm142 (*Mm-wt*::mCherry), ψmm145 (*Mm-luxR1* mutant::tdTomato) or both. (D-F) Nematode lower gut after 24 hours of infection to ψmm142, ψmm145 or both. (G-I) Nematode lower gut 6 hours post-infection. (P) *C. elegans* lower gut remained colonized with *Mm-wt* (mCherry) 6 hours post-infection (red). (Q) *C. elegans* lower gut shows reduced levels of colonization with *Mm-luxR1* (tdTomato) 6 hours post-infection (blue). (R) *C. elegans* lower gut shows much higher level of colonization with *Mm-luxR1* (tdTomato) 6 hours post-infection (red), essentially rescuing its attenuation phenotype.

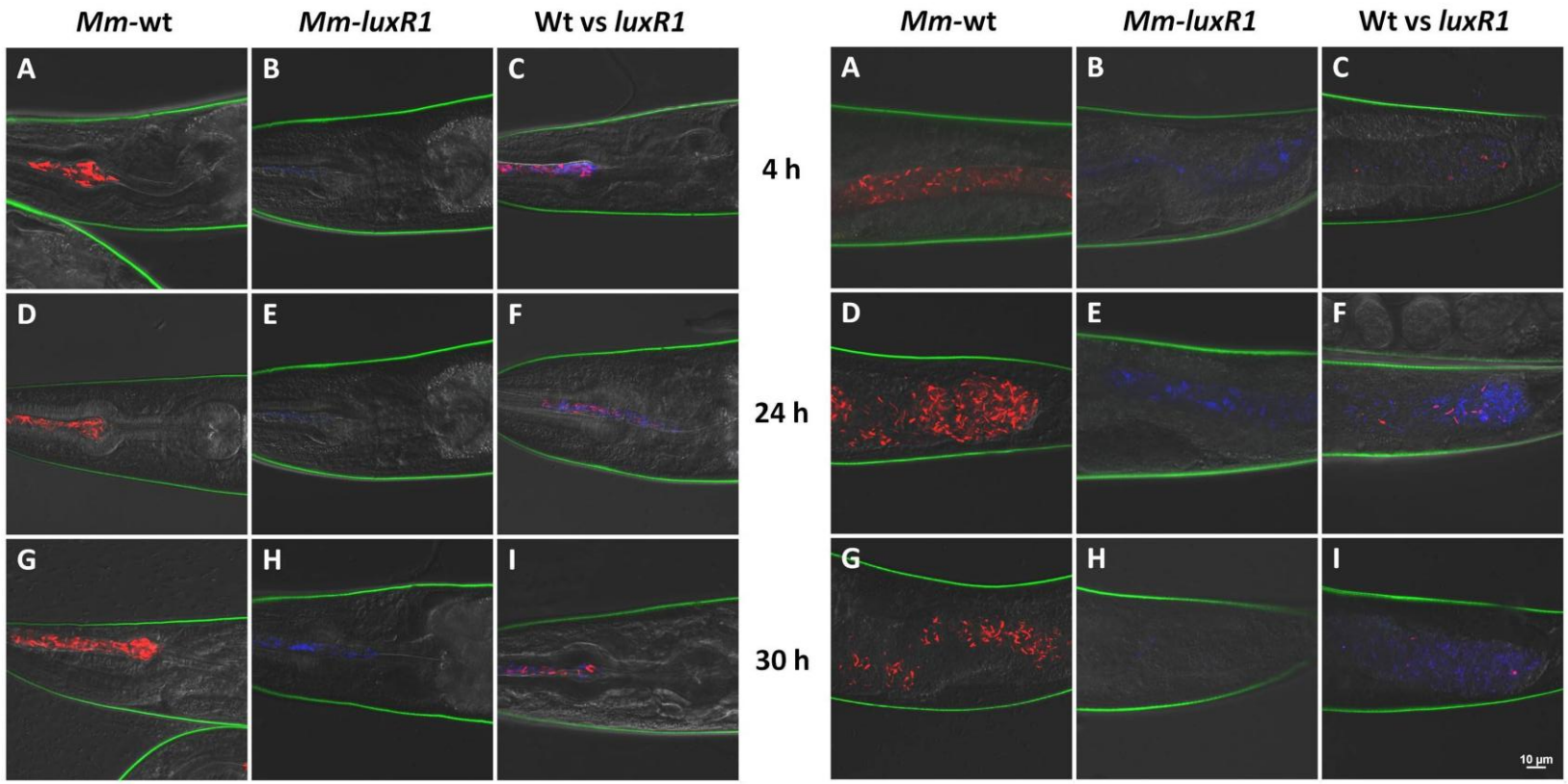

M. marinum wild-type vs. *luxR1* mutant

M. marinum wild-type vs. *luxR1* mutant

Figure 36. Proposed Model for the Function of Mycobacterial Virulence Factor LuxR1 Protein. The mycobacterial LuxR1 protein has a DNA binding helix-turn-helix motif and an auto-inducer binding domain. LuxR1 can act as a repressor under log phase and be displaced upon binding of an auto-inducer. LuxR1 can thereby regulate transcription of virulence factors that allow the pathogen to infect macrophages and *C. elegans*.

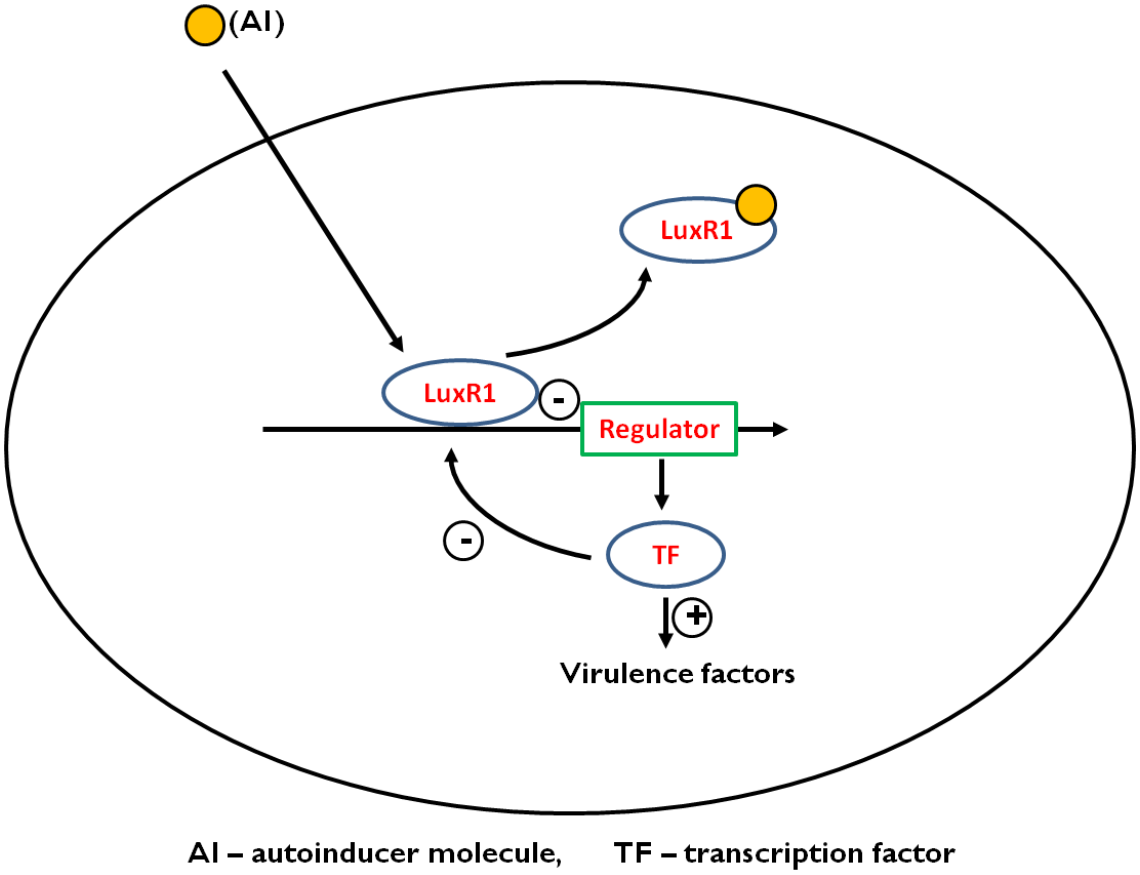

III.5 Discussion

Mycobacterial species have several genes with similarity to luxR in other species. However, most of these have not yet been characterized. We examined one of these genes, *Mm-luxR1* and evaluated its role in *M. marinum* virulence. *Mm-luxR1* was a of particular interest because a non-pathogenic mycobacteria, *M. smegmatis* does not have an ortholog for this gene, its deduced protein product has motifs similar to those found in *V. harveyi* LuxR and an *Mtb*-luxR1 mutant displays attenuation in macrophages. We propose that LuxR1 is a master regulator that controls virulence genes involved in mycobacterial pathogenesis (Figure 36).

In most bacterial species the *luxR* gene is part of an operon. We demonstrated that *Mm-luxR1* is most likely part of a common transcript with *Mm-pcd* and a hypothetical gene (MMAR-1241). Further studies are needed to better understand the function of this operon in *M. marinum*. It is also important to determine whether this operon is present and has a similar role in virulence of other pathogenic mycobacteria, such as and *Mtb* and *M. avium*. This operon could be confirmed using 5'-Rapid Amplification of cDNA Ends (RACE) and 3'-RACE. To demonstrate the specific nucleotides where transcription begins and ends. An understanding of the structure of this transcript will allow identification of promoter regions involved in repression and coordinated regulation of this operon.

In nutrient rich MADC media, we observed rapid growth of both the *Mm-pcd* mutant and *Mm-luxR1* mutant as compared to *Mm-wt*. We observed a similar trend in biofilm formation assays, where both the *Mm-luxR1* and *Mm-pcd* mutants display

increased biofilm formation. The observed increase in biofilm formation could be due to increased growth of the mutant strains or could be due to differences in the ability to form biofilms. Growth conditions that equalize the growth rates of these strains could be used to differentiate between these possibilities. In previous studies, *pcd* has been associated with biofilm formation in *M. avium* (Wu et al., 2009; Yamazaki et al., 2006). In these studies a *pcd* mutant displayed decreased in biofilm formation. It could be that our results were influenced by increased growth rates under the condition tested or *pcd* could have different functions in *M. marinum* than in *M. avium*. This is an area where further investigation is needed.

In order to use *M. marinum* as a model *Mtb* pathogen there should be parallels in the mechanisms used to parasitize the host. Since both the *Mtb-luxR1* and *Mm-luxR1* mutants have been tested in macrophages, their contribution to virulence can be compared. The *Mtb-luxR1* mutant displays a decrease in intracellular growth in macrophages, but does not differ in adherence, association or entry into macrophages as compared to *Mtb-wt*. The *Mm-luxR1* mutant, on the other hand, was attenuated in both entry and intracellular growth in macrophages, while displaying no differences in adherence and association as compared to *Mm-wt*. These observations validate our *M. marinum* model demonstrating that results we obtain in *M. marinum* can be translated to *Mtb*.

We also show that the *Mm-luxR1* mutant is attenuated in *C. elegans* infection. When *Mm-wt* and the *Mm-luxR1* mutant used to infect *C. elegans* together, we observe rescue of the *Mm-luxR1* mutant and colonization of the *C. elegans* gut. Our observations

using *C. elegans* and *M. marinum* competition assays open new possibilities for the use of the *C. elegans* model in study of the complex interactions involved in mixed bacterial infections.

CHAPTER IV

STUDYING THE INNATE IMMUNE RESPONSE TO MYCOBACTERIAL INFECTION UTILIZING *CAENORHABDITIS ELEGANS*

IV. 1 Summary

Mitogen activated protein kinase (MAPK) cell signaling pathways are critical mediators of host cell responses to pathogens. Pathogenic mycobacterial species activate all three major MAPK pathways, suggesting involvement in pathogenesis, but there is little evidence for their role in animals due to the developmentally detrimental effects of these mutations in mice. *Caenorhabditis elegans* has proven valuable for analysis of molecular host-pathogen interaction mechanisms, due to the vast array of tools available. Members of the genus *Mycobacterium* are important human pathogens, particularly due to infection of nearly one-third of the world's population by *Mycobacterium tuberculosis*. *Mycobacterium marinum*, an important aquatic pathogen that, due to its growth preference of <33°C, causes only skin infections in humans, is closely related to *M. tuberculosis*. We found that *C. elegans*, normally maintained at or near 20°C, infected with *M. marinum* for 24 h display >80% mortality. In contrast, when infected with the non-pathogenic mycobacteria *M. smegmatis*, <15% mortality is observed. Differences in bacterial load and localization suggest that pathogenic mycobacteria colonize *C. elegans* better than non-pathogenic mycobacteria. In addition, *C. elegans* display physiological and morphological changes when infected with pathogenic mycobacteria, implying that pathogenic mechanisms bring about these pathological

changes. Probing the potential role pathogenic and non-pathogenic *C. elegans* p38 MAPK revealed differences in the innate immune response against mycobacteria. A MAPK (*pmk-1*) mutant of *C. elegans* is hypersensitive to both *M. marinum* and *M. smegmatis*, while wild-type nematodes, with a functional copy of *pmk-1* resist *M. smegmatis* but not *M. marinum*. We propose that while a protctive innate immune response is triggered through p38 MAPK in *C. elegans*, pathogenic mycobacteria successfully inhibit this response, leading to increased mortality. Interestingly, *M. marinum* mutants affecting mammalian macrophage infection cause less mortality in *C. elegans* than wild type *M. marinum*. These observations establish *C. elegans* as a new host for study of mycobacterial pathogenic mechanisms and provide evidence for the importance of the MAPK-mediated innate immune response during infection.

IV.2 Introduction

The innate immune response acts as a key first line of defense in protecting the host against pathogens. Eukaryotic organisms recognize pathogen-associated molecular patterns (PAMPs) using a variety of pattern recognition receptors (PRRs) to trigger appropriate immune responses to invading pathogens (Kawai and Akira, 2010; Newton and Dixit, 2012). The innate immune response subsequently activates the adaptive immune response through expression of cytokines and chemokines, working in synergy with the adaptive immune response to defend the host (Iwasaki and Medzhitov, 2010). PRRs recognize conserved structures not present in eukaryotic cells, such as lipopolysaccharide (LPS), and trigger an initial immune response until the adaptive

immune response takes over (Janeway, 1989, 1992). Activation of the adaptive immune response takes 5 to 7 days and, in the absence of a functional innate immune response, this process is delayed or not appropriately activated (Medzhitov and Janeway, 1997). Among other functions, PRRs are important for activation of the inflammatory response and initiation of apoptosis (Medzhitov and Janeway, 1997). Several classes of PRRs are important in activation of innate immunity, including C-type lectin receptors (CLRs), Tol-like receptors (TLRs) and NOD-like receptors (NLRs) (Kingeter and Lin, 2012; Kleinnijenhuis et al., 2011). All PRPs identified activate a signaling cascade through the mitogen-activated protein kinase (MAPK) pathway in response to PAMPs (Kawai and Akira, 2010; Newton and Dixit, 2012), suggesting that MAPK is a key mediator of immunity. The MAP kinase pathways are highly conserved in eukaryotic species and MAPK-p38 and MAPK-JNK are primarily activated in response to environmental stresses and inflammation (Roach and Schorey, 2002; Sendide et al., 2005). As a result of this role, MAPK is one of the primary early signaling pathways that lead to the initiation of the inflammatory response after bacterial infection (Koul et al., 2004).

While most current therapeutics and interventions focus on the pathogen and host adaptive immune system, the innate immune response is also critical for suppressing mycobacterial growth (Brightbill et al., 1999; Pan et al., 2005). During mycobacterial infections, the innate immune response is first activated when mycobacteria encounter macrophages in the lung or other initial sites of infection (Roach and Schorey, 2002; Tse et al., 2002). The innate immune response continues to play a role throughout the early course of infection, while the T cell-mediated adaptive immune response is activated

shortly afterward and helps to reduce the bacterial load (Stenger and Modlin, 1999). When mycobacteria come in contact with macrophages, ERK and p38 are activated by phosphorylation leading to induction of the inflammatory response through production of IL-10 and TNF-α (Schorey and Cooper, 2003; Shiratsuchi et al., 2008; Souza et al., 2007). A major mycobacterial surface molecule, lipoarabinomannan (LAM), is known to act as a PAMP that activates the host innate immune response through MAPK (Chatterjee and Khoo, 1998; Strohmeier and Fenton, 1999). The LAM on the surface of pathogenic mycobacteria, such as *M. tuberculosis*, is mannose-capped (Man-LAM); whereas, non-pathogenic mycobacteria, such as *M. smegmatis*, have arabinosylated LAM (Ara-LAM). Ara-LAM induces high levels of cytokines and inflammatory mediators such as TNF-α, IL-1α, and IL-10, while Man-LAM suppresses activation of MAPK and, thereby, inflammatory cytokines (Dahl et al., 1996; Juffermans et al., 2000; Knutson et al., 1998; Roach et al., 1993). Despite the differences in activation of MAPK and the inflammatory response during in vitro interactions with host cells that correlate with mycobacterial virulence, the role of the MAPK pathway and its significance in mycobacterial infections in vivo is not well understood.

In *C. elegans*, there are three p38 isoforms, designated *pmk-1-3*, which coordinate the MAPK pathway responses to stresses, including pathogenic bacteria (Coleman and Mylonakis, 2009; Dierking et al., 2011; Padmanabhan et al., 2009; Shivers et al., 2009; Troemel et al., 2006; Ziegler et al., 2009). PMK-1, the best characterized of the p38 isoforms, modulates the immune response and helps reduce oxidative damage and egg laying defects during environmental stresses and in the

presence of pathogens (Mertenskotter et al., 2013; Montalvo-Katz et al., 2013; Papp et al., 2012; Yang et al., 2013).

We found that susceptibility of *C. elegans* to *M. marinum* is controlled by the p38 MAPK pathway, suggesting that the innate immune response is a key component of nematode resistance against mycobacterial infection. These studies demonstrate that *C. elegans* can be used as a virulence model for pathogenic mycobacteria that allows detailed analysis of both bacterial virulence factors and the innate immune response, in particular the MAPK pathway, a difficult pathway to analyze in mammalian hosts.

IV.3 Experimental Procedures

IV.3 (A) Bacterial Growth Conditions

A wild-type clinical isolate of *M. marinum* strain M (Ramakrishnan, 1997), *M. smegmatis* mc^2155 and *E. coli* OP50 were used for *C. elegans* infection to characterize host-pathogen interactions. Two constitutively expressing tdTomato fluorescent mycobacterial strains (ψmm91 and ψmm23) were derived by transforming *M. marinum* and *M. smegmatis* with a multi-copy plasmid, pJDC60 (pFJS8ΔGFP::tdTomato, under a PL5 promoter, with kanamycin selection). These strains were used to study mycobacterial localization within *C. elegans* nematodes after infection. *M. marinum* cultures were grown at 32ºC standing in T25 tissue culture flasks. *E. coli* and *M. smegmatis* cultures were grown at 37ºC shaking in sterile disposable glass test tubes. *M. marinum* and *M. smegmatis* were grown in Middlebrook 7H9 media (Difco, Sparks, MD) supplemented with 0.5% glycerol, 10% albumin-dextrose complex (ADC) and

0.25% Tween 80 (M-ADC-TW), while *E. coli* was grown in Miller's Luria Broth (NPI, Mt. Prospect, IL).

IV.3 (B) C. elegans *Maintenance and Synchronization*

N2 (Bristol, wild-type), KU25 [*pmk-1*(km25)], IG10 [*tol-1*(nr2033)], NU3 [*dbl-1*(nk3)], GR1307 [*daf-16*(mgDf50)], EU31 [*skn-1*(zu135)], JT366 [*vhp-1*(sa366)] and TP12 [*kaIs12*(col-19::GFP)] *C. elegans* strains were used in this study. The nematodes were grown and maintained on nematode growth media (NGM) plates using standard methods at room temperature (Brenner, 1974). Room temperature was regularly monitored and maintained at between 19ºC to 21ºC. Synchronous cohorts of *C. elegans* were obtained by lysing gravid nematodes using an alkaline bleach solution (Emmons et al., 1979). After removing the bleach solution and washing the embryos, they were stored in M9 buffer overnight to obtain L1 larvae. These L1 larvae were transferred onto NGM plates seeded with *E. coli* for growth of age-synchronized nematodes.

IV.3 (C) C. elegans *Infection with Bacterial Cultures and Recovery*

Bacterial cultures were grown until they reached stationary phase. 70 µl of *E. coli*, *M. smegmatis* or *M. marinum* were seeded on small tissue culture dishes (35x10 mm, Falcon), with NGM agar by spreading the bacteria to cover over $3/4^{th}$ of the infection plates. These plates were placed at room temperature overnight to allow bacterial cultures to grow, equilibrate/stabilize and become ready for infection the next day. Three day old age-synchronized adult *C. elegans* were washed with ddH_20 to remove residue *E. coli* and transferred onto plates seeded with *E. coli*, *M. smegmatis* or *M. marinum*. Cohorts of *C. elegans* were infected for a period of 4, 24 or 48 hours with each

individual bacterial strain. After the period of infection, the nematodes were transferred on to small NGM recovery plates with *E. coli* seeded in the center of each plate. 20 nematodes were incubated per small recovery NGM plate and cohorts of 60 nematodes were used for each bacterial infection. Nematodes were counted daily and transferred onto fresh *E. coli* plates every other day until experimental nematodes stopped laying eggs. Then they were transferred every 3-4 days to avoid overgrowth of *E. coli* until the nematodes reached senescence and died. The nematodes were considered dead if they were unresponsive to touch by the picker. Each bacterial infection was repeated at least three times with 20, 40 or 60 nematodes, unless stated otherwise. *C. elegans* were incubated at room temperature (19ºC to 21ºC) for all experiments.

IV.3 (D) Survival, Bagging and Morphological Characterization of C. elegans

C. elegans L1 larvae incubated on *E. coli* seeded NGM plates after synchronization were considered 0 days old. They were grown for three days at room temperature before bacterial infection. On day 4, they were recovered onto fresh *E. coli* seeded NGM plates and followed for survival and changes in morphology. The number of nematodes that died due to bagging of the adult nematode (where embryos hatch within the adult and cause the death of the adult) on day 5 and 6 was determined. Nematodes that lost their dark pigmentation after bacterial infection were designated as depigmented. Nematodes that were less than 2/3rd the length of a healthy nematode were designated as having a shortened length. On day 6, depigmented and shorter nematode numbers were determined. Nematodes that died prior to 15 days were considered to have a shortened lifespan.

IV.3 (E) RNAi Knock-Down Mutagenesis of C. elegans

After bleaching to age-synchronize the *C. elegans*, N2 L1 larvae were inoculated on small NGM plates seeded with *E. coli* strain HT115 (DE3) with RNAi constructs cloned into the pL4440-DESTvector and selected for ampicillin resistance (100 µg/ml). *E. coli* strains producing dsRNA of *pmk-1, tol-1*, *dbl-1*, *daf-16, skn-1* and *vhp-1* genes were used (Appendix Table 2). 50 µl of E. coli with each RNAi plasmid was added to the plates on day one and two of N2 knock-down mutant growth. Adult N2 knock-down mutants were then infected with wild-type *M. smegmatis* or *M. marinum* on day three as described above and their susceptibility to infection with mycobacteria was assessed.

IV.3 (F) Survival Assays for C. elegans *Mutants*

C. elegans L1 larvae were obtained for each of the *C. elegans* mutant strains *pmk-1, tol-1*, *dbl-1*, *daf-16, skn-1* and *vhp-1*. They were incubated on *E. coli* seeded NGM plates after synchronization and grown for three days at room temperature before subjecting to bacterial infection. On day 4, they were recovered onto fresh *E. coli* seeded NGM plates and followed for survival and changes in morphology.

IV.3 (G) C. elegans *Mutant Confirmation Through RT-PCR and qPCR*

Age-synchronized N2 L1 larvae were incubated on plates seeded with *E. coli* producing each of the individual dsRNA for the target gene (Appendix Table 2). Three day old adult nematodes were obtained and RNA was extracted after dissolving the nematodes in trizol. cDNA was produced using random primers and qPCR was run for each target gene (Appendix Table 3). *Cdc-42* and *pmp-3* were used as control constitutively expressed genes. Age-synchronized 3 day old nematodes from each mutant strain were used in this study and also used for RT-PCR confirmation.

IV.3 (H) Statistical Analyses

Parametric two tailed unpaired t-tests were used to compare the means of different bacterial infection groups at distinct time points using GraphPad Prism software. Means, standard deviations and standard errors were calculated using GraphPad Prism software and Microsoft Excel spreadsheets. A non-parametric log-rank statistical method was used to determine the difference in survival of groups of *C. elegans* after infection, using an online application for survival analysis of lifespan assays found on http://sbi.postech.ac.kr/oasis (released on May 2009; last accessed on March 20th 2014) (Yang et al., 2011).

IV.4 Results

IV.4 (A) MAPK Plays an Important Role in Protection From Mycobacteria

In mammalian macrophages, the MAP-kinase pathway is important in the initial response to mycobacterial infection (Roach and Schorey, 2002; Tse et al., 2002), but the importance of MAPK in the complex multi-cellular response of whole animals remains unclear, most likely due to the critical nature of this gene during development. In *C. elegans*, there is evidence that MAPK can play a role in defense against bacterial pathogens, but mycobacteria have not been examined (Jebamercy et al., 2013; Mertenskotter et al., 2013; Papp et al., 2012). We used our *C. elegans* virulence model to evaluate the role of MAPK in mycobacterial infection. *E. coli* expressing RNAi was used to knock-down *pmk-1* MAPK in *C. elegans* and found that the resulting nematodes were more susceptible to *M. marinum* infections, with significantly higher mortality at two days post-infection (Figure 37A-B). Interestingly, *C. elegans* with reduced MAPK expression are more susceptible to *M. marinum* and *M. smegmatis* (Figure 37B), suggesting that protection from both pathogenic and non-pathogenic mycobacteria involves MAPK. We also infected a *C. elegans pmk-1* mutant with *M. marinum* and *M. smegmatis* and found that they displayed a similar, and possibly greater, increase in mortality, with 100% mortality during the first 24 h of infection with *M. marinum* (Figure 37C-D). Our results suggest that the p38 MAPK pathway plays an important role in defense against mycobacterial infections.

Figure 37. *pmk-1* Gene Plays an Important Role in The *C. elegans* Innate Immune Response to Mycobacteria (A) The *pmk-1* RNAi knock-down strain has a significant reduction in viability after infection to *M. marinum* as compared to wild-type *C. elegans* (p = 0.0324). The *tol-1*, *dbl-1*, and *daf-16* RNAi knock-down strains do not display a significantly reduction in viability as compared to wild-type *C. elegans* (unpaired t-test). (B) Relative survival of *pmk-1* RNAi knock-down strains infected with *Ms* and *Mm* two days post infection as compared to wild-type *C. elegans*. (C) The *C. elegans pmk-1* mutant has a significantly reduction in viability two days after *M. marinum* infection (p <0.0001). (D) Survival of a *C. elegans pmk-1* mutant after 24 hours of infection. *Mm* vs. *Ms* Chi^2 statistic of 119.00 (p <0.0001); *Mm* and *E. coli* Chi^2 statistic of 119.00 (p <0.0001); *Ms* vs. *E. coli* Chi^2 statistic of 42.25 (p <0.0001).

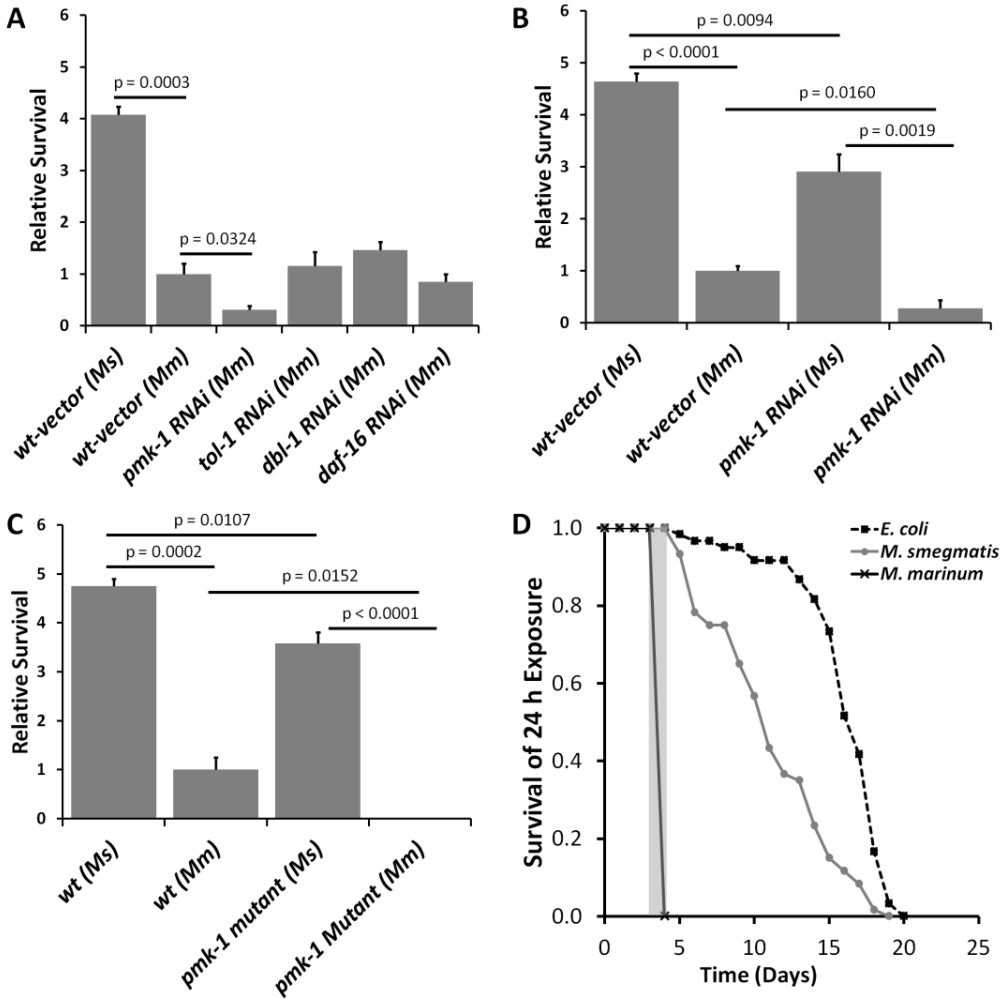

Figure 38. Morphological Changes in *pmk-1* Mutant *C. elegans* Infected with Bacteria. (A-D) 3 trials of 20 adult *pmk-1* (km25) mutant nematodes each (total n = 60) were infected with *E. coli* (OP50), *M. smegmatis* (MC^2155) or *M. marinum* (ψmm1) for 24 hours, and morphological changes were characterized. P-values are shown comparing *E. coli* to *M. smegmatis* infection and *M. smegmatis* to *M .marinum* infection (unpaired t-test). (A) Mean (±SEM) number of nematodes that died by 11 days post-infection (day 15), were characterized as having a shortened lifespan. (B) Mean (±SEM) number of nematodes that bagged and died by 2 days post-infection (day 6). (C-D) For each trial, the percentage of depigmentation and shortened length was determined for the remaining nematodes after initial mortalities due to bacterial infection. (C) Mean (±SEM) number of nematodes with a loss of pigmentation by 2 days post-infection (day 6), determined by a visible reduction in cuticular pigmentation. (D) Mean (±SEM) number of nematodes with a length of less than $2/3^{rd}$ the length of a healthy adult nematode by 2 days post-infection (day 6).

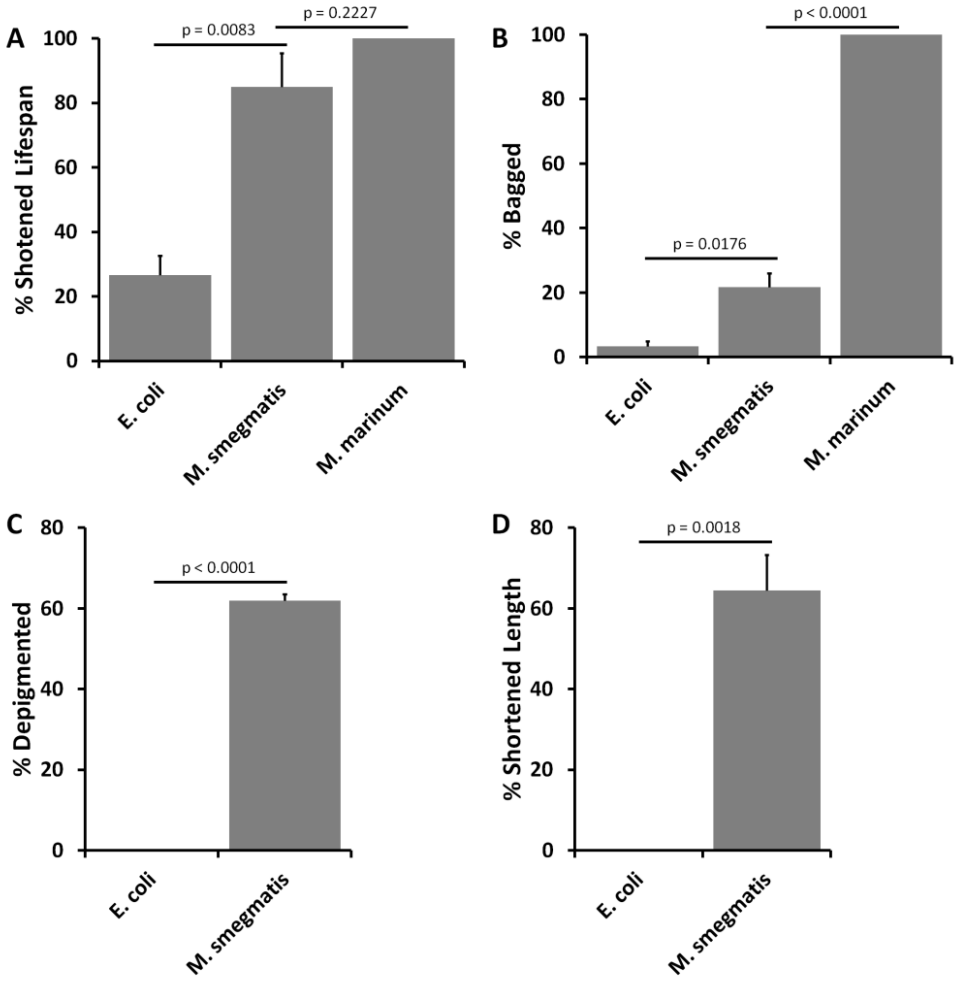

IV.4 (B) MAPK Is a Key Pathway for Protection from Mycobacterial Infection

In addition to the MAPK pathway, several alternative signaling pathways have been shown to play roles in *C. elegans* defense against pathogenic bacteria, including TOL-like receptor, TGF-β and insulin-like receptor pathways. The insulin-like signaling pathway is known to increase resistance to microbial invasion (Evans et al., 2008; Singh and Aballay, 2009). The TOL-like receptors and the TGF-β pathway have been shown to be important in both Gram-positive and -negative infections (Tenor and Aballay, 2008). We used RNAi knock-down, similar to that used for MAPK, to evaluate the role of the *C. elegans tol-1* (TOL-like pathway), *dbl-1* (TGF-β) and *daf-16* (insulin-like pathway) genes in the innate immune response to mycobacterial infection. The *tol-1*, *dbl-1* nor *daf-16* RNAi knock-down had an impact on viability of *C. elegans* after *M. marinum* infection (Figure 37A). We confirmed our results with RNAi knock-downs using *C. elegans* mutants in *tol-1, dbl-1* and *daf-16* (Figure 39). In fact, these mutants displayed a trend of increased resistance, rather than susceptibility to *M. marinum* infection, though they were not statistically significant. These observations suggest that knocking out alternative pathogen resistance pathways could stimulate or prepare the MAPK pathway for activation against mycobacterial infection. Our results indicate that while the MAPK pathway (*pmk-1)* plays an important role in the defense against *M. marinum* infections, TOL-like receptors, TGF-β and insulin-like signaling pathways, which are important for other pathogens, do not play an important role in *C. elegans* resistance to mycobacterial infection.

Figure 39. *tol-1, dbl-1* and *daf-16* Genes Play Less Important Roles in *C. elegans* Innate Immune Response To Mycobacteria (A) Survival of *tol-1*, *dbl-1* and *daf-16 C. elegans* mutants two days post-infection with *M. marinum*. (B) Survival of *tol-1 C. elegans* mutant after 24 hours of infection. *Mm* vs. *Ms* Chi^2 statistic of 85.22 ($p < 0.0001$); *Mm* vs. *E. coli* Chi^2 statistic of 88.00 ($p < 0.0001$); *Ms* vs. *E. coli* Chi^2 statistic of 0.01 ($p = 0.9219$). (C) Survival of *dbl-1 C. elegans* mutant after 24 hours of infection. *Mm* vs. *Ms* Chi^2 statistic of 15.98 ($p = 0.0001$); *Mm* vs. *E. coli* Chi^2 statistic of 23.10 ($p < 0.0001$); *Ms* vs. *E. coli* Chi^2 statistic of 1.69 ($p = 0.1939$). (D) Survival of *daf-16 C. elegans* mutant after 24 hours of infection. *Mm* vs. *Ms* Chi^2 statistic of 58.11 ($p < 0.0001$); *Mm* vs. *E. coli* Chi^2 statistic of 57.05 ($p < 0.0001$); *Ms* vs. *E. coli* Chi^2 statistic of 0.20 ($p = 0.6574$).

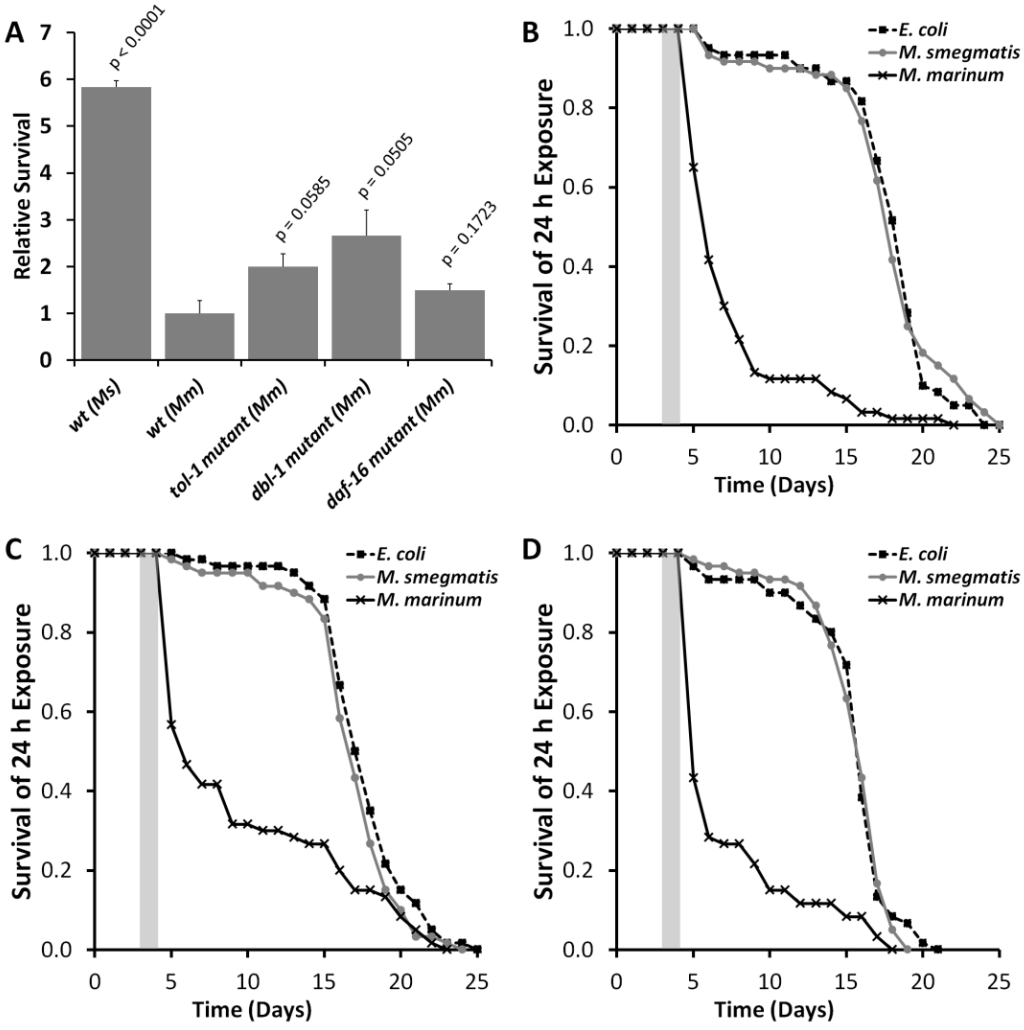

Figure 40. Morphological Changes in *tol-1* Mutant *C. elegans* Infected with Bacteria. (A-D) 3 trials of 20 adult *tol-1*(nr2033) mutant nematodes each (total n = 60) were infected with *E. coli* (OP50), *M. smegmatis* (MC^2155) and *M. marinum* (ψmm1) for 24 hours, and morphological changes were evaluated. P-values are shown comparing *E. coli* to *M. smegmatis* infection and *M. smegmatis* to *M. marinum* infection (unpaired t-test). (A) Mean (±SEM) number of nematodes that died by 11 days post-infection (day 15), designated as having a shortened lifespan. (B) Mean (±SEM) number of nematodes that bagged and died by 2 days post-infection (day 6). (C-D) For each trial, the percentage depigmentation and shortened length were was determined for the remaining nematodes after initial mortalities due to infection. (C) Mean (±SEM) number of nematodes with a loss of pigmentation by 2 days post-infection (day 6), determined through a visible reduction in cuticular pigmentation. (D) Mean (±SEM) number of nematodes with a length of less than $2/3^{rd}$ the length of a healthy adult nematode at 2 days post-infection (day 6).

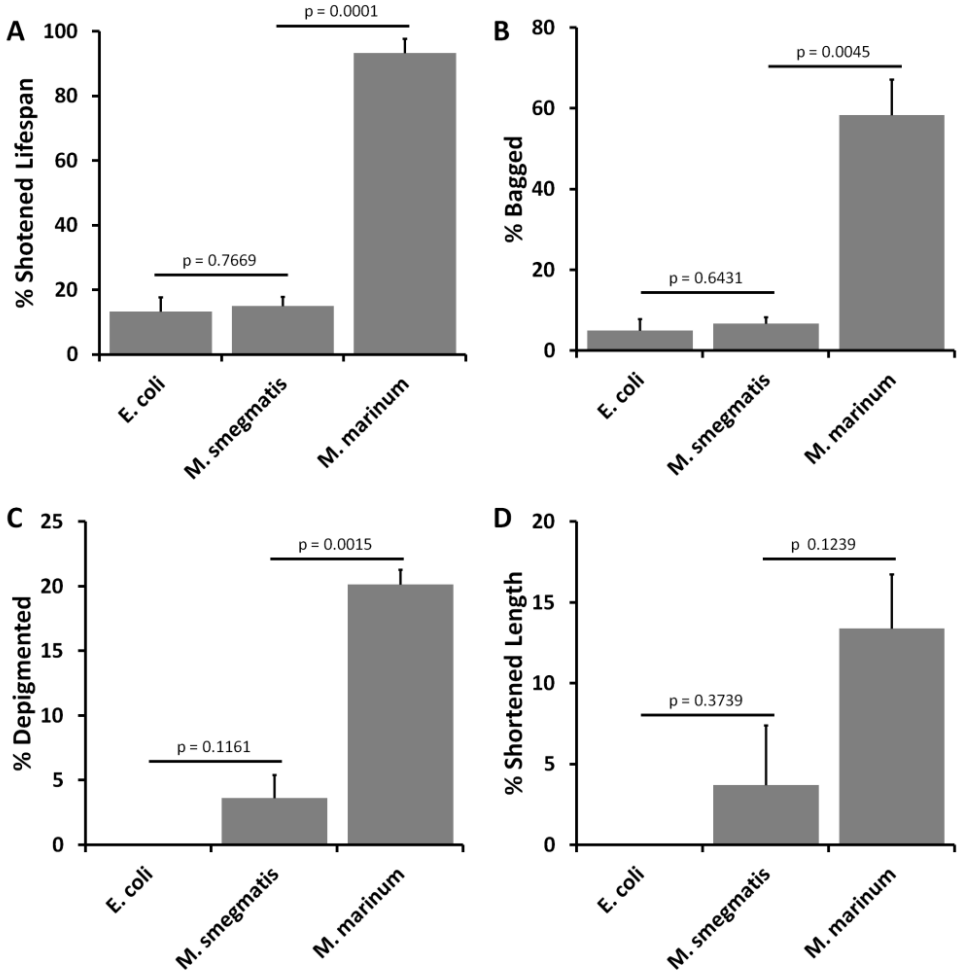

Figure 41. Morphological Changes in *dbl-1* Mutant *C. elegans* Infected with Bacteria. (A-D) 3 trials of 20 adult *dbl-1*(nk3) nematodes each (total n = 60) were infected with *E. coli* (OP50), *M. smegmatis* (MC^2155) and *M. marinum* (ψmm1) for 24 hours, and morphological changes were evaluated. P-values are shown comparing *E. coli* to *M. smegmatis* infection and *M. smegmatis* to *M. marinum* infection (unpaired t-test). (A) Mean (±SEM) number of nematodes that died by 11 days post-infection (day 15), designated as having a shortened lifespan. (B) Mean (±SEM) number of nematodes that bagged and died by 2 days post-infection (day 6). (C-D) For each trial, the percentage of depigmentation and shortened length were determined for the remaining nematodes after initial mortalities due to infection. (C) Mean (±SEM) number of nematodes with a loss of pigmentation by 2 days post-infection (day 6), determined through a visible reduction in cuticular pigmentation. (D) Mean (±SEM) number of nematodes with a length of less than 2/3rd the length of a healthy adult nematode at 2 days post-infection (day 6).

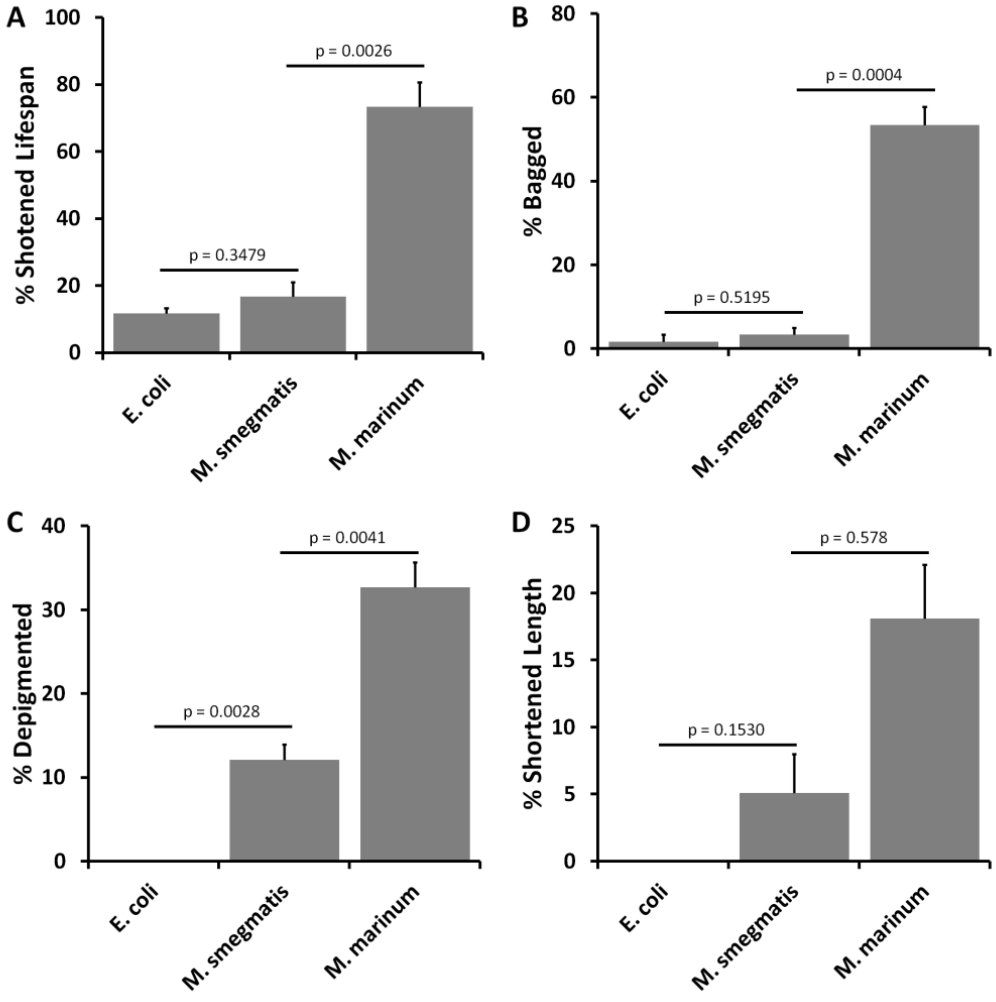

Figure 42. Morphological Changes in *daf-16* Mutant *C. elegans* Infected with Bacteria. (A-D) 3 trials of 20 adult *daf-16*(mgDf50) mutant nematodes each (total n = 60) were infected with *E. coli* (OP50), *M. smegmatis* (MC^2155) and *M. marinum* (ψmm1) for 24 hours, and morphological changes were evaluated. P-values are shown comparing *E. coli* to *M. smegmatis* infection and *M. smegmatis* to *M. marinum* infection (unpaired t-test). (A) Mean (±SEM) number of nematodes that died by 11 days post-infection (day 15), designated as having a shortened lifespan. (B) Mean (±SEM) number of nematodes that bagged and died by 2 days post-infection (day 6). (C-D) For each trial, the percentage depigmentation and shortened length were determined for the remaining nematodes after initial mortalities due to infection. (C) Mean (±SEM) number of nematodes with a loss of pigmentation by 2 days post-infection (day 6), determined through a visible reduction in cuticular pigmentation. (D) Mean (±SEM) number of nematodes with a length of less than 2/3rd the length of a healthy adult nematode at 2 days post-infection (day 6).

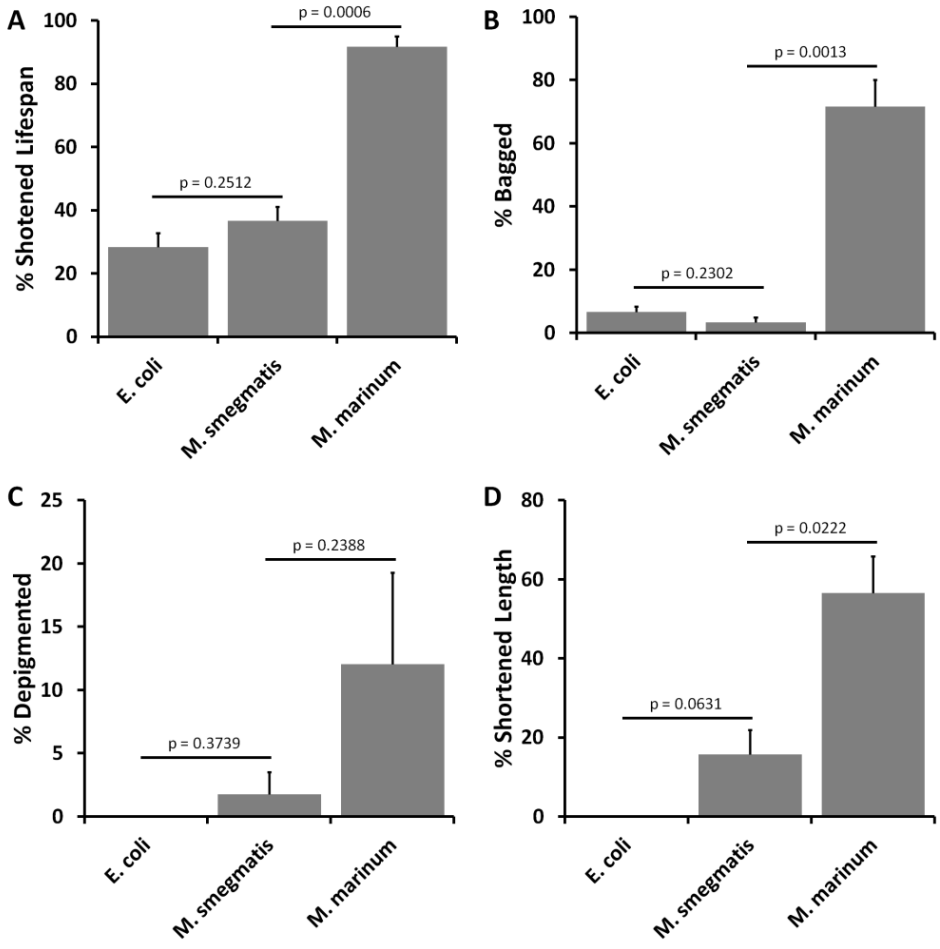

IV.4 (C) MAPK-Mediated Resistance to Mycobacteria is Partially Through skn-1 *Regulation*

One of the primary mechanisms by which the MAPK pathway in *C. elegans* controls innate immunity is through the down-stream transcription factor SKN-1 (Papp et al., 2012). The *skn-1* gene, analogous to the essential mammalian *nrf1* and *nrf2* cap-n-collar subfamily of basic leucine zipper transcription factors involved in protection from oxidative stress and regulation of the proteasome, is activated during the *C. elegans* response to stress, in particular oxidative stress and bacterial infection (Glover-Cutter et al., 2013; Papp et al., 2012; Staab et al., 2013). Based on the known function of *skn-1*, we felt that it was a likely candidate for playing a role in mediating resistance to mycobacterial infection. We infected *C. elegans skn-1* RNAi knock-down nematodes with *M. smegmatis* and *M. marinum* and found no difference in susceptibility to mycobacterial infection as compared to wild type *C. elegans* (Figure 43A).

Despite the apparent lack of mortality due to mycobacterial infection in the RNAi knock-down strains, the *M. marinum* infected nematodes did display some pathological changes, including depigmentation and low mortality (data not shown).When a *skn-1* mutant was used, rather than just knocking down expression, we observed significantly reduced survival for both the *M. marinum* and *M. smegmatis* infected nematodes (Figure 43C). Mortality of *M. marinum* and *M. smegmatis* infected nematodes were similar to that observed with the *pmk-1* mutant (Figure 37D); however, there was significantly less bagging ($p<0.0001$) in the *skn-1* mutant as compared to the *pmk-1* mutant (Figure 38B and 44B). However, the *skn-1* mutant displayed high frequencies of depigmentation and mortality (Figure 44C), similar to, but not as high as, the *pmk-1* mutant. These observations suggest that *skn-1* is involved in the mechanism of MAPK-mediated resistance to mycobacteria, but it is likely that MAPK also controls other transcriptional regulators that play a role in innate immunity to mycobacterial infections in *C. elegans*.

Figure 43. Modulation of *C. elegans* MAPK Pathway Determines the Extent of Resistance to Mycobacterial Infection. (A) Relative survival of *skn-1* and *vhp-1* RNAi knock-down strains of *C. elegans* at two days post-infection with *M. smegmatis* (Ms) and *M. marinum* (Mm) for 24 h. All calculations are relative to *C. elegans* infected with *E. coli*. (B) *skn-1* and *vhp-1* knock-down mutants infected with *Mm* and *Ms*. (C) Survival of the *C. elegans skn-1* mutant after 24 hours of infection. Log rank analysis: *Mm* vs. *Ms* $p < 0.0001$; *Mm* vs. *E. coli* $p < 0.0001$; *Ms* vs. *E. coli* $p < 0.0001$. (D) Survival of the *C. elegans vhp-1* mutant after 24 hours of infection. *Mm* vs. *Ms* Chi^2 statistic of 40.85 ($p < 0.0001$); *Mm* vs. *E. coli* Chi^2 statistic of 37.72 ($p < 0.0001$); *Ms* vs. *E. coli* Chi^2 statistic of 0.01 ($p = 0.9173$).

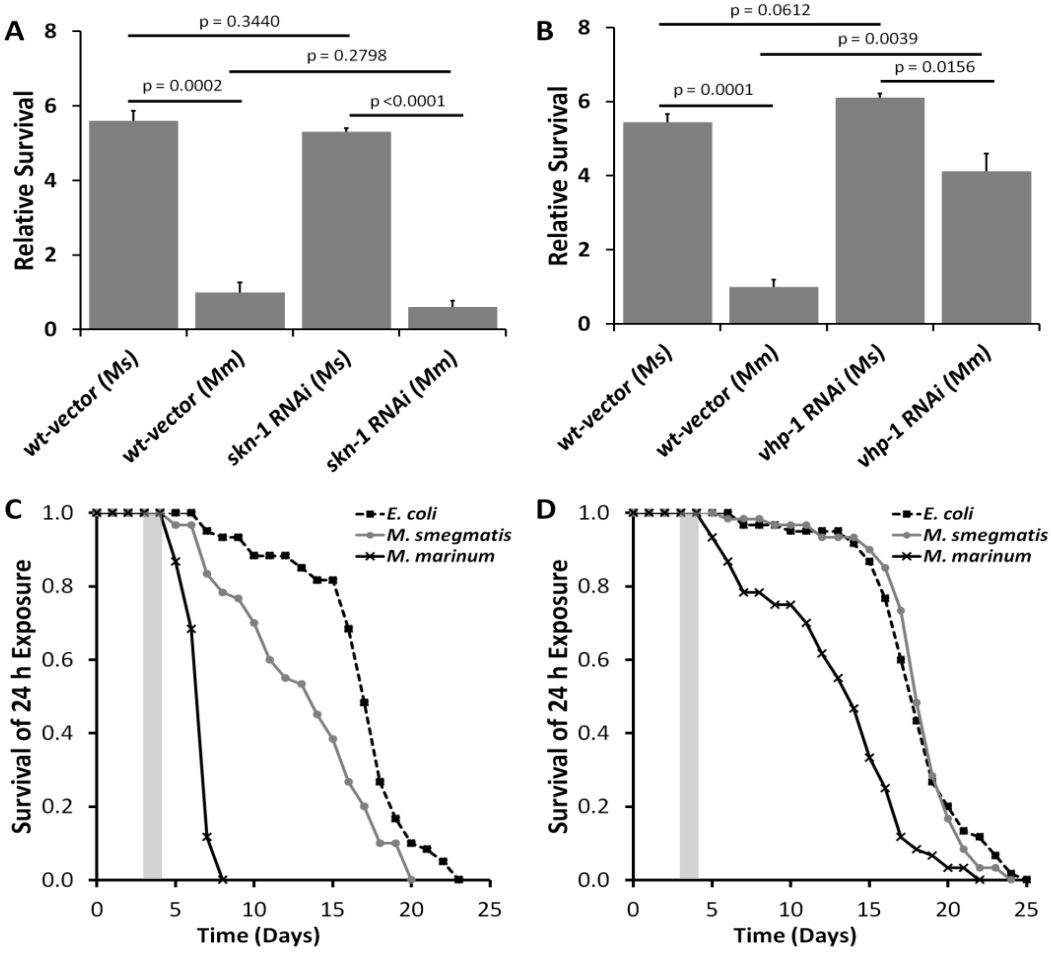

Figure 44. Morphological Changes in *skn-1* Mutant *C. elegans* Infected with Bacteria. (A-D) 3 trials of 20 adult *skn-1* (zu135) mutant nematodes each (total n = 60) were infected with *E. coli* (OP50), *M. smegmatis* (MC^2155) and *M. marinum* (ψmm1) for 24 hours, and morphological changes were evaluated. P-values are shown comparing *E. coli* to *M. smegmatis* infection and *M. smegmatis* to *M. marinum* infection (unpaired t-test). (A) Mean (±SEM) number of nematodes that died by 11 days post-infection (day 15), designated as having a shortened lifespan. (B) Mean (±SEM) number of nematodes that bagged and died by 2 days post-infection (day 6). (C-D) For each trial, the percentage depigmentation and shortened length were determined for the remaining nematodes after initial mortalities due to infection. (C) Mean (±SEM) number of nematodes with a loss of pigmentation by 2 days post-infection (day 6), determined through a visible reduction in cuticular pigmentation. (D) Mean (±SEM) number of nematodes with a length of less than 2/3rd the length of a healthy adult nematode at 2 days post-infection (day 6).

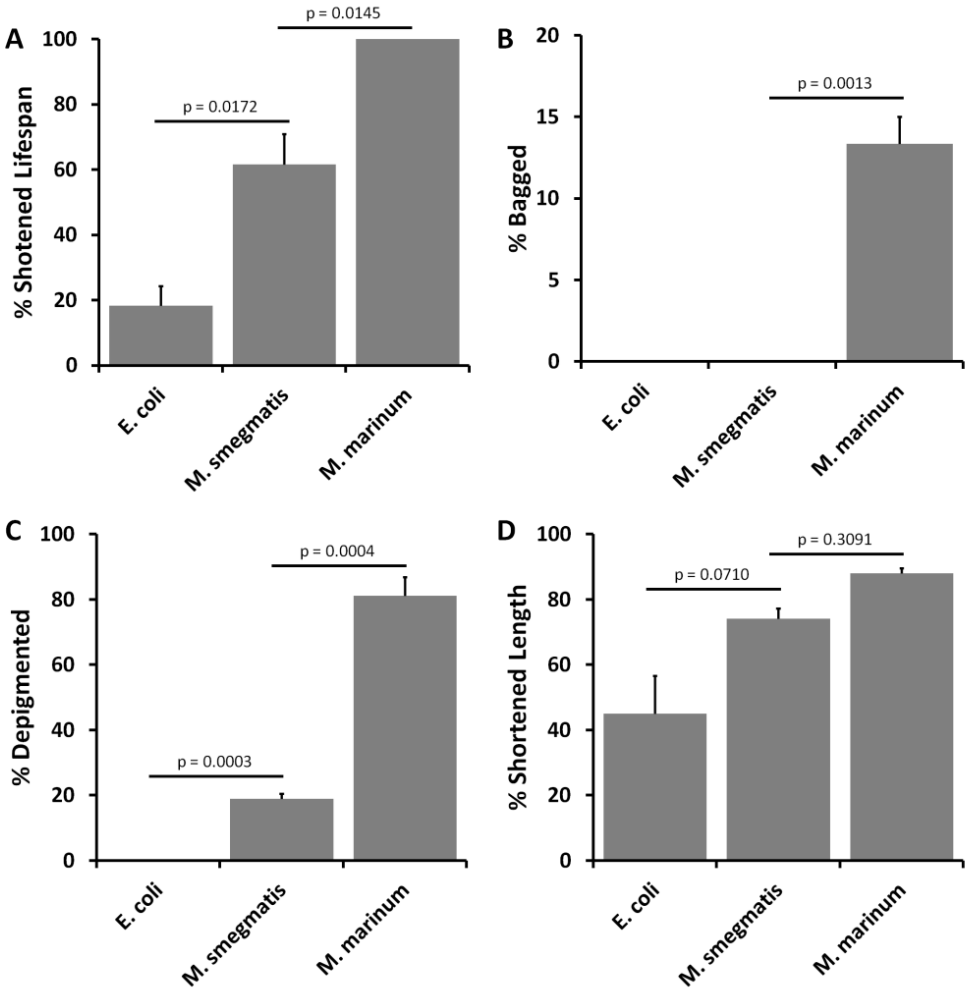

IV.4 (D) MAPK-Mediated Resistance is Inhibited by Pathogenic Mycobacteria Through vhp-1

In *C. elegans*, it is known that the MAPK phosphatase *vhp-1* acts as an inhibitor of the *pmk-1* MAPK pathway and can modulate the innate immune response (Kim et al., 2004). We infected *vhp-1* RNAi knock-down nematodes with *M. smegmatis* and *M. marinum* and we found that a *C. elegans vhp-1* knock-down strain displays resistance to killing by *M. marinum* as compared to wild type nematodes (Figure 43B). Similarly, a *vph-1* mutant displays significantly improved survival post-infection by *M. marinum* (Figure 43D). These observations suggest that one mechanism pathogenic mycobacteria may use to block MAPK activation and the innate immune response is induction of *vhp-1*. Induction of *vhp-1* would inhibit MAPK, increasing susceptibility of *C. elegans* to mycobacterial infection. These data suggest that the differences in MAPK induction by pathogenic and non-pathogenic mycobacteria could be important for innate immunity and may help explain why pathogenic mycobacteria can circumvent the innate immune response and cause disease in healthy individuals.

Figure 45. Morphological Changes in *vhp-1* Mutant *C. elegans* Infected with Bacteria. (A-D) 3 trials of 20 adult *vhp-1* (sa366) mutant nematodes each (total n = 60) were infected with *E. coli* (OP50), *M. smegmatis* (MC^2155) and *M. marinum* (ψmm1) for 24 hours, and morphological changes were evaluated. P-values are shown comparing *E. coli* to *M. smegmatis* infection and *M. smegmatis* to *M. marinum* infection (unpaired t-test). (A) Mean (±SEM) number of nematodes that died by 11 days post-infection (day 15), designated as having a shortened lifespan. (B) Mean (±SEM) number of nematodes that bagged and died by 2 days post-infection (day 6). (C-D) For each trial, the percentage depigmentation and shortened length were determined for the remaining nematodes after initial mortalities due to infection. (C) Mean (±SEM) number of nematodes with a loss of pigmentation by 2 days post-infection (day 6), determined through a visible reduction in cuticular pigmentation. (D) Mean (±SEM) number of nematodes with a length of less than $2/3^{rd}$ the length of a healthy adult nematode at 2 days post-infection (day 6).

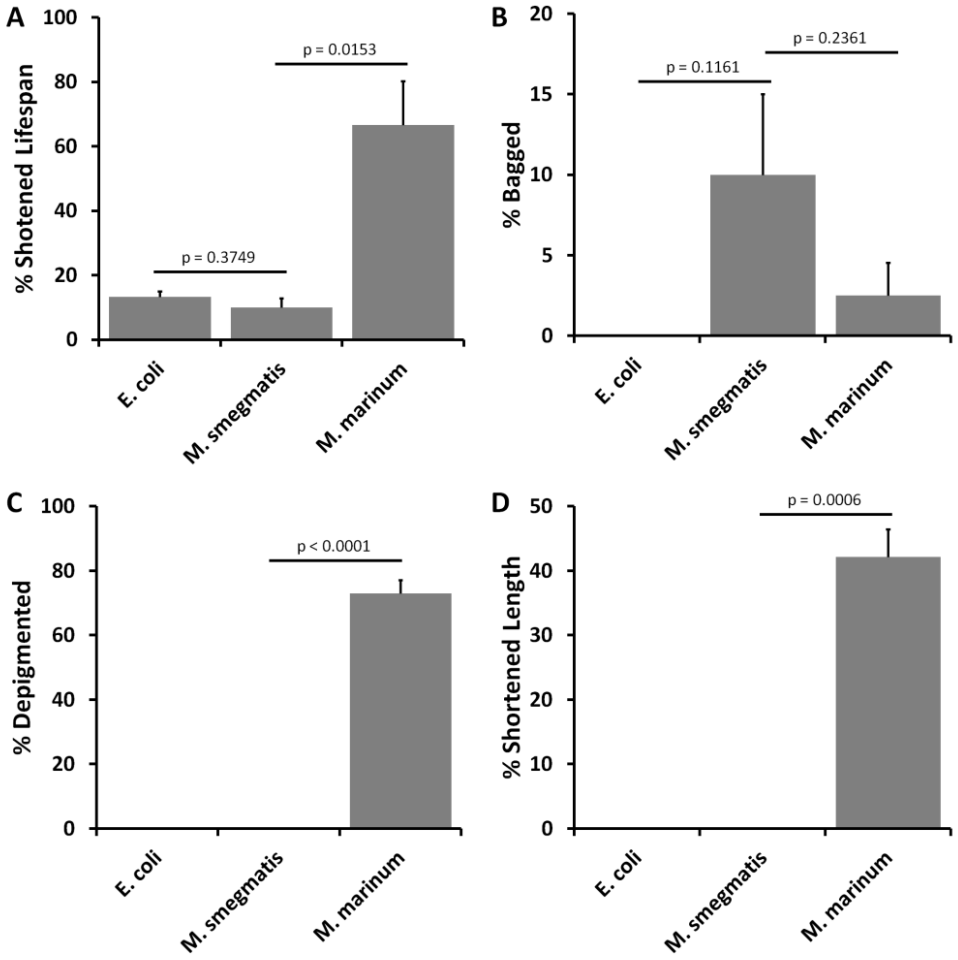

Figure 46. Activation of the MAPK Pathway is Important in the *C. elegans* Innate Immune Response to Mycobacterial Infection. (A) When infected with mycobacteria, the *C. elegans* MAPK pathway (*pmk-1*) is activated leading to an innate immune response to eliminate the pathogen. A MAPK phosphatase, VHP-1 inhibits the activation of MAPK, whereas nuclear respiratory factor (NRF), SKN-1 acts downstream of PMK-1 during activation of the innate immune response against mycobacteria. (B) The *C. elegans* innate immune response confers resistance to non-pathogenic mycobacteria (e.g. *M. smegmatis*) and survival of the nematodes, while pathogenic mycobacteria (e.g. *M. marinum*) modulate activation of the MAPK pathway in *C. elegans*, leading to persistence of the pathogen and death of the host.

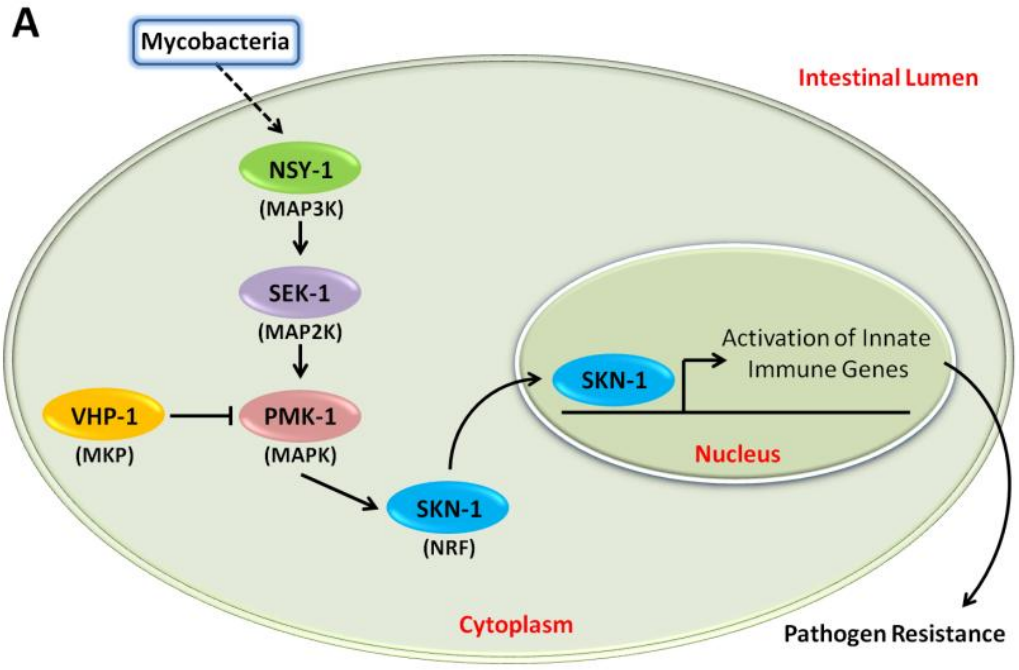
A
Mycobacteria
Intestinal Lumen
NSY-1
(MAP3K)
SEK-1
(MAP2K)
VHP-1
(MKP)
PMK-1
(MAPK)
SKN-1
(NRF)
SKN-1
Activation of Innate Immune Genes
Nucleus
Cytoplasm
Pathogen Resistance

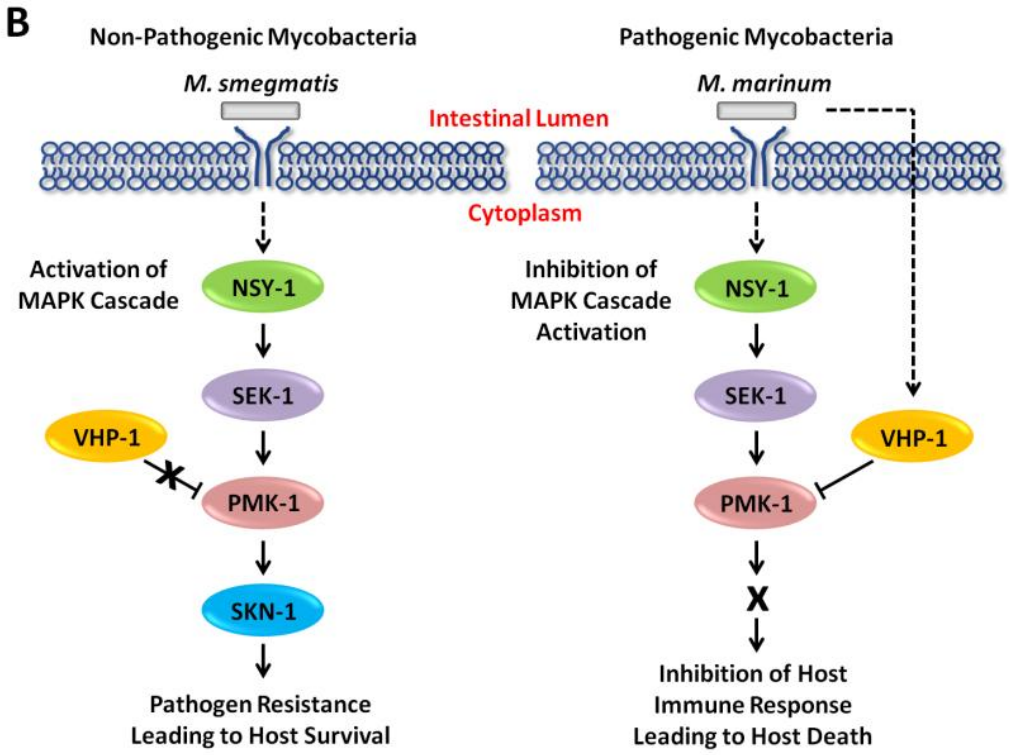
B
Non-Pathogenic Mycobacteria
Pathogenic Mycobacteria
M. smegmatis
M. marinum
Intestinal Lumen
Cytoplasm
Activation of MAPK Cascade
Inhibition of MAPK Cascade Activation
NSY-1
SEK-1
VHP-1
PMK-1
SKN-1
Pathogen Resistance Leading to Host Survival
Inhibition of Host Immune Response Leading to Host Death

IV.5 Discussion

The innate immune response acts in synergy with the adaptive response to defend against invading pathogens (Iwasaki and Medzhitov, 2010). In mycobacterial infections, the innate immune response activates the humoral response and continues to be active throughout infection (Stenger and Modlin, 1999). A great deal of research has focused on activation and inactivation of the adaptive immune response against pathogenic mycobacteria, but the innate immune response is less well understood. Interestingly, the mechanisms of susceptibility and resistance to mycobacterial infections in *C. elegans* appear to be unique as compared to other bacterial pathogens. Based on our observations, there are clear differences in activation of the innate immune response mediated by MAPK when comparing pathogenic to non-pathogenic mycobacteria infection in the multi-cellular *C. elegans* model, consistent with observations in mammalian in vitro homogeneous cell culture models (Dahl et al., 1996; Juffermans et al., 2000; Knutson et al., 1998; Roach et al., 1993). These observations confirm that *C. elegans* serves as a tractable model that is relevant to study of mammalian innate immune response mechanisms.

We found that the absence of *pmk-1* increases susceptibility to mycobacteria; whereas, the absence of *vhp-1* increases resistance, which suggests an important role for MAPK in the innate immune response to mycobacteria. It is interesting to note that, although the vhp-1 mutant increases resistance to *M. marinum*, *M. smegmatis* displays a nearly identical mortality curve to *E. coli* in this mutant and the same is true for the *tol-1*, *dbl-1* and *daf-16* mutants. However, the pmk-1 and *skn-1* mutants as well as wild type *C.*

elegans display a modest increase in mortality, even with *M. smegmatis*, suggesting that defense against non-pathogenic mycobacteria involves multiple signaling pathways, *pmk-1*, *tol-1*, *dbl-1* and *daf-16*, but susceptibility to pathogenic mycobacteria primarily involves *pmk-1*. Taken together, these observations suggest a key role for the *pmk-1* MAPK pathway in the innate immune response to mycobacterial infection (Figure 46A), where *C. elegans* respond differently to pathogenic and non-pathogenic mycobacterial infection through different levels or mechanisms of MAPK activation (Figure 46B). When infected with non-pathogenic mycobacteria, such as *M. smegmatis*, the *pmk-1* pathway is activated fully leading to bacterial killing and host survival. When infected with the pathogenic mycobacteria *M. marinum*, the *vhp-1* phosphatase is induced, reducing activation of *pmk-1*, leading to pathogen susceptibility and nematode pathology and death. Further analysis of the interaction of pathogenic mycobacteria with *C. elegans* is likely to lead to a better understanding these mechanistic differences and the regulation of downstream effectors that lead to pathogen resistance, which could offer new targets for therapeutics.

C. elegans is an excellent host for study of the innate immune response, including the MAPK pathway, which can be involved in control of antimicrobial responses (Coleman and Mylonakis, 2009; Dierking et al., 2011; Padmanabhan et al., 2009; Shivers et al., 2009; Troemel et al., 2006; Ziegler et al., 2009). *C. elegans* infected with *M. marinum* results in nematode mortality through the inhibition of the nematode's ability to lay eggs and by an increase in oxidative stress within the nematode. The inhibition of egg laying causes the infected adult nematodes to from bags of nematodes

(bagging), which is a form of protection for the progeny and provides them with a safer environment when environmental stresses occur such as infection with pathogens and starvation (Mosser et al., 2011; Seidel and Kimble, 2011). This morphological response invariably leads to death of the adult nematode within a period of 48 hours. Oxidative stress can cause a loss in pigmentation of the adult nematode and leads to a significantly lower survival rate. We have shown that the *pmk-1* regulated MAP Kinase pathway is important for pathogen resistance against mycobacterial infections in *C. elegans* by showing that *C. elegans* lacking functional *pmk-1* leads to 100% mortality within 24 hours and this mortality can be nearly completely reversed by deletion of *vhp-1*, a MKP gene that inhibits *pmk-1*. An Nrf analog, *skn-1* is be a key protein downstream of *pmk-1* in the response of *C. elegans* to both Gram-positive and Gram-negative bacteria (Mertenskotter et al., 2013; Papp et al., 2012). While *skn-1* mutants do not show the same bagging phenotype as the *C. elegans pmk-1* mutant infected with pathogenic mycobacteria, the *C. elegans skn-1* mutant displays higher levels of depigmentation and significantly reduced survival rates as compared to wild type nematodes. While this observation demonstrates the importance of skn-1 downstream of *pmk-1* gene in pathogen resistance, there could well be other genes acting downstream of *pmk-1* that impacts their ability to resist mycobacterial infections. Further studies should allow identification of other effectors involved in MAPK pathway induced protection from mycobacteria.

CHAPTER V

CONCLUSIONS AND DISCUSSION

V.1 Conclusions

C. elegans is a valuable model for study of pathogenesis and virulence factors of mycobacterial. *Mycobacterium marinum* causes increased pathology and mortality in infected nematodes making *C. elegans* a useful model host for study of mycobacterial virulence mechanisms. *C. elegans* mounts an immune response against mycobacteria mediated by the MAPK pathway. However, pathogenic mycobacteria are able to suppress this immune response. *M. marinum* mutants display attenuation in *C. elegans.* This fact allows *C. elegans* to be used to characterize the role of different mycobacterial genes in pathogenesis.

Infection with pathogenic *M. marinum* results in increased mortality *C. elegans* as compared to infection with non-pathogenic *M. smegmatis*. These observations suggest that *C. elegans* responds differently to pathogenic and non-pathogenic mycobacteria. *M. marinum* causes irreversible pathological and morphological changes in *C. elegans,* while *M. smegmatis* causes transient changes. Nematodes elicit a stress response when exposed to mycobacteria that helps them overcome the non-pathogenic strain but are unable to overcome *M. marinum* infections. *M. marinum* successfully colonizes the gut of the nematodes while *M. smegmatis* is either cleared or broken down. *M. marinum* appears to do so by attaching to the epithelium of the gut. Attachment most likely allows *M. marinum* to persist within the host for extended periods of time making study host-

pathogen interactions in this model possible. *C. elegans* display greater survival when infected with mutants in putative *M. marinum* virulence. Therefore *C. elegans* can be used to screen for additional *M. marinum* mutants that impact various aspects of pathogenesis in multi-cellular host.

Mm-luxR1 is a gene involved in macrophage infection. It regulates genes involved in the ability of *M. marinum* to enter macrophages and grow intracellularly. *Mm-luxR1* appears to play a role in modulating biofilm formation and is attenuated in *C. elegans* pathogenesis. When *Mm-wt* and *Mm-luxR1* mutant are used to competitively infect *C. elegans*, the *Mm-luxR1* attenuation is rescued by the wild type bacteria and *Mm-luxR1* is able to colonize the gut of *C. elegans*. This may be due to the fact that the function of *Mm-luxR1* can be provided by *Mm-wt* in trans or that when infected with *Mm-wt*, the *C. elegans* immune system is compromised allowing the *Mm-luxR1* mutants to colonize the nematode gut despite their defect.

The *C. elegans* MAPK pathway plays an important role in protecting nematodes from mycobacterial infections. The MAPK pathway is more efficient in protecting nematodes from non-pathogenic mycobacteria than pathogenic mycobacteria. Pathogenic mycobacteria modulate the MAPK pathway to their advantage and inhibit a protective response. The downstream Nrf protein is at least partially involved in mediating the response against mycobacterial infections in *C. elegans*. In the absence of a *nrf* gene, the nematode appears to undergo an oxidative stress response when infected with mycobacteria. When the MKP that blocks the activation of MAPK is removed, *C. elegans* are able to resist pathogenic mycobacteria better. Other *C. elegans* signaling

pathways involved in innate immunity, including TOL-like receptors, TGF-β and insulin-like signaling pathways do not appear to be as important in mycobacterial infections as the MAPK pathway.

C. elegans can also be used to study attenuated mutants of *M. marinum*, better understand their mechanisms of action in the host and identify new mycobacterial virulence factors. Therefore, *C. elegans* serves as a model for study of both the host response and mycobacterial virulence factors that are important for pathogenesis.

V.2 Significance of Findings

C. elegans provide a novel host to study *M. marinum* at a temperature optimal for growth (room temperature). *C. elegans* is a simple organism that can be handled with ease in the laboratory and large scale infections can be performed in a small amount of space. We have shown the importance of the MAPK pathway in the innate immune response against mycobacteria. The MAPK pathway is also likely to be important in the innate immune response against mycobacteria in humans. However, the involvement of the MAPK pathway has not been fully described. The most likely reason for the lack of clarity in this important aspect of the innate immune response is that there are not higher level eukaryotic hosts with complete knock-outs of MAPK. Since mutations are developmentally lethal. However, in *C. elegans* MAPK knock-outs exist and they are not lethal, making *C. elegans* a valuable model for studies focused on understanding the role of MAPK in pathogenesis.

C. elegans can be used to identify receptors and downstream effectors that mediate the host innate immune response against mycobacteria. *Mycobacterium marinum* causes morphological changes in *C. elegans* that allow us to measure pathogenic processes are important during infection. *C. elegans* is a useful novel model to study the innate immune response and mycobacterial virulence mechanisms. We also found that *C. elegans* allows use of competition assays to gain more detailed insight into the importance of mycobacterial virulence determinants as compared to other genes. Several useful molecular assays including, RNAi, high throughput sequencing can be used in *C. elegans* for detailed analysis of host-pathogen interactions. Furthermore, it is likely that *C. elegans* can be utilized in a similar manner to that used in the current study to identify novel therapeutic targets for mycobacterial infections.

V.3 Study Limitations

Mycobacteria are primarily intracellular pathogens (Vergne et al., 2004a) and reside within macrophages (Roach et al., 1993; Tascon et al., 2000). However, it is not known whether mycobacterial infections in *C. elegans* have an intracellular phase. *C. elegans* do not have macrophages or other phagocytic cells (Aballay et al., 2003). Therefore, *C. elegans* cannot necessarily be used to study the intracellular phase of mycobacterial infections. Since *C. elegans* do not have macrophages, they are unable to form granulomas, making it unlikely that finding in *C. elegans* will be directly relevant to granuloma formation.

Since *C. elegans* have only an innate immune system (Aballay et al., 2003; Jebamercy et al., 2013), they lack a defined adaptive immune response. Therefore, *C. elegans* cannot be used to characterize activation of the T cell response as it arises from the innate immune response. Mycobacterial diseases are usually chronic infections, making *C. elegans* a model for primarily acute phase of infection. *C. elegans* can be used for screening of virulence genes, identifying host-pathogen interaction and studying the host immune response, but it is not yet clear whether all pathways that are relevant to *C. elegans* will also be important in mammals.

A limitation of the current study is the absence of any protein analysis. We characterize the important role of the MAPK pathway plays in the innate immune response against mycobacterial infections and support our hypothesis with knock-down and knock-out mutants. However, to confirm the involvement of this signaling pathway in pathogenesis, it would be valuable to carryout phosphorylation analysis. These are some of the future directions of this work.

Despite these potential limitations, the apparent similarities of our finding to those in mammalian systems strongly supports to great potential for the *C. elegans* model for mycobacterial pathogenesis contributing a wealth of knowledge regarding molecular mechanisms of mycobacterial pathogenesis.

REFERENCES

Aaron, L., Saadoun, D., Calatroni, I., Launay, O., Memain, N., Vincent, V., Marchal, G., Dupont, B., Bouchaud, O., Valeyre, D., *et al.* (2004). Tuberculosis in HIV-infected patients: a comprehensive review. Clinical microbiology and infection : the official publication of the European Society of Clinical Microbiology and Infectious Diseases *10*, 388-398.

Aballay, A., Drenkard, E., Hilbun, L.R., and Ausubel, F.M. (2003). Caenorhabditis elegans innate immune response triggered by *Salmonella enterica* requires intact LPS and is mediated by a MAPK signaling pathway. Current biology : CB *13*, 47-52.

Aballay, A., Yorgey, P., and Ausubel, F.M. (2000). *Salmonella typhimurium* proliferates and establishes a persistent infection in the intestine of *Caenorhabditis elegans*. Current biology : CB *10*, 1539-1542.

Adams, K.N., Takaki, K., Connolly, L.E., Wiedenhoft, H., Winglee, K., Humbert, O., Edelstein, P.H., Cosma, C.L., and Ramakrishnan, L. (2011). Drug tolerance in replicating mycobacteria mediated by a macrophage-induced efflux mechanism. Cell *145*, 39-53.

Adhikesavan, L.G., and Harrington, T.M. (2008). Local and disseminated infections caused by *Mycobacterium marinum*: an unusual cause of subcutaneous nodules. Journal of clinical rheumatology : practical reports on rheumatic & musculoskeletal diseases *14*, 156-160.

Alibaud, L., Rombouts, Y., Trivelli, X., Burguiere, A., Cirillo, S.L., Cirillo, J.D., Dubremetz, J.F., Guerardel, Y., Lutfalla, G., and Kremer, L. (2011). A *Mycobacterium marinum* TesA mutant defective for major cell wall-associated lipids is highly attenuated in *Dictyostelium discoideum* and zebrafish embryos. Mol Microbiol *80*, 919-934.

Ando, N., Ueda, K., and Horinouchi, S. (1997). A *Streptomyces griseus* gene (sgaA) suppresses the growth disturbance caused by high osmolality and a high concentration of A-factor during early growth. Microbiology (Reading, England) *143 (Pt 8)*, 2715-2723.

Ang, P., Rattana-Apiromyakij, N., and Goh, C.L. (2000). Retrospective study of *Mycobacterium marinum* skin infections. International journal of dermatology *39*, 343-347.

Asad, S., and Opal, S.M. (2008). Bench-to-bedside review: Quorum sensing and the role of cell-to-cell communication during invasive bacterial infection. Critical Care (London, England) *12*, 236.

Ashrafi, K., Chang, F.Y., Watts, J.L., Fraser, A.G., Kamath, R.S., Ahringer, J., and Ruvkun, G. (2003). Genome-wide RNAi analysis of *Caenorhabditis elegans* fat regulatory genes. Nature *421*, 268-272.

Bae, T., Banger, A.K., Wallace, A., Glass, E.M., Aslund, F., Schneewind, O., and Missiakas, D.M. (2004). *Staphylococcus aureus* virulence genes identified by bursa aurealis mutagenesis and nematode killing. Proc Natl Acad Sci U S A *101*, 12312-12317.

Balasubramanian, V., Wiegeshaus, E.H., and Smith, D.W. (1994). Mycobacterial infection in guinea pigs. Immunobiology *191*, 395-401.

Bassler, B.L. (2002). Small talk. Cell-to-cell communication in bacteria. Cell *109*, 421-424.

Basu, J., Shin, D.M., and Jo, E.K. (2012). Mycobacterial signaling through toll-like receptors. Frontiers in cellular and infection microbiology *2*, 145.

Beck von Bodman, S., and Farrand, S.K. (1995). Capsular polysaccharide biosynthesis and pathogenicity in *Erwinia stewartii* require induction by an N-acylhomoserine lactone autoinducer. Journal of Bacteriology *177*, 5000-5008.

Bermudez, L.E., and Goodman, J. (1996). *Mycobacterium tuberculosis* invades and replicates within type II alveolar cells. Infect Immun *64*, 1400-1406.

Beutler, B., Jiang, Z., Georgel, P., Crozat, K., Croker, B., Rutschmann, S., Du, X., and Hoebe, K. (2006). Genetic analysis of host resistance: Toll-like receptor signaling and immunity at large. Annual Review of Immunology *24*, 353-389.

Bloom, B.R., and Murray, C.J. (1992). Tuberculosis: commentary on a reemergent killer. Science (New York, NY) *257*, 1055-1064.

Bobosha, K., Wilson, L., van Meijgaarden, K.E., Bekele, Y., Zewdie, M., van der Ploeg-van Schip, J.J., Abebe, M., Hussein, J., Khadge, S., Neupane, K.D., *et al.* (2014). T-cell regulation in lepromatous leprosy. PLoS neglected tropical diseases *8*, e2773.

Bodnar, K.A., Serbina, N.V., and Flynn, J.L. (2001). Fate of *Mycobacterium tuberculosis* within murine dendritic cells. Infect Immun *69*, 800-809.

Bolm, M., Jansen, W.T., Schnabel, R., and Chhatwal, G.S. (2004). Hydrogen peroxide-mediated killing of *Caenorhabditis elegans*: a common feature of different streptococcal species. Infect Immun *72*, 1192-1194.

Brenner, S. (1974). The genetics of *Caenorhabditis elegans*. Genetics *77*, 71-94.

Brightbill, H.D., Libraty, D.H., Krutzik, S.R., Yang, R.B., Belisle, J.T., Bleharski, J.R., Maitland, M., Norgard, M.V., Plevy, S.E., Smale, S.T., *et al.* (1999). Host defense mechanisms triggered by microbial lipoproteins through toll-like receptors. Science *285*, 732-736.

Brouillette, E., Hyodo, M., Hayakawa, Y., Karaolis, D.K., and Malouin, F. (2005). 3',5'-cyclic diguanylic acid reduces the virulence of biofilm-forming *Staphylococcus aureus* strains in a mouse model of mastitis infection. Antimicrobial Agents and Chemotherapy *49*, 3109-3113.

Broussard, G.W., and Ennis, D.G. (2007). *Mycobacterium marinum* produces long-term chronic infections in medaka: a new animal model for studying human tuberculosis. Comparative biochemistry and physiology Toxicology & pharmacology : CBP *145*, 45-54.

Brumell, J.H., and Grinstein, S. (2004). *Salmonella* redirects phagosomal maturation. Curr Opin Microbiol *7*, 78-84.

Calderon, V.E., Valbuena, G., Goez, Y., Judy, B.M., Huante, M.B., Sutjita, P., Johnston, R.K., Estes, D.M., Hunter, R.L., Actor, J.K., *et al.* (2013). A humanized mouse model of tuberculosis. PLoS One *8*, e63331.

Carter, G., Wu, M., Drummond, D.C., and Bermudez, L.E. (2003). Characterization of biofilm formation by clinical isolates of *Mycobacterium avium*. Journal of medical microbiology *52*, 747-752.

Carvalho, R., de Sonneville, J., Stockhammer, O.W., Savage, N.D., Veneman, W.J., Ottenhoff, T.H., Dirks, R.P., Meijer, A.H., and Spaink, H.P. (2011). A high-throughput screen for tuberculosis progression. PLoS One *6*, e16779.

Chatterjee, D., and Khoo, K.H. (1998). Mycobacterial lipoarabinomannan: an extraordinary lipoheteroglycan with profound physiological effects. Glycobiology *8*, 113-120.

Chen, J., and Caswell-Chen, E.P. (2004). Facultative Vivipary is a Life-History Trait in Caenorhabditis elegans. J Nematol *36*, 107-113.

Chiang, C.Y., Van Weezenbeek, C., Mori, T., and Enarson, D.A. (2013). Challenges to the global control of tuberculosis. Respirology *18*, 596-604.

Cirillo, S.L., Subbian, S., Chen, B., Weisbrod, T.R., Jacobs, W.R., Jr., and Cirillo, J.D. (2009). Protection of *Mycobacterium tuberculosis* from reactive oxygen species conferred by the mel2 locus impacts persistence and dissemination. Infect Immun *77*, 2557-2567.

Clark, H.F., and Shepard, C.C. (1963a). Effect of Environmental Temperatures on Infection with *Mycobacterium Marinum* (Balnei) of Mice and a Number of Poikilothermic Species. Journal of Bacteriology *86*, 1057-1069.

Coleman, J.J., and Mylonakis, E. (2009). The tangled web of signaling in innate immunity. Cell Host Microbe *5*, 313-315.

Corti, M., and Palmero, D. (2008). *Mycobacterium avium* complex infection in HIV/AIDS patients. Expert review of anti-infective therapy *6*, 351-363.

Cosma, C.L., Sherman, D.R., and Ramakrishnan, L. (2003). The secret lives of the pathogenic mycobacteria. Annu Rev Microbiol *57*, 641-676.

Cosma, C.L., Swaim, L.E., Volkman, H., Ramakrishnan, L., and Davis, J.M. (2006). Zebrafish and frog models of *Mycobacterium marinum* infection. Curr Protoc Microbiol *Chapter 10*, Unit 10B.12.

Couillault, C., and Ewbank, J.J. (2002). Diverse bacteria are pathogens of Caenorhabditis elegans. Infect Immun *70*, 4705-4707.

Coulthurst, S.J., Kurz, C.L., and Salmond, G.P. (2004). *luxS* mutants of *Serratia* defective in autoinducer-2-dependent 'quorum sensing' show strain-dependent impacts on virulence and production of carbapenem and prodigiosin. Microbiology *150*, 1901-1910.

Cruz-Knight, W., and Blake-Gumbs, L. (2013). Tuberculosis: an overview. Primary care *40*, 743-756.

Cywes, C., Hoppe, H.C., Daffe, M., and Ehlers, M.R. (1997). Nonopsonic binding of *Mycobacterium tuberculosis* to complement receptor type 3 is mediated by capsular polysaccharides and is strain dependent. Infect Immun *65*, 4258-4266.

Dahl, K.E., Shiratsuchi, H., Hamilton, B.D., Ellner, J.J., and Toossi, Z. (1996). Selective induction of transforming growth factor beta in human monocytes by lipoarabinomannan of *Mycobacterium tuberculosis*. Infect Immun *64*, 399-405.

Danelishvili, L., Cirillo, S.L., Cirillo, J.D., and Bermudez, L.E. (2007a). Virulent mycobacteria and the many aspects of macrophage uptake. Future Microbiol *2*, 461-464.

Danelishvili, L., Wu, M., Stang, B., Harriff, M., Cirillo, S.L., Cirillo, J.D., Bildfell, R., Arbogast, B., and Bermudez, L.E. (2007b). Identification of *Mycobacterium avium* pathogenicity island important for macrophage and amoeba infection. Proc Natl Acad Sci U S A *104*, 11038-11043.

Darby, C., Cosma, C.L., Thomas, J.H., and Manoil, C. (1999). Lethal paralysis of *Caenorhabditis elegans* by *Pseudomonas aeruginosa*. Proc Natl Acad Sci U S A *96*, 15202-15207.

Davis, J.M., and Ramakrishnan, L. (2009). The role of the granuloma in expansion and dissemination of early tuberculous infection. Cell *136*, 37-49.

Deng, W., Tang, X., Hou, M., Li, C., and Xie, J. (2011). New insights into the pathogenesis of tuberculosis revealed by *Mycobacterium marinum*: the zebrafish model from the systems biology perspective. Crit Rev Eukaryot Gene Expr *21*, 337-345.

Dierking, K., Polanowska, J., Omi, S., Engelmann, I., Gut, M., Lembo, F., Ewbank, J.J., and Pujol, N. (2011). Unusual regulation of a STAT protein by an SLC6 family transporter in *C. elegans* epidermal innate immunity. Cell Host Microbe *9*, 425-435.

Dong, D., Wang, D., Li, M., Wang, H., Yu, J., Wang, C., Liu, J., and Gao, Q. (2012). PPE38 modulates the innate immune response and is required for *Mycobacterium marinum* virulence. Infect Immun *80*, 43-54.

Dunlap, P.V. (1999). Quorum regulation of luminescence in Vibrio fischeri. Journal of Molecular Microbiology and Biotechnology *1*, 5-12.

Dunny, G.M., Leonard, B.A., and Hedberg, P.J. (1995). Pheromone-inducible conjugation in *Enterococcus faecalis*: interbacterial and host-parasite chemical communication. Journal of Bacteriology *177*, 871-876.

Dye, C. (2006). Global epidemiology of tuberculosis. Lancet *367*, 938-940.

Dye, C., Scheele, S., Dolin, P., Pathania, V., and Raviglione, M.C. (1999). Consensus statement. Global burden of tuberculosis: estimated incidence, prevalence, and mortality by country. WHO Global Surveillance and Monitoring Project. JAMA *282*, 677-686.

Eberl, L., Winson, M.K., Sternberg, C., Stewart, G.S., Christiansen, G., Chhabra, S.R., Bycroft, B., Williams, P., Molin, S., and Givskov, M. (1996). Involvement of N-acyl-L-hormoserine lactone autoinducers in controlling the multicellular behaviour of *Serratia liquefaciens*. Molecular microbiology *20*, 127-136.

Ehlers, S. (2010). TB or not TB? Fishing for Molecules Making Permissive granulomas. Cell Host Microbe *7*, 6-8.

El-Etr, S.H., Subbian, S., Cirillo, S.L., and Cirillo, J.D. (2004). Identification of two *Mycobacterium marinum* loci that affect interactions with macrophages. Infect Immun *72*, 6902-6913.

El-Etr, S.H., Yan, L., and Cirillo, J.D. (2001). Fish monocytes as a model for mycobacterial host-pathogen interactions. Infect Immun *69*, 7310-7317.

Emmons, S.W., Klass, M.R., and Hirsh, D. (1979). Analysis of the constancy of DNA sequences during development and evolution of the nematode *Caenorhabditis elegans*. Proc Natl Acad Sci U S A *76*, 1333-1337.

Evans, E.A., Kawli, T., and Tan, M.W. (2008). *Pseudomonas aeruginosa* suppresses host immunity by activating the DAF-2 insulin-like signaling pathway in *Caenorhabditis elegans*. PLoS Pathog *4*, e1000175.

Fenton, M.J., and Vermeulen, M.W. (1996). Immunopathology of tuberculosis: roles of macrophages and monocytes. Infect Immun *64*, 683-690.

Flynn, J.L. (2006). Lessons from experimental *Mycobacterium tuberculosis* infections. Microbes and infection / Institut Pasteur *8*, 1179-1188.

Flynn, J.L., Chan, J., Triebold, K.J., Dalton, D.K., Stewart, T.A., and Bloom, B.R. (1993). An essential role for interferon gamma in resistance to *Mycobacterium tuberculosis* infection. J Exp Med *178*, 2249-2254.

Fortune, S.M., and Rubin, E.J. (2007). The complex relationship between mycobacteria and macrophages: it's not all bliss. Cell Host Microbe *2*, 5-6.

Fuqua, C., and Greenberg, E.P. (2002). Listening in on bacteria: acyl-homoserine lactone signalling. Nature reviewsMolecular cell biology *3*, 685-695.

Gambello, M.J., Kaye, S., and Iglewski, B.H. (1993). LasR of *Pseudomonas aeruginosa* is a transcriptional activator of the alkaline protease gene (apr) and an enhancer of exotoxin A expression. Infection and immunity *61*, 1180-1184.

Gan, Y.H., Chua, K.L., Chua, H.H., Liu, B., Hii, C.S., Chong, H.L., and Tan, P. (2002). Characterization of Burkholderia pseudomallei infection and identification of novel virulence factors using a *Caenorhabditis elegans* host system. Mol Microbiol *44*, 1185-1197.

Garigan, D., Hsu, A.L., Fraser, A.G., Kamath, R.S., Ahringer, J., and Kenyon, C. (2002). Genetic analysis of tissue aging in *Caenorhabditis elegans*: a role for heat-shock factor and bacterial proliferation. Genetics *161*, 1101-1112.

Garsin, D.A., Sifri, C.D., Mylonakis, E., Qin, X., Singh, K.V., Murray, B.E., Calderwood, S.B., and Ausubel, F.M. (2001). A simple model host for identifying Gram-positive virulence factors. Proc Natl Acad Sci U S A *98*, 10892-10897.

Garsin, D.A., Villanueva, J.M., Begun, J., Kim, D.H., Sifri, C.D., Calderwood, S.B., Ruvkun, G., and Ausubel, F.M. (2003). Long-lived *C. elegans* daf-2 mutants are resistant to bacterial pathogens. Science *300*, 1921.

Gauthier, D.T., and Rhodes, M.W. (2009). Mycobacteriosis in fishes: a review. Veterinary journal (London, England : 1997) *180*, 33-47.

Gaynor, C.D., McCormack, F.X., Voelker, D.R., McGowan, S.E., and Schlesinger, L.S. (1995). Pulmonary surfactant protein A mediates enhanced phagocytosis of *Mycobacterium tuberculosis* by a direct interaction with human macrophages. Journal of immunology (Baltimore, Md : 1950) *155*, 5343-5351.

Glaziou, P., Falzon, D., Floyd, K., and Raviglione, M. (2013). Global epidemiology of tuberculosis. Semin Respir Crit Care Med *34*, 3-16.

Glover-Cutter, K.M., Lin, S., and Blackwell, T.K. (2013). Integration of the unfolded protein and oxidative stress responses through SKN-1/Nrf. PLoS Genet *9*, e1003701.

Gonzalez-Juarrero, M., and Orme, I.M. (2001). Characterization of murine lung dendritic cells infected with *Mycobacterium tuberculosis*. Infect Immun *69*, 1127-1133.

Griffitts, J.S., Whitacre, J.L., Stevens, D.E., and Aroian, R.V. (2001). Bt toxin resistance from loss of a putative carbohydrate-modifying enzyme. Science *293*, 860-864.

Gutierrez, M.C., Supply, P., and Brosch, R. (2009). Pathogenomics of mycobacteria. Genome Dyn *6*, 198-210.

Haber, C.L., Heckaman, C.L., Li, G.P., Thompson, D.P., Whaley, H.A., and Wiley, V.H. (1991). Development of a mechanism of action-based screen for anthelmintic microbial metabolites with avermectinlike activity and isolation of milbemycin-producing *Streptomyces* strains. Antimicrob Agents Chemother *35*, 1811-1817.

Hall, D.H., Hartwieg, E., and Nguyen, K.C. (2012). Modern electron microscopy methods for *C. elegans*. Methods Cell Biol *107*, 93-149.

Harjai, K., Gupta, R.K., and Sehgal, H. (2014). Attenuation of quorum sensing controlled virulence of *Pseudomonas aeruginosa* by cranberry. The Indian journal of medical research *139*, 446-453.

He, Y., Li, W., Liao, G., and Xie, J. (2012). *Mycobacterium tuberculosis*-specific phagosome proteome and underlying signaling pathways. J Proteome Res *11*, 2635-2643.

Henderson, R.A., Watkins, S.C., and Flynn, J.L. (1997). Activation of human dendritic cells following infection with *Mycobacterium tuberculosis*. Journal of immunology (Baltimore, Md : 1950) *159*, 635-643.

Hernandez-Pando, R., and Rook, G.A. (1994). The role of TNF-alpha in T-cell-mediated inflammation depends on the Th1/Th2 cytokine balance. Immunology *82*, 591-595.

Hesseling, A.C., Kim, S., Madhi, S., Nachman, S., Schaaf, H.S., Violari, A., Victor, T.C., McSherry, G., Mitchell, C., Cotton, M.F., *et al.* (2012). High prevalence of drug resistance amongst HIV-exposed and -infected children in a tuberculosis prevention trial. The international journal of tuberculosis and lung disease : the official journal of the International Union against Tuberculosis and Lung Disease *16*, 192-195.

Hirsch, C.S., Ellner, J.J., Russell, D.G., and Rich, E.A. (1994). Complement receptor-mediated uptake and tumor necrosis factor-alpha-mediated growth inhibition of *Mycobacterium tuberculosis* by human alveolar macrophages. Journal of immunology (Baltimore, Md : 1950) *152*, 743-753.

Hirsch, C.S., Toossi, Z., Othieno, C., Johnson, J.L., Schwander, S.K., Robertson, S., Wallis, R.S., Edmonds, K., Okwera, A., Mugerwa, R., *et al.* (1999). Depressed T-cell interferon-gamma responses in pulmonary tuberculosis: analysis of underlying mechanisms and modulation with therapy. J Infect Dis *180*, 2069-2073.

Hodgkin, J., Kuwabara, P.E., and Corneliussen, B. (2000). A novel bacterial pathogen, *Microbacterium nematophilum*, induces morphological change in the nematode *C. elegans*. Current biology : CB *10*, 1615-1618.

Horinouchi, S., and Beppu, T. (1992). Autoregulatory factors and communication in actinomycetes. Annual Review of Microbiology *46*, 377-398.

Horinouchi, S., and Beppu, T. (1994). A-factor as a microbial hormone that controls cellular differentiation and secondary metabolism in Streptomyces griseus. Molecular microbiology *12*, 859-864.

Howard, S.T., Rhoades, E., Recht, J., Pang, X., Alsup, A., Kolter, R., Lyons, C.R., and Byrd, T.F. (2006). Spontaneous reversion of Mycobacterium abscessus from a smooth to a rough morphotype is associated with reduced expression of glycopeptidolipid and reacquisition of an invasive phenotype. Microbiology (Reading, England) *152*, 1581-1590.

Iwasaki, A., and Medzhitov, R. (2010). Regulation of adaptive immunity by the innate immune system. Science *327*, 291-295.

Janeway, C.A., Jr. (1989). Approaching the asymptote? Evolution and revolution in immunology. Cold Spring Harb Symp Quant Biol *54 Pt 1*, 1-13.

Janeway, C.A., Jr. (1992). The immune system evolved to discriminate infectious nonself from noninfectious self. Immunol Today *13*, 11-16.

Jansen, W.T., Bolm, M., Balling, R., Chhatwal, G.S., and Schnabel, R. (2002). Hydrogen peroxide-mediated killing of *Caenorhabditis elegans* by *Streptococcus pyogenes*. Infect Immun *70*, 5202-5207.

Jansson, H.B., von Hofsten, A., and von Mecklenburg, C. (1984). Life cycle of the endoparasitic nematophagous fungus *Meria coniospora*: a light and electron microscopic study. Antonie Van Leeuwenhoek *50*, 321-327.

JebaMercy, G., and Balamurugan, K. (2012). Effects of sequential infections of *Caenorhabditis elegans* with *Staphylococcus aureus* and *Proteus mirabilis*. Microbiol Immunol *56*, 825-835.

JebaMercy, G., Pandian, S.K., and Balamurugan, K. (2011). Changes in *Caenorhabditis elegans* life span and selective innate immune genes during Staphylococcus aureus infection. Folia Microbiol (Praha) *56*, 373-380.

Jebamercy, G., Vigneshwari, L., and Balamurugan, K. (2013). A MAP Kinase pathway in *Caenorhabditis elegans* is required for defense against infection by opportunistic Proteus species. Microbes and infection / Institut Pasteur.

Jernigan, J.A., and Farr, B.M. (2000). Incubation period and sources of exposure for cutaneous *Mycobacterium marinum* infection: case report and review of the literature. Clinical infectious diseases : an official publication of the Infectious Diseases Society of America *31*, 439-443.

Joshua, G.W., Karlyshev, A.V., Smith, M.P., Isherwood, K.E., Titball, R.W., and Wren, B.W. (2003). A *Caenorhabditis elegans* model of *Yersinia* infection: biofilm formation on a biotic surface. Microbiology *149*, 3221-3229.

Juang, B.T., Gu, C., Starnes, L., Palladino, F., Goga, A., Kennedy, S., and L'Etoile, N.D. (2013). Endogenous nuclear RNAi mediates behavioral adaptation to odor. Cell *154*, 1010-1022.

Juffermans, N.P., Verbon, A., Belisle, J.T., Hill, P.J., Speelman, P., van Deventer, S.J., and van der Poll, T. (2000). *Mycobacterial lipoarabinomannan* induces an inflammatory response in the mouse lung. A role for interleukin-1. Am J Respir Crit Care Med *162*, 486-489.

Kaattari, I.M., Rhodes, M.W., Kaattari, S.L., and Shotts, E.B. (2006). The evolving story of *Mycobacterium tuberculosis* clade members detected in fish. Journal of Fish Diseases *29*, 509-520.

Kadirvel, M., Fanimarvasti, F., Forbes, S., McBain, A., Gardiner, J.M., Brown, G.D., and Freeman, S. (2014). Inhibition of quorum sensing and biofilm formation in *Vibrio*

harveyi by 4-fluoro-DPD; a novel potent inhibitor of signalling. Chemical communications (Cambridge, England) *50*, 5000-5002.

Kang, P.B., Azad, A.K., Torrelles, J.B., Kaufman, T.M., Beharka, A., Tibesar, E., DesJardin, L.E., and Schlesinger, L.S. (2005). The human macrophage mannose receptor directs *Mycobacterium tuberculosis* lipoarabinomannan-mediated phagosome biogenesis. J Exp Med *202*, 987-999.

Karaolis, D.K., Rashid, M.H., Chythanya, R., Luo, W., Hyodo, M., and Hayakawa, Y. (2005). c-di-GMP (3'-5'-cyclic diguanylic acid) inhibits *Staphylococcus aureus* cell-cell interactions and biofilm formation. Antimicrobial Agents and Chemotherapy *49*, 1029-1038.

Kawai, T., and Akira, S. (2010). The role of pattern-recognition receptors in innate immunity: update on Toll-like receptors. Nat Immunol *11*, 373-384.

Keane, J., Balcewicz-Sablinska, M.K., Remold, H.G., Chupp, G.L., Meek, B.B., Fenton, M.J., and Kornfeld, H. (1997). Infection by *Mycobacterium tuberculosis* promotes human alveolar macrophage apoptosis. Infect Immun *65*, 298-304.

Kendall, M.M., Rasko, D.A., and Sperandio, V. (2007). Global effects of the cell-to-cell signaling molecules autoinducer-2, autoinducer-3, and epinephrine in a *luxS* mutant of enterohemorrhagic *Escherichia coli*. Infection and immunity *75*, 4875-4884.

Khounlotham, M., Subbian, S., Smith, R., 3rd, Cirillo, S.L., and Cirillo, J.D. (2009). *Mycobacterium tuberculosis* interferes with the response to infection by inducing the host EphA2 receptor. J Infect Dis *199*, 1797-1806.

Kim, D.H., Liberati, N.T., Mizuno, T., Inoue, H., Hisamoto, N., Matsumoto, K., and Ausubel, F.M. (2004). Integration of *Caenorhabditis elegans* MAPK pathways mediating immunity and stress resistance by MEK-1 MAPK kinase and VHP-1 MAPK phosphatase. Proc Natl Acad Sci U S A *101*, 10990-10994.

Kim, J.K., Gabel, H.W., Kamath, R.S., Tewari, M., Pasquinelli, A., Rual, J.F., Kennedy, S., Dybbs, M., Bertin, N., Kaplan, J.M., *et al.* (2005). Functional genomic analysis of RNA interference in *C. elegans*. Science *308*, 1164-1167.

Kindler, V., Sappino, A.P., Grau, G.E., Piguet, P.F., and Vassalli, P. (1989). The inducing role of tumor necrosis factor in the development of bactericidal granulomas during BCG infection. Cell *56*, 731-740.

Kingeter, L.M., and Lin, X. (2012). C-type lectin receptor-induced NF-kappaB activation in innate immune and inflammatory responses. Cell Mol Immunol *9*, 105-112.

Kleinnijenhuis, J., Oosting, M., Joosten, L.A., Netea, M.G., and Van Crevel, R. (2011). Innate immune recognition of *Mycobacterium tuberculosis*. Clinical & developmental immunology *2011*, 405310.

Knutson, K.L., Hmama, Z., Herrera-Velit, P., Rochford, R., and Reiner, N.E. (1998). Lipoarabinomannan of *Mycobacterium tuberculosis* promotes protein tyrosine dephosphorylation and inhibition of mitogen-activated protein kinase in human mononuclear phagocytes. Role of the Src homology 2 containing tyrosine phosphatase 1. J Biol Chem *273*, 645-652.

Kong, Y., Yao, H., Ren, H., Subbian, S., Cirillo, S.L., Sacchettini, J.C., Rao, J., and Cirillo, J.D. (2010). Imaging tuberculosis with endogenous beta-lactamase reporter enzyme fluorescence in live mice. Proc Natl Acad Sci U S A *107*, 12239-12244.

Kothe, M., Antl, M., Huber, B., Stoecker, K., Ebrecht, D., Steinmetz, I., and Eberl, L. (2003). Killing of *Caenorhabditis elegans* by *Burkholderia cepacia* is controlled by the cep quorum-sensing system. Cell Microbiol *5*, 343-351.

Koul, A., Herget, T., Klebl, B., and Ullrich, A. (2004). Interplay between mycobacteria and host signalling pathways. Nature reviews Microbiology *2*, 189-202.

Kurz, C.L., Chauvet, S., Andres, E., Aurouze, M., Vallet, I., Michel, G.P., Uh, M., Celli, J., Filloux, A., De Bentzmann, S., *et al.* (2003). Virulence factors of the human opportunistic pathogen *Serratia marcescens* identified by in vivo screening. The EMBO journal *22*, 1451-1460.

Labrousse, A., Chauvet, S., Couillault, C., Kurz, C.L., and Ewbank, J.J. (2000). *Caenorhabditis elegans* is a model host for *Salmonella typhimurium*. Current biology : CB *10*, 1543-1545.

Ladel, C.H., Szalay, G., Riedel, D., and Kaufmann, S.H. (1997). Interleukin-12 secretion by *Mycobacterium tuberculosis*-infected macrophages. Infect Immun *65*, 1936-1938.

Liu, P.T., and Modlin, R.L. (2008). Human macrophage host defense against *Mycobacterium tuberculosis*. Curr Opin Immunol *20*, 371-376.

Lynch, J.B. (2013). Multidrug-resistant Tuberculosis. Med Clin North Am *97*, 553-579, ix-x.

Maadani, A., Fox, K.A., Mylonakis, E., and Garsin, D.A. (2007). *Enterococcus faecalis* mutations affecting virulence in the *Caenorhabditis elegans* model host. Infect Immun *75*, 2634-2637.

Mahajan-Miklos, S., Tan, M.W., Rahme, L.G., and Ausubel, F.M. (1999). Molecular mechanisms of bacterial virulence elucidated using a *Pseudomonas aeruginosa-Caenorhabditis elegans* pathogenesis model. Cell *96*, 47-56.

Malmberg, L.H., Hu, W.S., and Sherman, D.H. (1993). Precursor flux control through targeted chromosomal insertion of the lysine epsilon-aminotransferase (lat) gene in cephamycin C biosynthesis. Journal of Bacteriology *175*, 6916-6924.

Marcenaro, E., Carlomagno, S., Pesce, S., Moretta, A., and Sivori, S. (2011). Bridging innate NK cell functions with adaptive immunity. Advances in experimental medicine and biology *780*, 45-55.

Mazzaccaro, R.J., Gedde, M., Jensen, E.R., van Santen, H.M., Ploegh, H.L., Rock, K.L., and Bloom, B.R. (1996). Major histocompatibility class I presentation of soluble antigen facilitated by *Mycobacterium tuberculosis* infection. Proc Natl Acad Sci U S A *93*, 11786-11791.

McMurray, D.N. (2001). Disease model: pulmonary tuberculosis. Trends in molecular medicine *7*, 135-137.

Means, T.K., Lien, E., Yoshimura, A., Wang, S., Golenbock, D.T., and Fenton, M.J. (1999a). The CD14 ligands lipoarabinomannan and lipopolysaccharide differ in their requirement for Toll-like receptors. Journal of immunology (Baltimore, Md : 1950) *163*, 6748-6755.

Means, T.K., Wang, S., Lien, E., Yoshimura, A., Golenbock, D.T., and Fenton, M.J. (1999b). Human toll-like receptors mediate cellular activation by *Mycobacterium tuberculosis*. Journal of immunology (Baltimore, Md: 1950) *163*, 3920-3927.

Medzhitov, R., and Janeway, C.A., Jr. (1997). Innate immunity: impact on the adaptive immune response. Curr Opin Immunol *9*, 4-9.

Mehta, P.K., Pandey, A.K., Subbian, S., El-Etr, S.H., Cirillo, S.L., Samrakandi, M.M., and Cirillo, J.D. (2006). Identification of *Mycobacterium marinum* macrophage infection mutants. Microb Pathog *40*, 139-151.

Mertenskotter, A., Keshet, A., Gerke, P., and Paul, R.J. (2013). The p38 MAPK PMK-1 shows heat-induced nuclear translocation, supports chaperone expression, and affects the heat tolerance of *Caenorhabditis elegans*. Cell Stress Chaperones *18*, 293-306.

Miller, M.B., and Bassler, B.L. (2001). Quorum sensing in bacteria. Annual Review of Microbiology *55*, 165-199.

Miltner, E., Daroogheh, K., Mehta, P.K., Cirillo, S.L., Cirillo, J.D., and Bermudez, L.E. (2005). Identification of Mycobacterium avium genes that affect invasion of the intestinal epithelium. Infect Immun *73*, 4214-4221.

Mohan, V.P., Scanga, C.A., Yu, K., Scott, H.M., Tanaka, K.E., Tsang, E., Tsai, M.M., Flynn, J.L., and Chan, J. (2001). Effects of tumor necrosis factor alpha on host immune response in chronic persistent tuberculosis: possible role for limiting pathology. Infect Immun *69*, 1847-1855.

Montalvo-Katz, S., Huang, H., Appel, M.D., Berg, M., and Shapira, M. (2013). Association with soil bacteria enhances p38-dependent infection resistance in *Caenorhabditis elegans*. Infect Immun *81*, 514-520.

Mooren, O.L., Galletta, B.J., and Cooper, J.A. (2012). Roles for actin assembly in endocytosis. Annu Rev Biochem *81*, 661-686.

Mor, N., and Levy, L. (1985). Importance of the footpad lesion in the mouse response to local inoculation of *Mycobacterium marinum*. Annales de l'Institut Pasteur Microbiologie *136a*, 191-201.

Mor, N., Lutsky, I., and Levy, L. (1980). Response in distant lymph nodes of mice to infection in the hind footpad with *Mycobacterium marinum*. Infect Immun *28*, 225-229.

Mosser, T., Matic, I., and Leroy, M. (2011). Bacterium-induced internal egg hatching frequency is predictive of life span in *Caenorhabditis elegans* populations. Appl Environ Microbiol *77*, 8189-8192.

Moy, T.I., Mylonakis, E., Calderwood, S.B., and Ausubel, F.M. (2004). Cytotoxicity of hydrogen peroxide produced by *Enterococcus faecium*. Infect Immun *72*, 4512-4520.

Munsiff, S.S., Joseph, S., Ebrahimzadeh, A., and Frieden, T.R. (1997). Rifampin-monoresistant tuberculosis in New York City, 1993-1994. Clinical infectious diseases : an official publication of the Infectious Diseases Society of America *25*, 1465-1467.

Neth, O., Jack, D.L., Dodds, A.W., Holzel, H., Klein, N.J., and Turner, M.W. (2000). Mannose-binding lectin binds to a range of clinically relevant microorganisms and promotes complement deposition. Infect Immun *68*, 688-693.

Newton, K., and Dixit, V.M. (2012). Signaling in innate immunity and inflammation. Cold Spring Harb Perspect Biol *4*.

Noss, E.H., Pai, R.K., Sellati, T.J., Radolf, J.D., Belisle, J., Golenbock, D.T., Boom, W.H., and Harding, C.V. (2001). Toll-like receptor 2-dependent inhibition of macrophage class II MHC expression and antigen processing by 19-kDa lipoprotein of *Mycobacterium tuberculosis*. Journal of immunology (Baltimore, Md : 1950) *167*, 910-918.

O'Quinn, A.L., Wiegand, E.M., and Jeddeloh, J.A. (2001). *Burkholderia pseudomallei* kills the nematode *Caenorhabditis elegans* using an endotoxin-mediated paralysis. Cell Microbiol *3*, 381-393.

Ohnishi, Y., Kameyama, S., Onaka, H., and Horinouchi, S. (1999). The A-factor regulatory cascade leading to streptomycin biosynthesis in *Streptomyces griseus* : identification of a target gene of the A-factor receptor. Molecular microbiology *34*, 102-111.

Osorio, F., Magina, S., Carvalho, T., Goncalves, M.H., and Azevedo, F. (2010). *Mycobacterium marinum* skin infection with tenosynovitis successfully treated with doxycycline. Dermatology online journal *16*, 7.

Padmanabhan, S., Mukhopadhyay, A., Narasimhan, S.D., Tesz, G., Czech, M.P., and Tissenbaum, H.A. (2009). A PP2A regulatory subunit regulates *C. elegans* insulin/IGF-1 signaling by modulating AKT-1 phosphorylation. Cell *136*, 939-951.

Pan, H., Yan, B.S., Rojas, M., Shebzukhov, Y.V., Zhou, H., Kobzik, L., Higgins, D.E., Daly, M.J., Bloom, B.R., and Kramnik, I. (2005). Ipr1 gene mediates innate immunity to tuberculosis. Nature *434*, 767-772.

Papp, D., Csermely, P., and Soti, C. (2012). A role for SKN-1/Nrf in pathogen resistance and immunosenescence in *Caenorhabditis elegans*. PLoS Pathog *8*, e1002673.

Parish, T., and Stoker, N.G. (2000). Use of a flexible cassette method to generate a double unmarked *Mycobacterium tuberculosis* tlyA plcABC mutant by gene replacement. Microbiology (Reading, England) *146 (Pt 8)*, 1969-1975.

Park, B., Subbian, S., El-Etr, S.H., Cirillo, S.L., and Cirillo, J.D. (2008). Use of gene dosage effects for a whole-genome screen to identify *Mycobacterium marinum* macrophage infection loci. Infect Immun *76*, 3100-3115.

Park, J.O., El-Tarabily, K.A., Ghisalberti, E.L., and Sivasithamparam, K. (2002). Pathogenesis of *Streptoverticillium albireticuli* on *Caenorhabditis elegans* and its antagonism to soil-borne fungal pathogens. Letters in applied microbiology *35*, 361-365.

Petrini, B. (2006). *Mycobacterium marinum*: ubiquitous agent of waterborne granulomatous skin infections. European journal of clinical microbiology & infectious diseases : official publication of the European Society of Clinical Microbiology *25*, 609-613.

Prouty, M.G., Correa, N.E., Barker, L.P., Jagadeeswaran, P., and Klose, K.E. (2003). Zebrafish-*Mycobacterium marinum* model for mycobacterial pathogenesis. FEMS Microbiol Lett *225*, 177-182.

Pujol, N., Link, E.M., Liu, L.X., Kurz, C.L., Alloing, G., Tan, M.W., Ray, K.P., Solari, R., Johnson, C.D., and Ewbank, J.J. (2001). A reverse genetic analysis of components of the Toll signaling pathway in *Caenorhabditis elegans*. Current biology : CB *11*, 809-821.

Ramakrishnan, L. (1997). Images in clinical medicine. *Mycobacterium marinum* infection of the hand. N Engl J Med *337*, 612.

Ramakrishnan, L. (2013). Looking within the zebrafish to understand the tuberculous granuloma. Advances in experimental medicine and biology *783*, 251-266.

Ramakrishnan, L., Valdivia, R.H., McKerrow, J.H., and Falkow, S. (1997). *Mycobacterium marinum* causes both long-term subclinical infection and acute disease in the leopard frog (Rana pipiens). Infection and immunity *65*, 767-773.

Roach, S.K., and Schorey, J.S. (2002). Differential regulation of the mitogen-activated protein kinases by pathogenic and nonpathogenic mycobacteria. Infect Immun *70*, 3040-3052.

Roach, T.I., Barton, C.H., Chatterjee, D., and Blackwell, J.M. (1993). Macrophage activation: lipoarabinomannan from avirulent and virulent strains of *Mycobacterium tuberculosis* differentially induces the early genes c-fos, KC, JE, and tumor necrosis factor-alpha. Journal of immunology (Baltimore, Md : 1950) *150*, 1886-1896.

Robinson, N., Wolke, M., Ernestus, K., and Plum, G. (2007). A mycobacterial gene involved in synthesis of an outer cell envelope lipid is a key factor in prevention of phagosome maturation. Infect Immun *75*, 581-591.

Rodrigues, L.C., and Lockwood, D. (2011). Leprosy now: epidemiology, progress, challenges, and research gaps. The Lancet infectious diseases *11*, 464-470.

Rosenberger, C.M., and Finlay, B.B. (2003). Phagocyte sabotage: disruption of macrophage signalling by bacterial pathogens. Nat Rev Mol Cell Biol *4*, 385-396.

Rovina, N., Panagiotou, M., Pontikis, K., Kyriakopoulou, M., Koulouris, N.G., and Koutsoukou, A. (2013). Immune response to mycobacterial infection: lessons from flow cytometry. Clinical & developmental immunology *2013*, 464039.

Sauder, D.N., and Hanke, C.W. (1978). *Mycobacterium marinum* infections of the skin. Canadian Medical Association journal *118*, 900-901.

Schauder, S., Shokat, K., Surette, M.G., and Bassler, B.L. (2001). The LuxS family of bacterial autoinducers: biosynthesis of a novel quorum-sensing signal molecule. Molecular microbiology *41*, 463-476.

Scherr, N., Jayachandran, R., Mueller, P., and Pieters, J. (2009). Interference of *Mycobacterium tuberculosis* with macrophage responses. Indian journal of experimental biology *47*, 401-406.

Schlesinger, L.S. (1993). Macrophage phagocytosis of virulent but not attenuated strains of *Mycobacterium tuberculosis* is mediated by mannose receptors in addition to complement receptors. Journal of immunology (Baltimore, Md : 1950) *150*, 2920-2930.

Schorey, J.S., and Cooper, A.M. (2003). Macrophage signalling upon mycobacterial infection: the MAP kinases lead the way. Cell Microbiol *5*, 133-142.

Seidel, H.S., and Kimble, J. (2011). The oogenic germline starvation response in *C. elegans*. PLoS One *6*, e28074.

Sem, X., and Rhen, M. (2012). Pathogenicity of *Salmonella enterica* in *Caenorhabditis elegans* relies on disseminated oxidative stress in the infected host. PLoS One *7*, e45417.

Senaldi, G., Yin, S., Shaklee, C.L., Piguet, P.F., Mak, T.W., and Ulich, T.R. (1996). *Corynebacterium parvum*- and *Mycobacterium bovis* bacillus Calmette-Guerin-induced granuloma formation is inhibited in TNF receptor I (TNF-RI) knockout mice and by

treatment with soluble TNF-RI. Journal of immunology (Baltimore, Md : 1950) *157*, 5022-5026.

Sendide, K., Reiner, N.E., Lee, J.S., Bourgoin, S., Talal, A., and Hmama, Z. (2005). Cross-talk between CD14 and complement receptor 3 promotes phagocytosis of mycobacteria: regulation by phosphatidylinositol 3-kinase and cytohesin-1. Journal of immunology (Baltimore, Md : 1950) *174*, 4210-4219.

Shaw, T.C., Thomas, L.H., and Friedland, J.S. (2000). Regulation of IL-10 secretion after phagocytosis of *Mycobacterium tuberculosis* by human monocytic cells. Cytokine *12*, 483-486.

Shi, C., Shi, J., and Xu, Z. (2011). A review of murine models of latent tuberculosis infection. Scandinavian journal of infectious diseases *43*, 848-856.

Shiloh, M.U., and Champion, P.A. (2010). To catch a killer. What can mycobacterial models teach us about *Mycobacterium tuberculosis* pathogenesis? Curr Opin Microbiol *13*, 86-92.

Shiratsuchi, H., Ellner, J.J., and Basson, M.D. (2008). Extracellular-regulated kinase activation regulates replication of *Mycobacterium avium* intracellularly in primary human monocytes. Cell Tissue Res *332*, 237-244.

Shivers, R.P., Kooistra, T., Chu, S.W., Pagano, D.J., and Kim, D.H. (2009). Tissue-specific activities of an immune signaling module regulate physiological responses to pathogenic and nutritional bacteria in *C. elegans*. Cell Host Microbe *6*, 321-330.

Sifri, C.D., Begun, J., Ausubel, F.M., and Calderwood, S.B. (2003). *Caenorhabditis elegans* as a model host for *Staphylococcus aureus* pathogenesis. Infect Immun *71*, 2208-2217.

Sifri, C.D., Mylonakis, E., Singh, K.V., Qin, X., Garsin, D.A., Murray, B.E., Ausubel, F.M., and Calderwood, S.B. (2002). Virulence effect of *Enterococcus faecalis* protease genes and the quorum-sensing locus fsr in *Caenorhabditis elegans* and mice. Infect Immun *70*, 5647-5650.

Singh, V., and Aballay, A. (2009). Regulation of DAF-16-mediated Innate Immunity in *Caenorhabditis elegans*. J Biol Chem *284*, 35580-35587.

Sirisinha, S. (2014). Evolutionary insights into the origin of innate and adaptive immune systems: different shades of grey. Asian Pacific journal of allergy and immunology / launched by the Allergy and Immunology Society of Thailand *32*, 3-15.

Sizaire, V., Nackers, F., Comte, E., and Portaels, F. (2006). *Mycobacterium ulcerans* infection: control, diagnosis, and treatment. The Lancet infectious diseases *6*, 288-296.

Slany, M., Jezek, P., Fiserova, V., Bodnarova, M., Stork, J., Havelkova, M., Kalat, F., and Pavlik, I. (2012). *Mycobacterium marinum* infections in humans and tracing of its possible environmental sources. Canadian journal of microbiology *58*, 39-44.

Smith, M.G., Des Etages, S.G., and Snyder, M. (2004). Microbial synergy via an ethanol-triggered pathway. Molecular and cellular biology *24*, 3874-3884.

Sousa, A.O., Mazzaccaro, R.J., Russell, R.G., Lee, F.K., Turner, O.C., Hong, S., Van Kaer, L., and Bloom, B.R. (2000). Relative contributions of distinct MHC class I-dependent cell populations in protection to tuberculosis infection in mice. Proc Natl Acad Sci U S A *97*, 4204-4208.

Souza, C.D., Evanson, O.A., and Weiss, D.J. (2007). Role of the mitogen-activated protein kinase pathway in the differential response of bovine monocytes to *Mycobacterium avium* subsp. *paratuberculosis* and *Mycobacterium avium* subsp. *avium*. Microbes and infection / Institut Pasteur *9*, 1545-1552.

Staab, T.A., Griffen, T.C., Corcoran, C., Evgrafov, O., Knowles, J.A., and Sieburth, D. (2013). The conserved SKN-1/Nrf2 stress response pathway regulates synaptic function in *Caenorhabditis elegans*. PLoS Genet *9*, e1003354.

Stenger, S., and Modlin, R.L. (1999). T cell mediated immunity to *Mycobacterium tuberculosis*. Curr Opin Microbiol *2*, 89-93.

Stinear, T.P., Seemann, T., Harrison, P.F., Jenkin, G.A., Davies, J.K., Johnson, P.D., Abdellah, Z., Arrowsmith, C., Chillingworth, T., Churcher, C., *et al.* (2008). Insights from the complete genome sequence of *Mycobacterium marinum* on the evolution of *Mycobacterium tuberculosis*. Genome research *18*, 729-741.

Stone, A.C., Wilbur, A.K., Buikstra, J.E., and Roberts, C.A. (2009). Tuberculosis and leprosy in perspective. Am J Phys Anthropol *140 Suppl 49*, 66-94.

Strohmeier, G.R., and Fenton, M.J. (1999). Roles of lipoarabinomannan in the pathogenesis of tuberculosis. Microbes and infection / Institut Pasteur *1*, 709-717.

Styer, K.L., Hopkins, G.W., Bartra, S.S., Plano, G.V., Frothingham, R., and Aballay, A. (2005). *Yersinia pestis* kills *Caenorhabditis elegans* by a biofilm-independent process that involves novel virulence factors. EMBO reports *6*, 992-997.

Subbian, S., Mehta, P.K., Cirillo, S.L., Bermudez, L.E., and Cirillo, J.D. (2007a). A *Mycobacterium marinum* mel2 mutant is defective for growth in macrophages that produce reactive oxygen and reactive nitrogen species. Infect Immun *75*, 127-134.

Subbian, S., Mehta, P.K., Cirillo, S.L., and Cirillo, J.D. (2007b). The *Mycobacterium marinum mel2* locus displays similarity to bacterial bioluminescence systems and plays a role in defense against reactive oxygen and nitrogen species. BMC Microbiol *7*, 4.

Swaim, L.E., Connolly, L.E., Volkman, H.E., Humbert, O., Born, D.E., and Ramakrishnan, L. (2006a). *Mycobacterium marinum* infection of adult zebrafish causes caseating granulomatous tuberculosis and is moderated by adaptive immunity. Infection and immunity *74*, 6108-6117.

Swaim, L.E., Connolly, L.E., Volkman, H.E., Humbert, O., Born, D.E., and Ramakrishnan, L. (2006b). *Mycobacterium marinum* infection of adult zebrafish causes caseating granulomatous tuberculosis and is moderated by adaptive immunity. Infect Immun *74*, 6108-6117.

Tabach, Y., Billi, A.C., Hayes, G.D., Newman, M.A., Zuk, O., Gabel, H., Kamath, R., Yacoby, K., Chapman, B., Garcia, S.M., *et al.* (2013). Identification of small RNA pathway genes using patterns of phylogenetic conservation and divergence. Nature *493*, 694-698.

Takaki, K., Davis, J.M., Winglee, K., and Ramakrishnan, L. (2013). Evaluation of the pathogenesis and treatment of *Mycobacterium marinum* infection in zebrafish. Nat Protoc *8*, 1114-1124.

Takano, E. (2006). Gamma-butyrolactones: *Streptomyces* signalling molecules regulating antibiotic production and differentiation. Current opinion in microbiology *9*, 287-294.

Talaat, A.M., Reimschuessel, R., Wasserman, S.S., and Trucksis, M. (1998). Goldfish, *Carassius auratus*, a novel animal model for the study of *Mycobacterium marinum* pathogenesis. Infect Immun *66*, 2938-2942.

Tan, M.W., Rahme, L.G., Sternberg, J.A., Tompkins, R.G., and Ausubel, F.M. (1999). *Pseudomonas aeruginosa* killing of *Caenorhabditis elegans* used to identify *P. aeruginosa* virulence factors. Proc Natl Acad Sci U S A *96*, 2408-2413.

Tascon, R.E., Soares, C.S., Ragno, S., Stavropoulos, E., Hirst, E.M., and Colston, M.J. (2000). *Mycobacterium tuberculosis*-activated dendritic cells induce protective immunity in mice. Immunology *99*, 473-480.

Taylor, R.C., and Dillin, A. (2013). XBP-1 is a cell-nonautonomous regulator of stress resistance and longevity. Cell *153*, 1435-1447.

Teasdale, M.E., Donovan, K.A., Forschner-Dancause, S.R., and Rowley, D.C. (2011). Gram-positive marine bacteria as a potential resource for the discovery of quorum sensing inhibitors. Marine biotechnology (New York, NY) *13*, 722-732.

Tebruegge, M., and Curtis, N. (2011). *Mycobacterium marinum* infection. Advances in experimental medicine and biology *719*, 201-210.

Tenor, J.L., and Aballay, A. (2008). A conserved Toll-like receptor is required for *Caenorhabditis elegans* innate immunity. EMBO reports *9*, 103-109.

Tenor, J.L., McCormick, B.A., Ausubel, F.M., and Aballay, A. (2004). *Caenorhabditis elegans*-based screen identifies *Salmonella* virulence factors required for conserved host-pathogen interactions. Current biology : CB *14*, 1018-1024.

Tobin, D.M., and Ramakrishnan, L. (2008). Comparative pathogenesis of *Mycobacterium marinum* and *Mycobacterium tuberculosis*. Cellular microbiology *10*, 1027-1039.

Tobin, D.M., Roca, F.J., Oh, S.F., McFarland, R., Vickery, T.W., Ray, J.P., Ko, D.C., Zou, Y., Bang, N.D., Chau, T.T., *et al.* (2012). Host genotype-specific therapies can optimize the inflammatory response to mycobacterial infections. Cell *148*, 434-446.

Toossi, Z., Gogate, P., Shiratsuchi, H., Young, T., and Ellner, J.J. (1995). Enhanced production of TGF-beta by blood monocytes from patients with active tuberculosis and presence of TGF-beta in tuberculous granulomatous lung lesions. Journal of immunology (Baltimore, Md : 1950) *154*, 465-473.

Troemel, E.R., Chu, S.W., Reinke, V., Lee, S.S., Ausubel, F.M., and Kim, D.H. (2006). p38 MAPK regulates expression of immune response genes and contributes to longevity in *C. elegans*. PLoS Genet *2*, e183.

Tse, H.M., Josephy, S.I., Chan, E.D., Fouts, D., and Cooper, A.M. (2002). Activation of the mitogen-activated protein kinase signaling pathway is instrumental in determining the ability of *Mycobacterium avium* to grow in murine macrophages. Journal of immunology (Baltimore, Md : 1950) *168*, 825-833.

van Crevel, R., Ottenhoff, T.H., and van der Meer, J.W. (2002). Innate immunity to *Mycobacterium tuberculosis*. Clin Microbiol Rev *15*, 294-309.

van der Sar, A.M., Abdallah, A.M., Sparrius, M., Reinders, E., Vandenbroucke-Grauls, C.M., and Bitter, W. (2004a). *Mycobacterium marinum* strains can be divided into two distinct types based on genetic diversity and virulence. Infect Immun *72*, 6306-6312.

van der Sar, A.M., Appelmelk, B.J., Vandenbroucke-Grauls, C.M., and Bitter, W. (2004b). A star with stripes: zebrafish as an infection model. Trends in microbiology *12*, 451-457.

VanHeyningen, T.K., Collins, H.L., and Russell, D.G. (1997). IL-6 produced by macrophages infected with *Mycobacterium* species suppresses T cell responses. Journal of immunology (Baltimore, Md : 1950) *158*, 330-337.

Vergne, I., Chua, J., Singh, S.B., and Deretic, V. (2004a). Cell biology of *Mycobacterium tuberculosis* phagosome. Annu Rev Cell Dev Biol *20*, 367-394.

Vergne, I., Fratti, R.A., Hill, P.J., Chua, J., Belisle, J., and Deretic, V. (2004b). *Mycobacterium tuberculosis* phagosome maturation arrest: mycobacterial phosphatidylinositol analog phosphatidylinositol mannoside stimulates early endosomal fusion. Mol Biol Cell *15*, 751-760.

Vieira, O.V., Botelho, R.J., and Grinstein, S. (2002). Phagosome maturation: aging gracefully. Biochem J *366*, 689-704.

Vilcheze, C., Baughn, A.D., Tufariello, J., Leung, L.W., Kuo, M., Basler, C.F., Alland, D., Sacchettini, J.C., Freundlich, J.S., and Jacobs, W.R., Jr. (2011). Novel inhibitors of InhA efficiently kill *Mycobacterium tuberculosis* under aerobic and anaerobic conditions. Antimicrob Agents Chemother *55*, 3889-3898.

Weerdenburg, E.M., Abdallah, A.M., Mitra, S., de Punder, K., van der Wel, N.N., Bird, S., Appelmelk, B.J., Bitter, W., and van der Sar, A.M. (2012). ESX-5-deficient *Mycobacterium marinum* is hypervirulent in adult zebrafish. Cell Microbiol *14*, 728-739.

Whitehead, N.A., Barnard, A.M., Slater, H., Simpson, N.J., and Salmond, G.P. (2001). Quorum-sensing in Gram-negative bacteria. FEMS microbiology reviews *25*, 365-404.

Wilkins, C., Dishongh, R., Moore, S.C., Whitt, M.A., Chow, M., and Machaca, K. (2005). RNA interference is an antiviral defence mechanism in *Caenorhabditis elegans*. Nature *436*, 1044-1047.

Wu, C.W., Schmoller, S.K., Bannantine, J.P., Eckstein, T.M., Inamine, J.M., Livesey, M., Albrecht, R., and Talaat, A.M. (2009). A novel cell wall lipopeptide is important for biofilm formation and pathogenicity of *Mycobacterium avium* subspecies paratuberculosis. Microb Pathog *46*, 222-230.

Yamazaki, H., Ohnishi, Y., and Horinouchi, S. (2000). An A-factor-dependent extracytoplasmic function sigma factor (sigma(AdsA)) that is essential for morphological development in *Streptomyces griseus*. Journal of Bacteriology *182*, 4596-4605.

Yamazaki, Y., Danelishvili, L., Wu, M., Macnab, M., and Bermudez, L.E. (2006). *Mycobacterium avium* genes associated with the ability to form a biofilm. Appl Environ Microbiol *72*, 819-825.

Yang, H.C., Chen, T.L., Wu, Y.H., Cheng, K.P., Lin, Y.H., Cheng, M.L., Ho, H.Y., Lo, S.J., and Chiu, D.T. (2013). Glucose 6-phosphate dehydrogenase deficiency enhances germ cell apoptosis and causes defective embryogenesis in *Caenorhabditis elegans*. Cell Death Dis *4*, e616.

Yang, J.S., Nam, H.J., Seo, M., Han, S.K., Choi, Y., Nam, H.G., Lee, S.J., and Kim, S. (2011). OASIS: online application for the survival analysis of lifespan assays performed in aging research. PLoS One *6*, e23525.

Yoshida, A., Inagawa, H., Kohchi, C., Nishizawa, T., and Soma, G. (2009). The role of toll-like receptor 2 in survival strategies of *Mycobacterium tuberculosis* in macrophage phagosomes. Anticancer Research *29*, 907-910.

Zaffran, Y., and Ellner, J.J. (1997). A coat of many complements. Nature medicine *3*, 1078-1079.

Ziegler, K., Kurz, C.L., Cypowyj, S., Couillault, C., Pophillat, M., Pujol, N., and Ewbank, J.J. (2009). Antifungal innate immunity in *C. elegans*: PKCdelta links G protein signaling and a conserved p38 MAPK cascade. Cell Host Microbe *5*, 341-352.

Zumla, A., Abubakar, I., Raviglione, M., Hoelscher, M., Ditiu, L., McHugh, T.D., Squire, S.B., Cox, H., Ford, N., McNerney, R., *et al.* (2012). Drug-resistant tuberculosis--current dilemmas, unanswered questions, challenges, and priority needs. The Journal of infectious diseases *205 Suppl 2*, S228-240.

APPENDIX

Appendix Tables

Table 1. Mutants in *M. marinum*.

Gene[1]	Putative activity[2]	*Mtb homolog*[3]
fadD29	fatty acid-CoA ligase	Rv2950c
fadD30	fatty acid-CoA ligase	Rv0404
mimA	membrane protein	Rv0246
mimB	integrase/recombinase	None
mimC	o-phosphotransferase	Rv2636
mimD	hypothetical protein	None
mimE	copper amine oxidase	None
mimF	phage protein	None
mimG	Amidophosphoribosyltransferase	Rv3242c
mimH	secretion (extRD1)	Rv3881c
mimI	hypothetical protein	Rv1502
mimJ	hypothetical protein	None
mimK	hypothetical protein	None
Nrp	glycopeptidolipid synthesis	Rv0101
pks12	polyketide synthesis	Rv2048c
ppe24	PPE24	Rv1753c
ppe53	PPE53	Rv3159c
sdhD	succinate dehydrogenase	Rv3317

[1] Mutants were constructed previously (Mehta et al., 2006).

[2] Putative activities are as described in NCBI Gene Bank.

[3] Homolog annotation are listed as previously reported (Mehta et al., 2006).

Table 2. *C. elegans* RNAi Constructs and Mutant Strains.

Gene	RNAi Construct[1]	Mutant Strain[2]	Mutant Genotype
daf-16	R13H8.1	GR1307	*daf-16* (mgDf50)
dbl-1	T25F10.2	NU3	*dbl-1* (nk3)
pmk-1	B0218.3	KU25	*pmk-1* (km25)
skn-1	T19E7.2	EU31	*skn-1* (zu135)
tol-1	C07F11.1	IG10	*tol-1* (nr2033)
vhp-1	F08B1.1	JT366	*vhp-1* (sa366)

[1] RNAi constructs were cloned into pL4440-DEST vector that confirms resistance to ampicillin (100 µg/ml). *E. coli* host strain is HT115 (DE3) (obtained from the Fire Lab).

[2] Mutant strains were obtained from *Caenorhabditis* Genetics Center (CGC), University of Minnesota.

Table 3. Primers Used for Confirmation of *C. elegans* Mutants and RNAi Knock-Down Mutants.

Gene	Forward primers[1]	Reverse primers[1]	Product length
pmk-1	AACTGGAACACCAGATGAAG	TTGAAATCACGGCGAGTC	99bp
daf-16	CGGTTCCAGCAATTCCA	GCTTCGACTCCTGCTTAAT	102bp
dbl-1	ACTGAGCTCATTGCCCTA	TTTGTGCACTCCGTTTCC	101bp
tol-1	GCTGGACGTGTCGAATAAT	GTAAGCAGATTGCCCTTCA	99bp
vhp-1	TGTTGTCGAGAACCCATTT	GCAGATGCTGGAGTTGAT	96bp
skn-1	CGTCAACAGCAGACTCAAA	CGAGTGTCTCTGTGAGTGA	96bp
cdc-42	GCTCGAGAAACTGGCAAA	CGCTGAGCATTCAACGTA	103bp
pmp-3	TCGCTAACTGAATGGAGAAT	TGATGAACACGGGAACAC	103bp

[1] Forward and Reverse primers were selected using the Oligo Analyzer Tools available on the Integrated DNA Technologies website, to have a melt temperature of ~60 ºC.

Table 4. List of Primers Used for Amplification of Full-Length MMAR_1239 Genes to Obtain Functional Complementing Clones.

Primer Name	Tm (°C)	Length (bp)	Pimer Sequence
MMAR1239F	62	34	TATAAAGCTTGCATGCCTCCACCGAGCTGCCGCT
MMAR1239R	62	29	TATAGATATCGCCATGGTGCCAACGGGCA
MMAR1239F2	62	36	TATAAAGCTTGCATGCCGAGCTGCCGCTGGCCCAGG
MMAR1239R2	62	31	TATAGATATCGCCATGGTGCCAACGGGCACC
MMAR1239F-HindIII	58	29	TATAAAGCTTGGATGCCTGGAAGGCGTAT
MMAR1239R-PacI	58	32	TATATTAATTAACGGGCACCGACAAAAACTAT
MMAR1240F1	62	31	TATAAGCTTGCTAGCGACCCGTACTCGCTCT
MMAR1240R1	62	29	ATATTAATTAAGCCAGGCTCACCCAAACTG
MMAR1239-40F1	60	33	ATATTAATTAAGCTTGACCCGTACTCGCTCTAC
MMAR1239-40R1	60	35	ATATTAATTAAGCATGCCTAGCCATGGTGCCAACG

Table 5. List of Primers Used for Amplification of Entire MMAR_1239 Gene Locus for Insertional Mutagenesis.

Primer Name	Tm (°C)	Length (bp)	Pimer Sequence
MMAR1239-10KF1	60	30	TATAACCTAGGAGACCGAAAGACCGGCACTG
MMAR1239-10KR1	60	30	TATAACTAGTCCAAGGCAAACCAGCGGTAG
MMAR1239-10KF2	60	29	TATACCTAGGCATCATCGGGTTGGGAAGG
MMAR1239-10KR2	60	30	TATAACTAGTGGGATTCAACGGTGGTGCTG
MMAR1239-8KF1	60	30	TATACCTAGGCCCACATCAACCACCTCACG
MMAR1239-8KR1	60	30	TATAACTAGTGAATATCGCAGCGGGTCAGC
MMAR1239-8KF2	60	27	TATACCTAGGACCCAGCCACGATCTGG
MMAR1239-8KR2	60	31	TATAACTAGTGATGATTCGTGCTGGTGGTC
MMAR1239-5KF1	60	30	TATACCTAGGCAGGGCACACCATGAGTTCG
MMAR1239-5KR1	60	30	TATAACTAGTACTTGCCCGACAGCAGATCC
MMAR1239-5KR2	60	30	TATAACTAGTACGGATACTTGCCCGACAGC
MMAR1239-2KF1	60	27	TATACCTAGGTGGCCGACGATGTGGTG
MMAR1239-2KR1	60	29	TATAACTAGTGTCGTACGGTCGCCGATAG
MMAR1239-2KF2	60	28	TATACCTAGGATCGGCCGACCTGGACCT
MMAR1239-2KR2	60	29	TATAACTAGTGAGTCGCTCCAGGGATAGC

Table 6. List of Primers Used for MMAR_1239 Operon Structure Determination and To Quantify Transcript Levels Using RT-PCR and qPCR.

Primer Name	Tm (°C)	Length (bp)	Pimer Sequence
MMAR1240-1241F	55	18	CATCGACCGCGACATTTG
MMAR1240-1241R	55	18	TCGAACGCCTTGCGTACC
MMAR1239-1240F	55	18	CGCCACCAACACCATCAA
MMAR1239-1240R	55	18	CGCTTGCCGAAAACTTCC
MMAR1238-1239F	55	18	CCACACGCTGCTGGACTC
MMAR1238-1239R	55	18	ACCATTCGCGAGTGATCG
MMAR1237-1238F	55	18	ACCGGAGTGCCGGTGCTA
MMAR1237-1238R	55	18	ATATCGCAGCGGGTCAGC
MMAR1241F-RT	55	18	CACGATCTGGAGCGACCA
MMAR1241R-RT	55	18	TAATCGGGGTCGCTGTCC
MMAR1240F-RT	55	18	CGCACACAAGCACGACCT
MMAR1240R-RT	55	18	GAGCGGATGCCAGGTCTC
MMAR1239F-RT	55	18	GGCTCTACGAGGCCACCA
MMAR1239R-RT	55	18	CCATCTGGCGGTTCTTGG
MMAR1238F-RT	55	18	CTGGCGCTATCCCTGGAG
MMAR1238R-RT	55	18	ATGTCAGCCACCGGAACC
MMAR1237F-RT	55	18	ACGATATCCGGGCAGTGG
MMAR1237R-RT	55	18	CAGCACCCGTTGATCGAG
MMAR1240F2-RT	55	18	CTCTCGTCGGCGATCTTC
MMAR1240R2-RT	55	18	GCGCATATACGCCTTCCA
MMAR1236-37 F	55	17	GGGTGGGAGGCGATTGT
MMAR1236-37R	55	16	GCCGGTCGGCAGTTGT
MMAR1237-38F2	55	18	AGCGGGTCAGCGTTTTTC
MMAR1237-38R2	55	18	TGGTCGAGCGAATCAACG
MMAR1241-42F	55	19	TGCTGTATGCGGGGACTTC
MMAR1241-42R	55	17	ACGCCCATCGGAGACCA
MMAR5519F	55	20	TTCATGTCCTGTGGTGGAAA
MMAR5519R	55	20	GTGCAATATTCCCCACTGCT

Appendix Figures

Figure 47. Plasmid pJDC279a With a 5 kbp region of MMAR_1239 Gene Locus.

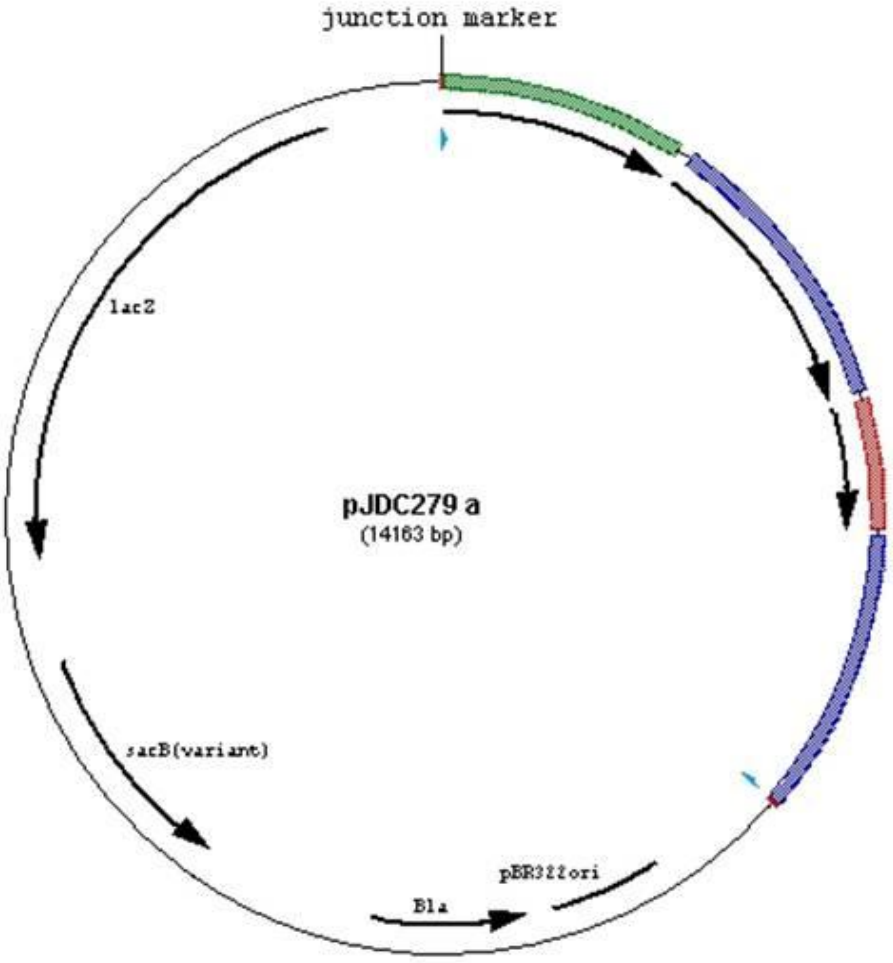

Figure 48. pJDC282 and pJDC284 Constructs With a Kanamycin Insertion in MMAR_1239 and MMAR_1240.

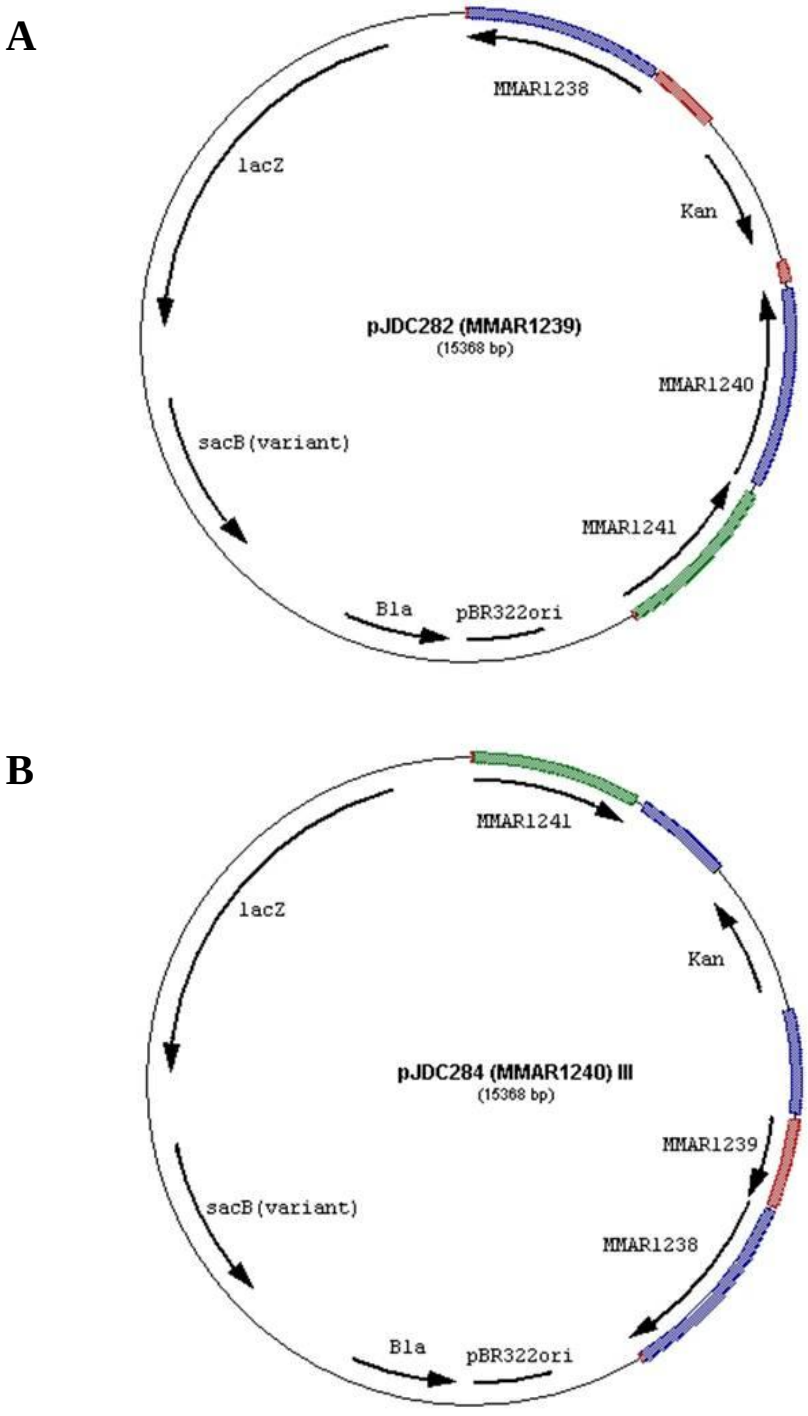

Figure 49. Full length MMAR_1239 and MMAR_1240 Genes Were Used to Complement Insertion Mutants *Mm-luxR1* and *Mm-pcd*.

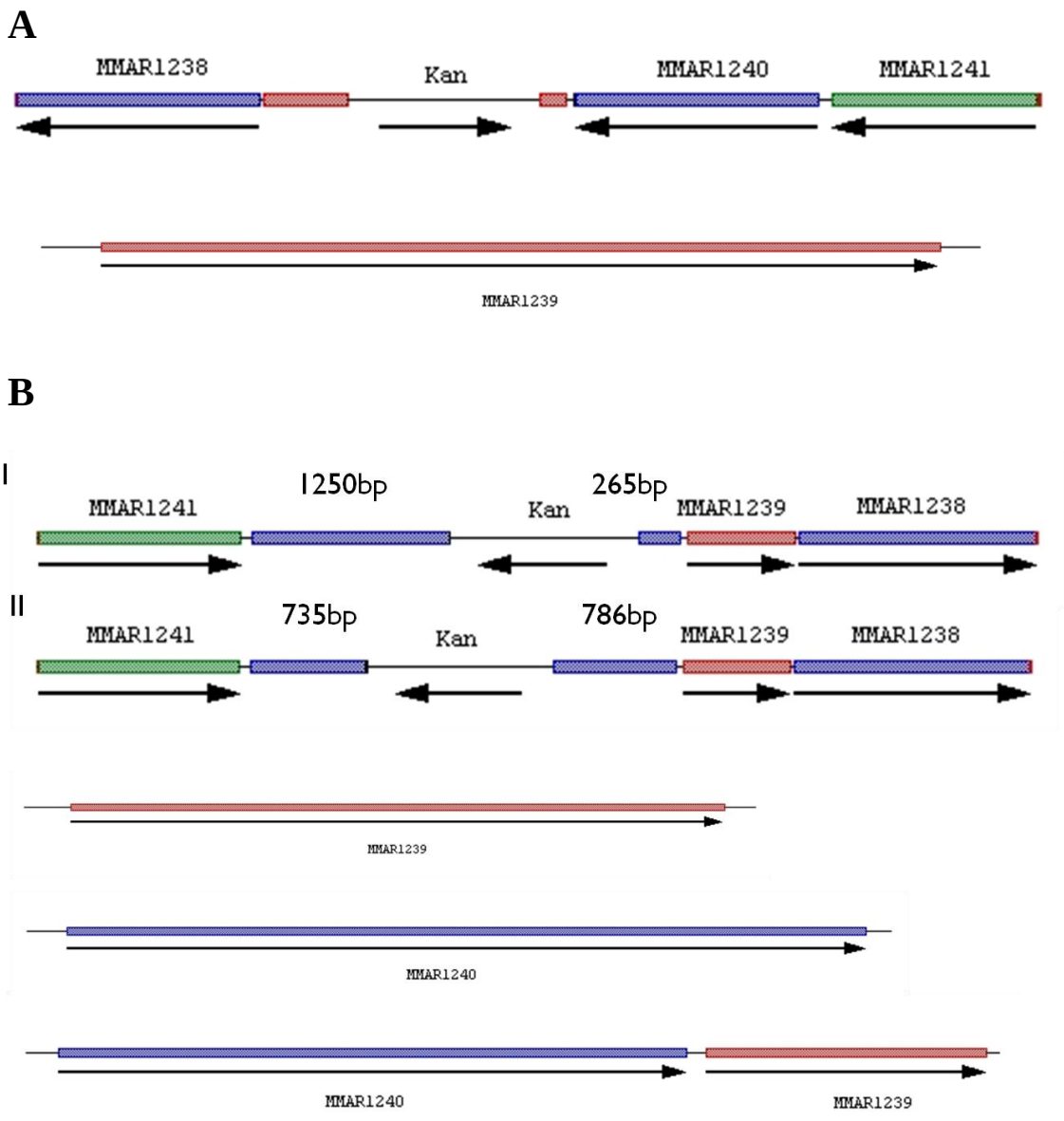

Figure 50. Representative Plasmid Constructs Depicting the Primer SeqE and SeqW Binding Sites Used for Insertion Mutant Confirmation

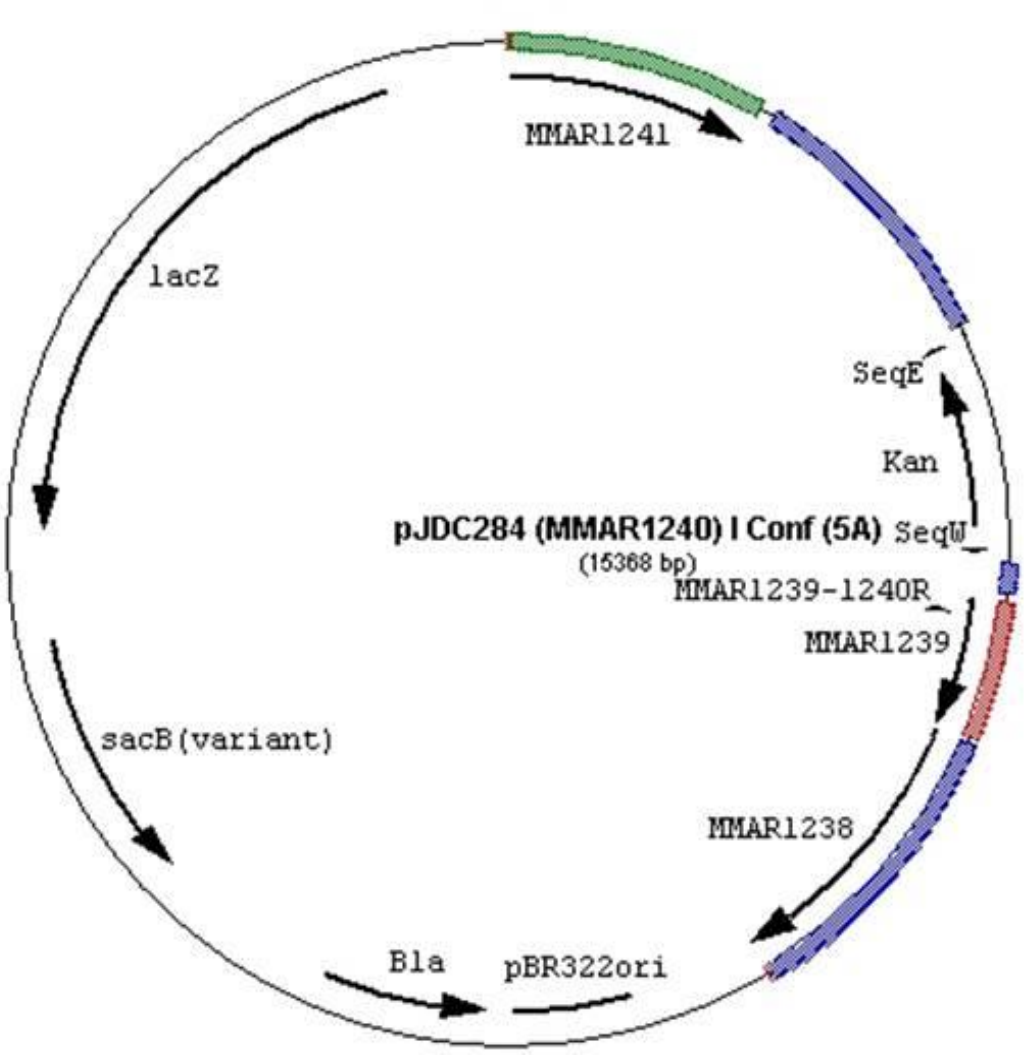

Figure 51. Plasmid Used for Single Copy Complementation of Mutants.

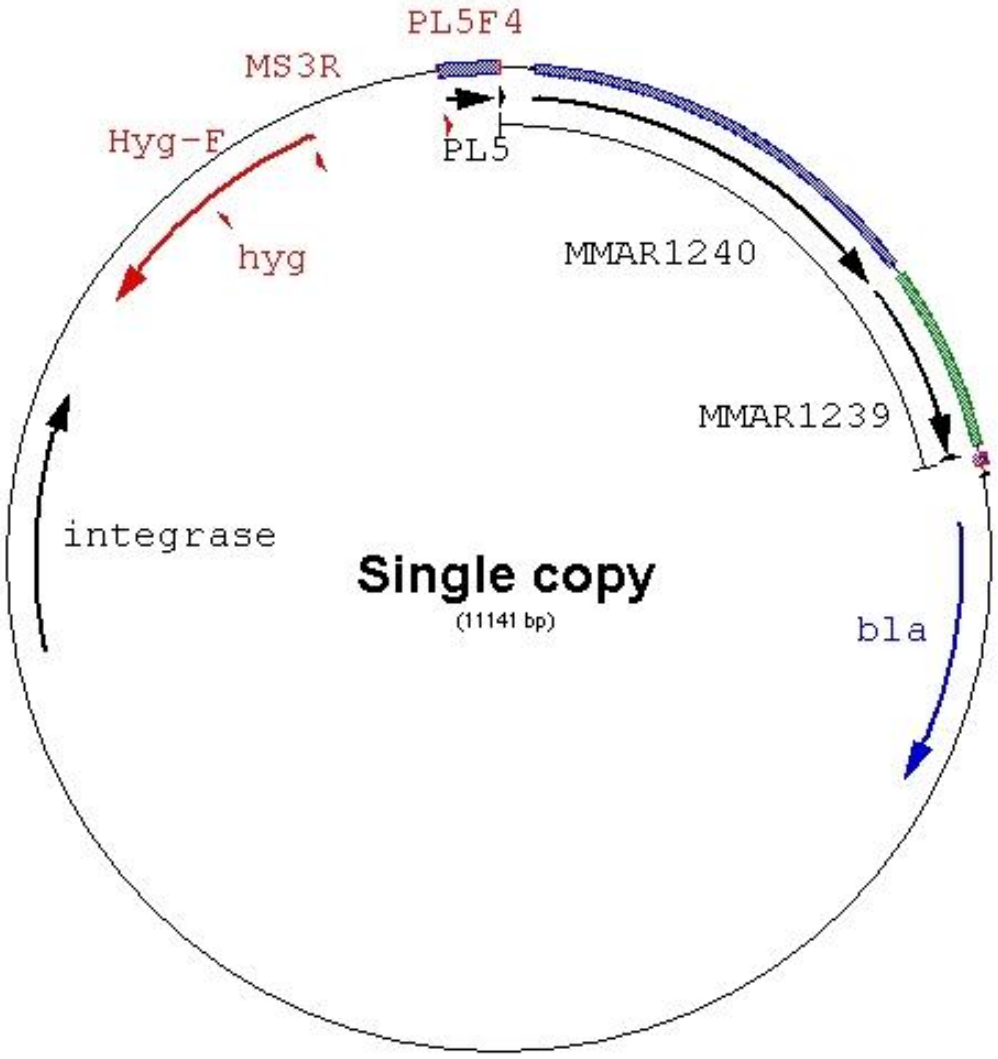

Figure 52. Plasmid Used for Multi-Copy Complementation of Mutants.

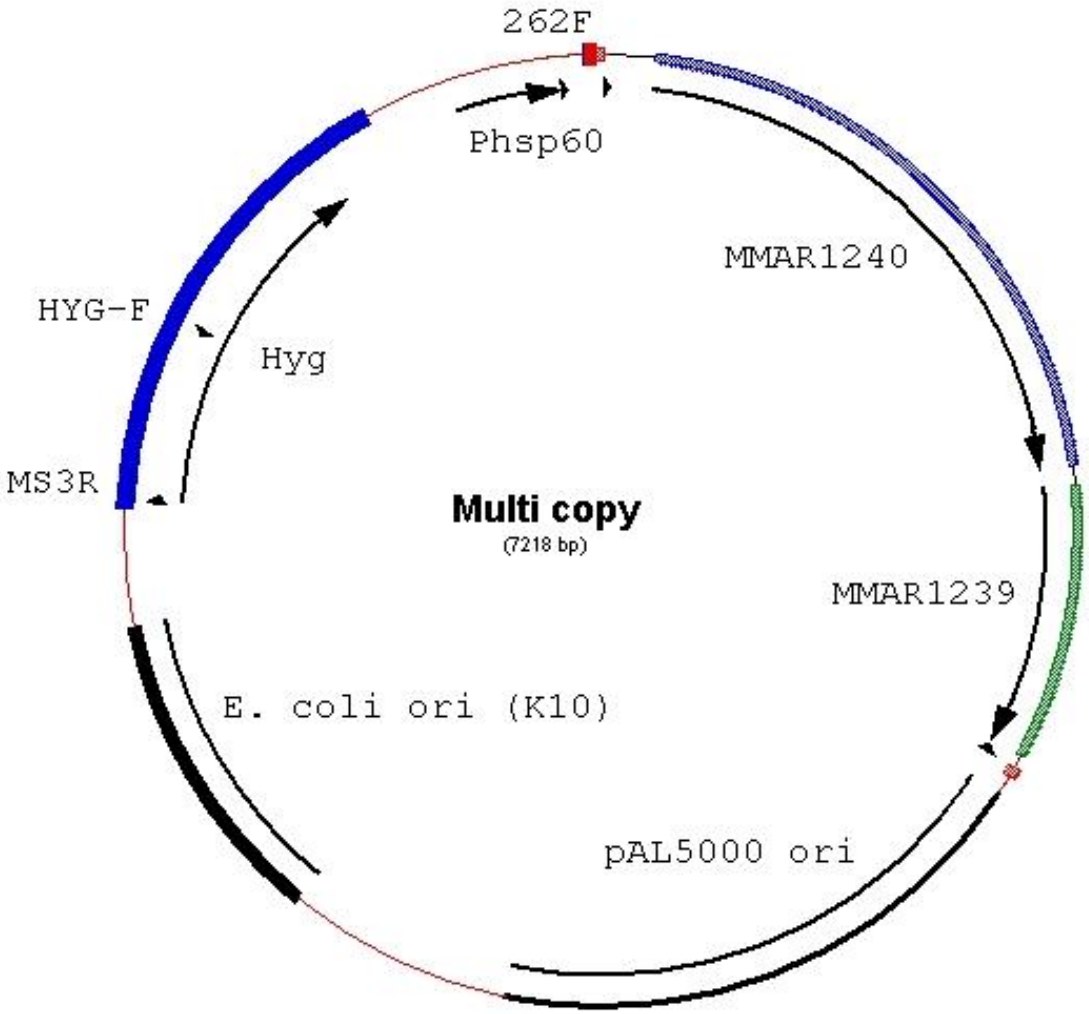

Figure 53. Confirmation of *Mm-pcd* Complementing Strain.

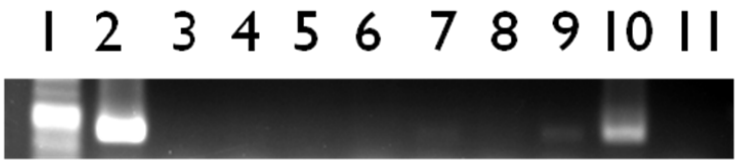

1 – 100bp ladder
2 – (+)ve control (pJDC240)
3 – (-)ve control (*luxR1* mutant w/o complement)
4 – *pcd* mutant w/ single copy empty vector (1)
5 – *pcd* mutant w/ single copy empty vector (2)
6 – *pcd* mutant w/ single copy *pcd* (1)
7 – *pcd* mutant w/ single copy *pcd* (2)
8 – *pcd* mutant w/ single copy *pcd/luxR1* (1)
9 – *pcd* mutant w/ single copy *pcd/luxR1* (2)
10 – (+)ve control (plasmid with *luxR1*)
11 – (-)ve control (*pcd* mutant w/o complement)

Confirmed Complement Clones
7 – *pcd* mutant w/ single copy *pcd* (2)
9 – *pcd* mutant w/ single copy *pcd/luxR1* (2)

Figure 54. Initial Confirmation of *Mm-luxR1* Complementing Strain.

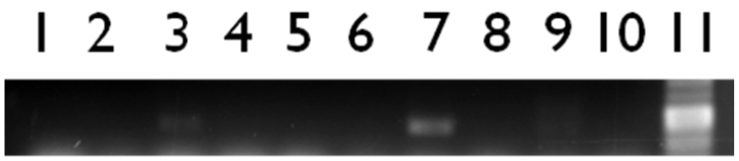

1 – wt w/ single copy empty vector (1)
2 – wt w/ single copy empty vector (2)
3 – *luxR1* mutant w/ single copy *luxR1*(1)
4 – *luxR1* mutant w/ single copy *luxR1*(2)
5 – *luxR1* mutant w/ single copy empty vector (1)
6 – *luxR1* mutant w/ single copy empty vector (2)
7 – *luxR1* mutant w/ muti copy *luxR1* (1)
8 – *luxR1* mutant w/ muti copy *luxR1* (2)
9 – *luxR1* mutant w/ muti copy empty vector (1)
10 – *luxR1* mutant w/ muti copy empty vector (2)
11 – 100bp ladder

Confirmed Complement Clones
3 – *luxR1* mutant w/ single copy *luxR1* (1)
7 – *luxR1* mutant w/ muti copy *luxR1* (1)

Figure 55. Secondary Confirmation of *Mm-luxR1* Complementing Strain.

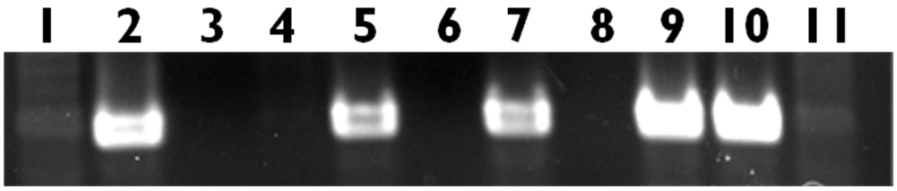

1 – 100 bp ladder
2 – plasmid (+)ve control
4 – *Mm-wt* gDNA
5 – *Mm-wt* w/ vector (1)
6 – *Mm-wt* w/ vector (2)
7 – *Mm-luxR1* mutant w/ vector (1)
8 – *Mm-luxR1* mutant w/ vector (2)
9 – *Mm-luxR1* complement (1)
10 – *Mm-luxR1* complement (2)
11 – 100 bp ladder